Universitetet i Stavanger

DET TEKNISK-NATURVITENSKAPELIGE FAKULTET

MASTEROPPGAVE

Study program: Engineering structures and materials / Building structures	Spring semester, 2021 Open
Authors: Torunn Gjerdset, Ingvild Nordvik	
Faculty supervisor: Associate professor Samindi Samarakoon Supervisors: Sindre Sandbakk, Dr.techn. Olav Olsen AS Fredrik Fosdal, Rambøll Bergen	
Title of master thesis: Punching shear resistance in fiber-reinforced PT-slabs	
Credits: 30	
Keywords: Punching shear Flat slab Post-tensioning Fiber reinforced concrete Concrete SFRC Eurocode 2	Number of pages: 84 + supplemental material/other: 69 Stavanger, 30.06.2021 date/year

PUNCHING SHEAR RESISTANCE IN FIBER-REINFORCED PT SLABS

PUNCHING SHEAR RESISTANCE IN POST-TENSIONED FLAT SLABS WITH FIBER-REINFORCEMENT IN ACCORDANCE WITH PROPOSED PROVISIONS IN prEN 1992-1-1

Torunn Gjerdset
Ingvild Nordvik

University of Stavanger
department of mechanical and structural engineering and materials science

2021 Stavanger

1 Acknowledgements

This master thesis marks the ending of our master's degree at the department of mechanical, civil, and materials technology at the University of Stavanger.

We would like to thank our supervisor Associate Professor Samindi Samarakoon, for all the guidance, knowledge, and support during the work with this thesis.

We would also like to thank our colleagues at Dr.techn. Olav Olsen AS and Rambøll. Your knowledge and professional support have been of great importance for our work.

Last, we would like to thank Steinar Trygstad. Your knowledge and enthusiasm regarding this subject cannot be overstated.

Torunn Gjerdset

Torunn Gjerdset

Ingvild Nordvik

Ingvild Nordvik

2 Abstract

Post-tensioned flat slabs with fiber-reinforced concrete can reduce cracking and deflections, provide longer spans, thinner slabs and provide a reduction in the weight of the structure due to reduced floor dead load. The solution also provides benefits such as reduced storey height, a large reduction in conventional reinforcement, as well as an overall more flexible design (The concrete society , 2005). However, the local shear per unit of length around columns in flat slabs can become very high, and this can result in local punching shear failure (Sørensen, 2013). Hence, this thesis aims to investigate the punching shear resistance in post-tensioned flat slabs with fiber reinforcement in accordance with proposed provisions in prEN 1992-1-1.

Initially the thesis presents a general study of different theory, design and calculations regarding flat slabs, fiber-reinforced concrete, and prestressed concrete. This part also includes a study of the current Eurocode 2, the proposed version of Eurocode 2, ACI 318-19, and FIB's Model Code. Thereafter a parametric study of a flat slab was performed. In this study, the punching shear resistance around different critical control sections was controlled, and then compared with results from ADAPT and FEM-Design. Furthermore, the effect from different parameters in prEN 1992-1-1 and EN 1992-1-1 were compared.

The study showed that the fiber-reinforcement had the greatest contribution to the punching shear resistance according to the proposed provisions in Eurocode 2. The shear reinforcement had the second greatest contribution, although this contribution will vary. The purpose of the shear reinforcement is to account for the residual shear capacity and depending on the contribution from the fiber-reinforcement, post-tensioning and shear force, this value will therefore be different depending on the given case. If the contribution is e.g. sufficiently high from the fiber, the required amount of shear reinforcement will be lower/not required, because there will be a higher capacity in the slab to withstand the shear force.

Furthermore, the study showed that the prestressing affected the punching shear resistance in a relatively small manner. The study also showed that the punching shear resistance was lower for EN-1992-1-1 compared to prEN 1992-1-1. However, the proposed version will give a lower capacity because the design shear force is increased due to the decreased critical control section.

The design methods presented in this study is intended to be read in conjunction with Eurocode 2 and the Norwegian National Annex. It should be noted that during the preparation of this thesis the final version of Eurocode 2 was not published, and the reader should confirm numerical values given in this method with the final version of Eurocode 2 and the Norwegian National Annex.

Sammendrag

Etteroppspente flatdekker med fiberarmert betong kan redusere riss og nedbøyning, gi lengre spenn, tynnere dekker og en reduksjon i vekt på grunn av redusert egenvekt. Løsningen gir også fordeler som redusert etasjehøyde, en betydelig reduksjon i konvensjonell armering, samt et mer fleksibelt design (The concrete society , 2005). Det er imidlertid slik at lokal skjærkraft per lengdeenhet rundt søylene i flatdekker kan bli veldig høy, noe som kan medføre lokale gjennomlokkingsbrudd (Sørensen, 2013). Denne masteroppgaven tar derfor sikte på å undersøke gjennomlokkingskapasiteten i slike dekker, i samsvar med foreløpig versjon av prEN 1992-1-1.

Innledningsvis presenterer oppgaven relevant teori og beregningsmetoder knyttet til flatdekker, fiberarmert betong og prinsippet med etteroppspent betong. Denne delen inneholder også en studie av gjeldende Eurokode 2, revidert versjon av Eurokode 2, den amerikanske betongstandarden 318-19 og FIBs Model Code. Deretter ble en parametrisk studie gjennomført der et flatdekke ble analysert, og kritisk kontrollsnitt rundt innersøyler, hjørnesøyler og kantsøyler ble undersøkt. Disse resultatene ble sammenlignet med resultater fra FE-analyser i ADAPT og FEM-Design. Til slutt er det gjort en parametersammenligning fra prEN 1992-1-1 og EN 1992-1-1.

Studien viste at fiberarmeringen hadde størst innvirkning på gjennomlokkingskapasiteten i henhold til revidert utgave av Eurokode 2. Skjærarmeringen hadde det nest største bidraget, selv om dette bidraget vil variere. Formålet med skjærarmeringen er å ivareta den manglende skjærkapasiteten, og dette vil avhenge av bidraget fra fiberarmeringen, forspenningen og den opptredende skjærkraften. Dermed vil denne verdien være forskjellig ut ifra de andre bidragene. Hvis bidraget f.eks. er tilstrekkelig høyt fra fiberen, vil den nødvendige mengden skjærarmering være lavere/ikke nødvendig, fordi det vil være en høyere kapasitet i platen til å motstå skjærkraften.

Videre viste studien at forspenningen påvirket kapasiteten relativt lite. Studien viste også at dimensjonerende gjennomlokkingskapasitet var lavere for EN-1992-1-1 sammenlignet med prEN 1992-1-1. Imidlertid gir den foreslåtte versjonen høyere skjærkraft på grunn av redusert kritisk kontrollsnitt.

Beregningsmetodene som presenteres i denne oppgaven er tiltenkt å bli lest i sammenheng med Eurokode 2 og det norske nasjonale tillegget. Det bemerkes her at den endelige versjonen av Eurokode 2 ikke var publisert ved utarbeidelsen av denne oppgaven, og leseren bør bekrefte numeriske verdier gitt i denne metoden med den endelige versjonen av Eurokoden og det norske nasjonale tillegget.

Contents

List of figures

List of tables

Notations

Latin Upper-Case Letters

A	Cross sectional area
A_c	Cross sectional area of concrete
A_s	Cross-sectional area of ordinary reinforcement
A_{sw}	Cross sectional area of shear reinforcement
D_{lower}	Smallest value of the sieve size of the coarsest fraction of aggregates permitted by the specification of concrete
V_{Rd}	Design Value of shear resistance
SCC	Self-consolidating concrete

Latin Lower-Case Letters

b_w	The minimum width of the cross-section between tension and compression chords
d	Effective depth of a cross-section
d_{dg}	Size parameter for describing the crack and the failure zone roughness taking account of concrete type and its aggregate properties
f_{cd}	Design value of concrete compressive strength
f_{ck}	Characteristic compressive cylinder strength of concrete in [MPa]
$f_{ck,cube}$	Characteristic compressive cube strength of concrete in [MPa]
f_{cm}	Mean concrete cylinder compressive strength at age t_{ref}
f_{ctm}	Mean axial tensile strength of concrete at age t_{ref}
f_{Ftuk}	Characteristic residual tensile strength
f_{ywd}	Design yield strength of shear reinforcement

Greek Letters

γ_c	Partial factor of safety for concrete
γ_{sf}	Partial factor of safety for SFRC
η_c	Strength reduction coefficient for shear resistance $\tau_{Rd,c}$
κ_O	Factor taking into account the orientation of the steel fibers in the concrete matrix in relation to the orientation of the principle longitudinal stress arising from the action effects
ρ	Reinforcement ratio
$\tau_{Rd,c}$	Shear stress resistance of members without shear reinforcement
$\tau_{Rdc,min}$	Minimum shear stress resistance
ϕ	Diameter of a reinforcing bar

Abbreviations

CMOD	Crack Mouth Opening Displacement
FRC	Fiber-reinforced Concrete
SFRC	Steel Fiber Reinforced Concrete

INTRODUCTION

2.1 Background

Reinforced concrete is the world's most widely used structural material, and it has maintained this position since the end of the nineteenth century.

Because reinforced concrete's tensile strength is limited and the compressive strength is excessive, prestressing becomes essential in many applications in order to fully utilize that compressive strength. Prestressing can either be done before or after the concrete is cast. If the prestressing is done after the concrete is cast, and as indicated by the name, it is called post-tensioning (G.Nawy, 2003).

Fiber-reinforced concrete is not a new concept, but there has been a lack of design guidelines, and today EN 1992-1-1 does not include guidelines for fiber-reinforced concrete, although the work with a new revision is under preparation. However, the Norwegian Concrete Society issued NB38 in 2019 which united the industry in the development of guidelines regarding fiber-reinforced concrete.

For the design of slabs, there are numerous structural solutions, depending on the loading, geometry, economic factors and maybe also the preference of the designer and the customer. A common way to design slabs is by using a slab that is directly supported by columns without beams. This solution is called flat slabs and can provide a flexible and good structural design with many advantages.

The critical failure mode for flat slabs is punching shear. This is a phenomenon in slabs that is caused by concentrated support reactions inducing a cone shaped perforation starting from the top surface of the slab. The design approach with respect to punching shear is in various codes based on empirical results and observations from reinforced concrete slabs supported on concrete columns (Ericsson, 2010).

The combination of fiber-reinforcement and post-tensioning in flat slabs can offer numerous advantages, and the following chapters presents the structural behavior, the critical areas in the slab that tends to exceed the punching shear limits, and different parameters that govern the punching shear resistance.

2.2 Scope of the study and limitations

The scope of this study was to investigate the punching shear resistance in post-tensioned flat slabs with fiber-reinforcement in accordance with prEN 1992-1-1. This also included a comparison between prEN 1992-1-1 and EN-1992-1-1. The thesis investigated many aspects of these subjects, however some delimitations existed:

- Openings and inserts were not included
- The thesis did not investigate flat slabs with drop panels

- The prestressing only included post-tensioned mono-strands (unbonded tendons)
- The fiber-reinforcement only included one type of steel fibers
- The load combinations only included distributed loads
- Different spans were not reviewed

2.3 Objectives

The objectives of this thesis are:

- Carry out a literature review on punching shear and the calculation models given in standards/codes
- To study punching shear resistance for different cases, including the calculation of punching shear resistance in the critical control sections for columns in the center of a slab, around slab edges and in the corners of the slab
- To study the influence of different parameters in calculation models on punching shear resistance using a parametric study

METHOD

2.4 Literature study

Initially, the thesis presents a literature study to increase knowledge and understanding about the theory behind the structural behavior in flat slabs. This includes background theory about prestressing, fiber-reinforcement, flat slabs, and punching shear failure.

2.5 Code requirements

In order to increase knowledge and understanding about the current and the proposed provisions in Eurocode 2 regarding punching shear, a review of the current and proposed version, including a comparison of them was performed. Throughout the thesis the proposed version is referred to as prEN 1992-1-1, and the current version as EN 1992-1-1. In addition, the American Building Code and FIB's model code was studied.

2.6 Parametric Study

A parametric study was performed in order to investigate and analyze the effect on the punching shear resistance in a flat slab with post-tensioning and fiber-reinforcement. The study was performed on a flat slab that included different cases of the critical control sections, as presented initially.

The calculations were done using Mathcad, as it provided a way to create a template that simplified the calculation procedure, and they were done in accordance with prEN 1992-1-1 and EN 1992-1-1 (including factors from the Norwegian National Annex). Thereafter these calculations were compared with results from analysis done in ADAPT and FEM-Design. It should be noted that neither ADAPT or FEM-Design have the possibilities to include the contribution from steel fiber-reinforcement, and therefore this contribution had to be investigated separately.

THEORETICAL BACKGROUND

3 Post-tensioning

3.1 Introduction

Concrete is strong in compression, but weak in tension. Due to this, flexural cracks develop at early stages of loading. To prevent or reduce such cracks from developing, an eccentric or concentric force is imposed. The force is imposed in the longitudinal direction of the structural element, and it prevents the cracks from developing by eliminating or reducing the tensile stresses at critical midspan and support sections at service load. This will increase the shear, bending and torsional capacities of the sections, and the sections are then able to behave elastically. Such an imposed longitudinal force is called a prestressing force (G.Nawy, 2003).

There are two main methods of prestressing: Pre-tensioning and post-tensioning. Pre-tensioning is, as the name implies, a tensioning of steel strands prior to the casting of the concrete. Post-tensioning is a tensioning operation that occur after the concrete is cast. Prestress may also be imposed on new or existing members using external tendons. These systems are useful for temporary pre-stressing operations (Ranzi, 2018). Pre-tensioning and external prestressing will not be discussed further in this study.

3.2 General

Post-tensioning of concrete is used in a wide range of structures to apply prestress, and the method offers significant flexibility in the way the prestress is applied to a structure, with the tendon profiles fit to the support conditions and loading (Ranzi, 2018).

The primary advantages of post-tensioning slabs over conventional reinforced concrete slabs are

- Thinner slabs
- Increased clear spans
- Reduced cracking
- Reduced deflection
- Lighter structure; reduced dead load
- Better water resistance
- Rapid construction
- Reduced storey height
- Large reduction of conventional reinforcement

(The concrete society , 2005)

3.3 Bonded and unbonded systems

Post-tensioned slabs can be constructed using either unbonded or bonded tendons, and the two techniques offers different advantages and disadvantages, and are therefore subjects to debate (The concrete society , 2005).

3.3.1 Unbonded system

In an unbonded system the strands are encapsulated in a polyurethane sheath, and the voids between the sheath and the strands are filled with grease.
The main features of a unbonded system are

- The tendons are flexible, can be curved easily in the horizontal direction to accommodate curved buildings, and divert around openings in the slab
- Tendons can be replaced
- The tendons can be prefabricated off site
- The ultimate flexural capacity is less with unbonded tendons than with bonded, but much greater deflections will take place before yielding of the steel
- The friction loss is lower than for bonded tendons due to the action of the grease
- Attention is required in design to ensure against progressive collapse
- A broken tendon causes prestress to be lost for full tendon length
- The tendon can be prefabricated off site and the installation process can be quicker due to the prefabrication and reduced site operations
- The smaller tendon diameter and reduced cover requirements allow the eccentricity from the neutral axis to be increased
  (The concrete society , 2005)

3.3.2 Bonded system

In a bonded post-tensioning system, the strands are installed in a galvanized steel or plastic duct and once the strands have been stressed, the voids around the strands are filled with grout.

The main features of a bonded system are:

- The prestressing tendons can contribute to the shear capacity in the concrete
- Less reliance on the anchorages once the duct has been grouted
- Accidental damage to a tendon results in a local loss of prestress force only
- The full strength of the strand can be utilized at the ULS and hence there is generally a lower requirement for the use of unstressed reinforcement
- A high force can be applied to a small concrete section due to the concentrated arrangement of strands within the duct

(The concrete society , 2005)

3.3.3 Comparison: Bonded and unbonded system

There are advantages and disadvantages of bonded and unbonded systems, and the use of either is dependent on the design and construction requirements. Durability is an important consideration for all forms of construction, and the provision of active corrosion protection is therefore of significant importance. By grouting the tendons, an alkaline environment is provided around the steel, and this provides active corrosion protection (Ranzi, 2018).

A bonded system ensures that any change in strain at the tendon level is the same in the tendon and the surrounding concrete. When a concrete member deforms and the strain at the tendon level increases, the full capacity of the bonded tendon can be utilized, and the ultimate capacity of the cross-section can be increased substantially by grouting. Furthermore, a bonded system will be better than unbonded tendons for controlling cracking and resisting progressive collapse, if local failure should occur (Ranzi, 2018).

In an unbonded system the prestressing forces can, with appropriate design consideration, theoretically be adjusted throughout the life of the structure. Tendons may be able to be inspected, re-stressed or replaced (Ranzi, 2018).

Unbonded tensons are often used in flat slabs. Because this is a construction method that is more simple without grouting, it enables this to be a more favorable solution in the economic aspect (Sørensen, 2013).

3.4 Prestressed concrete

The deformation of a prestressed concrete member throughout the full range of loading depends on the behavior and loading of the materials. In order to satisfy the design objective of adequate structural strength, material strength, non-linear behavior and factors affecting these must be considered (Ranzi, 2018). The following subsections highlights the structural behavior and properties related to prestressed concrete.

3.4.1 Concrete

Concrete, particularly high-strength concrete, is a major constituent of all prestressed elements, and hence its long-term endurance and strength have to be achieved through proper quality assurance and quality control in the production stage (G.Nawy, 2003).

3.4.1.1 Quality-affecting parameters

Endurance and strength are two major qualities that are important in prestressed concrete structures, and long-term detrimental effects can rapidly reduce the prestressing force. This could result in unexpected failure, and therefore measures have to be taken to ensure

quality control and assurance at the different stages of production, construction, and maintenance (G.Nawy, 2003).

3.4.1.2 Properties of hardened concrete

The mechanical properties of hardened concrete can be classified in short-term and long-term properties. The short-term properties are strength in compression, tension, shear, and stiffness, and the long-term properties can be classified in terms of creep and shrinkage (G.Nawy, 2003).

3.4.1.3 Compressive strength

The strength of concrete is specified in NS-EN 1992-1-1 in terms of strength classes. These classes relate to the lower characteristic compressive strength at 28 days measured on cylinders f_{ck} or on cubes $f_{ck,cube}$.

3.4.1.4 Tensile strength

The tensile strength of concrete is low compared to the compressive strength. The uniaxial tensile strength of concrete is also defined in NS-EN 1990-1-1 as the maximum stress that the concrete can withstand when subjected to concentric uniaxial tension (Ranzi, 2018)

3.4.1.5 Shear strength

Shear strength is more difficult to determine experimentally, due the difficulty of isolating shear from other stresses. This is one of the reasons why there is a large variation in the literature on shear-strength values, varying from 20 percent of the compressive strength in normal loading up to 85 percent of the compressive strength in cases where direct shear exists in combination with compression (G.Nawy, 2003).

3.5 Structural behavior

3.5.1 Effects of prestress

The primary effects of prestress are axial pre-compression of the slab, and an upward load within the span. This upward load balances part of the downward dead and live loads and cause a transverse effect that carries the load directly to the supports. For the remaining load the slab will have an increased resistance to torsion, shear and punching due to the compressive stresses from the axial effect (Ranzi, 2018).

3.5.2 Load balancing and equivalent loads

For a general tendon profile in the x-y plane

Tendon profile $$y = f(x)$$

Tendon-angle $$\theta(x) \approx tan\theta(x) = \frac{dy}{dx}$$

Equivalent load along dx $$q = q(x)$$

Approx. equilibrium in y-direction $$q(x) \cdot dx \approx Pd\theta$$

The equivalent load in the y-direction then becomes:

$$q(x) = P \cdot \frac{d\theta}{dx} = P \cdot \frac{d^2y}{dx^2} \quad (3.0)$$

(Sørensen, 2013)

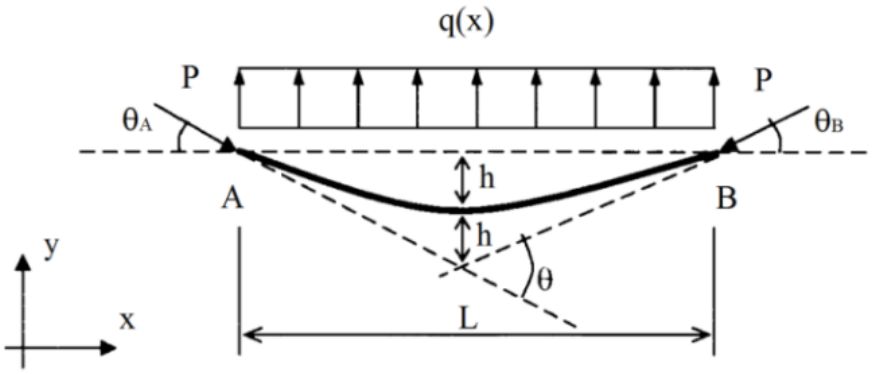

Figure 1 Parabolic tendon (Sørensen 2013)

3.5.3 Parabolic tendon profile and load-balancing distributed

For post-tensioning with non-straight prestressing tendons, a useful approach in the design is load balancing. This is a technique based on utilizing the vertical force of the draped or harped prestressing tendon to counteract or balance the imposed gravity loading (G.Nawy, 2003).

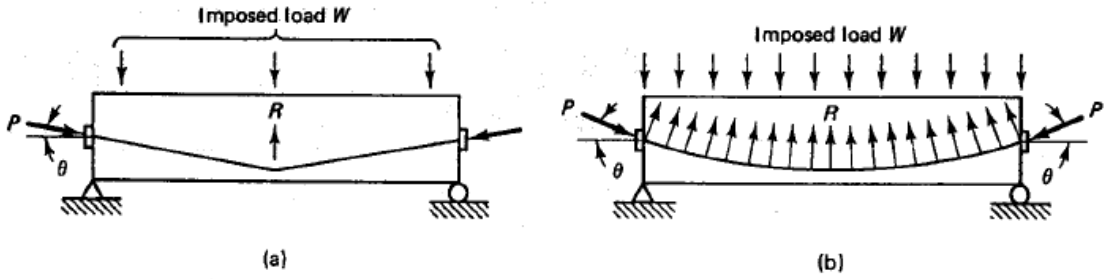

Figure 2 Load balancing forces a) Harped tendon b) Draped tendon (G.Nawy, 2003)

For a parabolic tendon shown under in Figure 3, the tendon drape can be expressed with the parabolic function:

$$y = ax^2 + bx + c \quad (3.0)$$

$$\frac{dy}{dx} = 2ax + b$$

$$\frac{d^2y}{dx} = 2a$$

When: $x = 0$ $y = c = 0$

When: $x = \frac{L}{2}$ $y = -e$ $-e = a \cdot \left(\frac{L}{2}\right)^2 + b \cdot \frac{L}{2} = a \cdot \frac{L^2}{4} + b \cdot \frac{L}{2}$

When: $x = \frac{L}{2}$ $\frac{dy}{dx} = 0$ $0 = 2a \cdot \frac{L}{2} + b = a \cdot L + b$ $b = -a \cdot L$

Substituting b into -e:

$$-e = a \cdot \frac{L^2}{4} + b \cdot \frac{L}{2}$$

$$-e = a \cdot \frac{L^2}{4} + -a \cdot L \cdot \frac{L}{2}$$

$$-e = a \cdot \frac{L^2}{4} + -a\frac{L^2}{2}$$

$$-e = a \cdot \frac{L^2}{4} - a\frac{L^2}{2}$$

$$-e = -a \cdot \frac{L^2}{4}$$

$$e = a \cdot \frac{L^2}{4}$$

$$a = \frac{4e}{L^2}$$

Substituting a into b:

$$b = -a \cdot L$$

$$b = -\left(\frac{4e}{L^2}\right) \cdot L$$

$$b = -\frac{4e}{L^2} \cdot L$$

$$b = -\frac{4e}{L}$$

Substituting a and b into the function of y:

$$y = ax^2 + bx + c$$

$$y = \frac{4e}{L^2}x^2 + -\frac{4e}{L}x + 0$$

$$y = \frac{4e}{L^2}x^2 - \frac{4e}{L}x$$

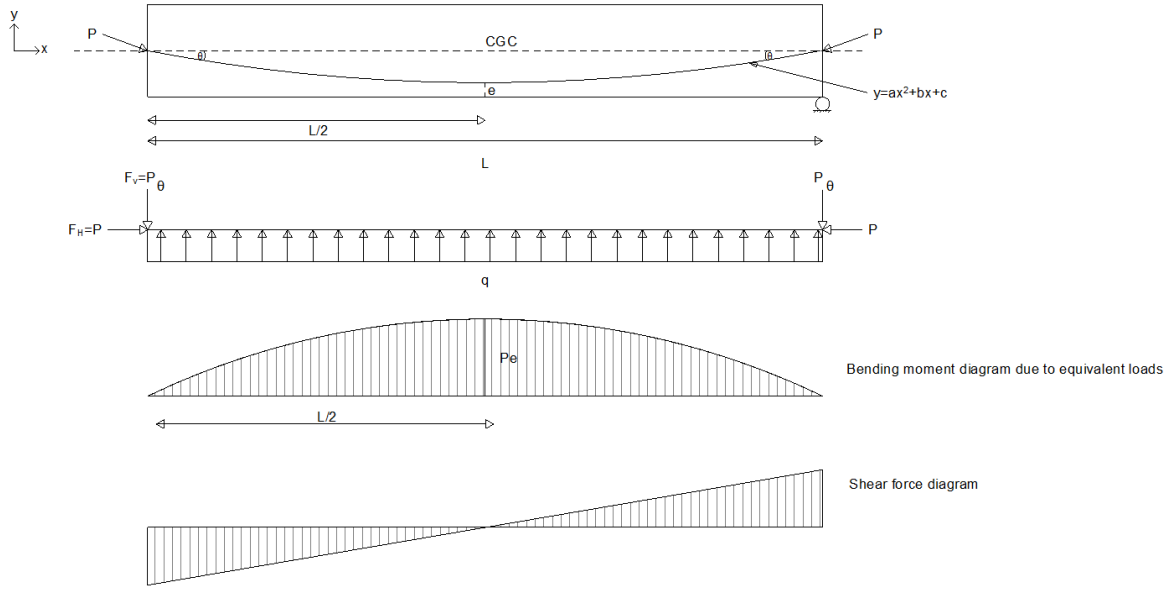

Figure 3 Parabolic tendon profile

Equation 3.1 provides the equivalent load for the parabolic tendon-profile

$$q(x) = P \cdot \frac{d^2y}{dx^2} = P \cdot 2a = constant \tag{3.1}$$

Finding $\frac{d^2y}{dx^2}$ in equation 3.1 and substituting into equation 3.2 yields

$$q(x) = P \cdot \frac{d^2y}{dx^2} = P \cdot 2a = P \cdot 2\frac{4e}{L^2} = \frac{8Pe}{L^2}$$

$$q = \frac{8Pe}{L^2} \tag{3.2}$$

3.6 Post-tensioned pre-stressed concrete structures

3.6.1 Slab thickness

The slab thickness must meet two primary functional requirements: deflection and structural strength. In addition, vibration should also be considered. The selection of type or thickness is also influenced by loading and concrete strength. There are likely several alternative solutions to the same problem, and a preliminary costing exercise may be necessary in order to choose the most beneficial solution in terms of economic aspects (Ranzi, 2018).

3.6.2 Tendon layout and post-tensioned flat slab behavior

Tests and applications have shown that a post-tensioned flat slab behaves as a flat plate almost regardless of tendon arrangement. However, the effects of the tendons are critical to the behavior as they exert loads on the slab as well as provide reinforcement (The concrete society , 2005).

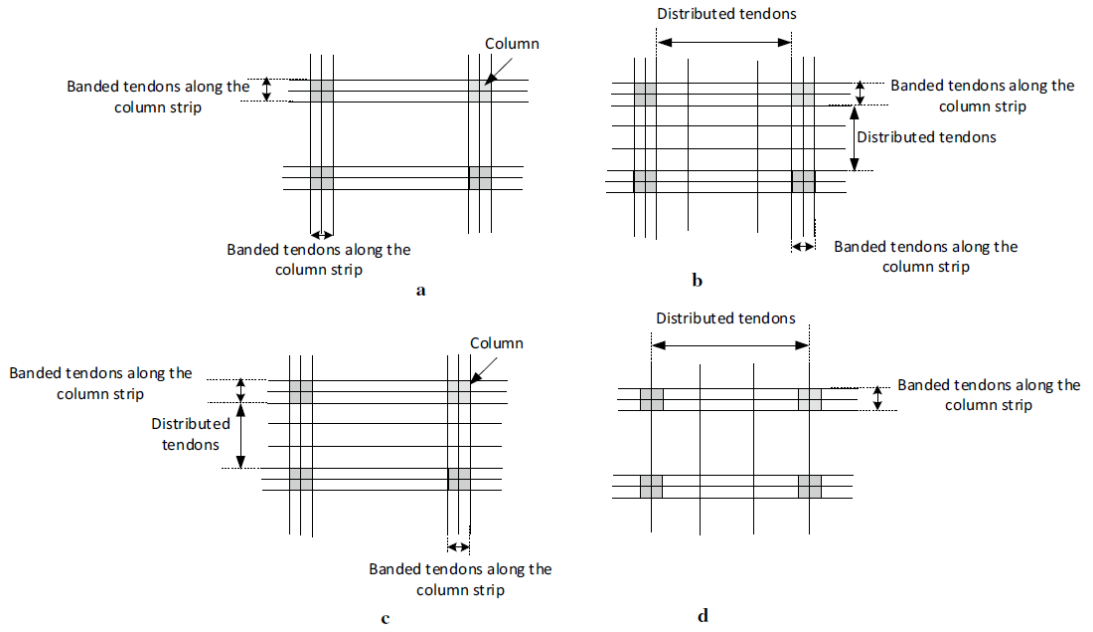

Figure 4 Different tendon layouts (Sørensen 2013)

3.7 Shear- moment transfer to columns supporting PT flat slabs

The shear behavior of flat slabs is a three-dimensional stress problem, where the critical shear failure plane follows the perimeter of the loaded area. This area is located at a distance that gives a minimum shear perimeter (G.Nawy, 2003).

3.7.1 Shear moment transfer

The unbalanced moment at the column face support is one of the more critical design considerations in proportioning a flat slab. To ensure an adequate shear strength it requires a moment transfer to the column by flexure across the perimeter of the column and by eccentric shearing stress such that approximately 60% is transferred by flexure and 40% by shear (G.Nawy, 2003).

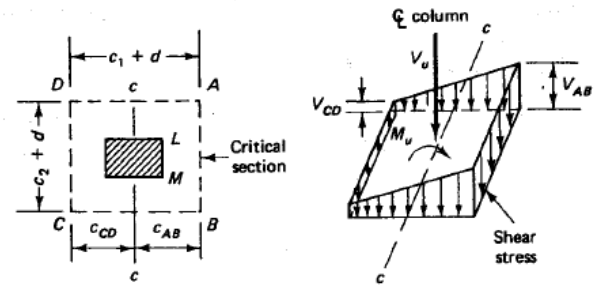

Figure 5 Shear stress distribution around interior column edge (G.Nawy, 2003)

3.7.2 Consideration of prestressing

Prestressing has three potential influences on the shear strength:

- The vertical component of the prestressing force related to the longitudinal axis. This effect can be accounted for by considering prestressing as an external action
- The horizontal component influencing the normal force N_E

- The eccentricity of the tendon, influencing the reinforcement force and thus the shear strength. This effect can be accounted for by considering prestressing as an external action and thus influencing the bending moment at the control section (Aurelio Muttoni A. P., 2018).

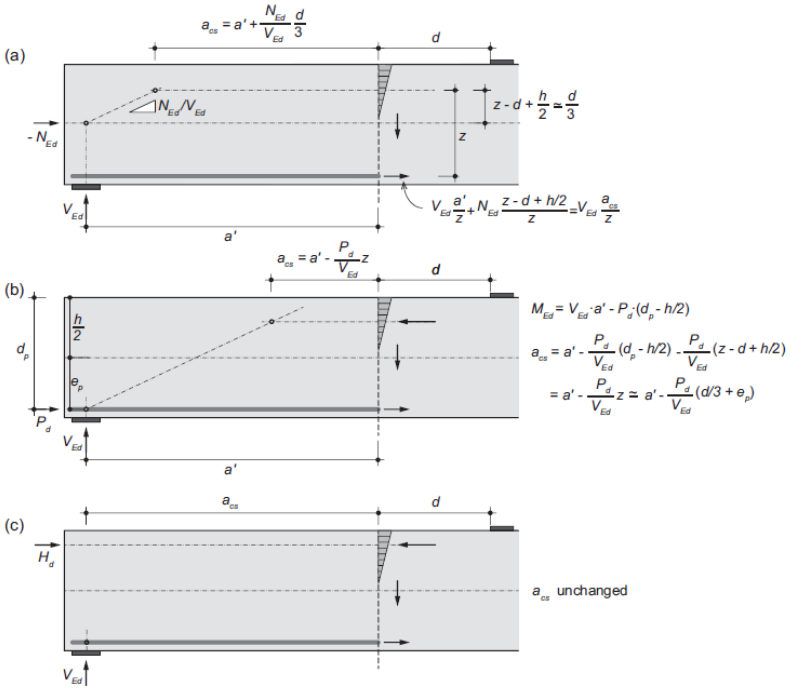

Figure 6 Equilibrium of internal forces: members subjected to (a) centered axial force; (b) prestressing force on the tension side c) prestressing force on the compression side (Aurelio Muttoni A. P., 2018).

4 Fiber-reinforced concrete

4.1 Introduction

Fiber-reinforced concrete extends the versatility of concrete as a construction material and offers a potential to simplify the construction process. In addition, it has also been shown that fiber-reinforced concrete can be used in combination with low reinforcement ratios, and that the amount of conventional reinforcement could be reduced to half of the conventional reinforced concrete, but still lead to improved structural performance (Löfgren, 2005).

4.2 General

Fiber-reinforcement is not a new concept and has been around since 1874. It can be described as concrete containing hydraulic cement, water, fine and coarse aggregate and discontinuous discrete fibers (Löfgren, 2005).

Extensive research and development in recent years has provided new insight into difficulties and opportunities associated with the use of fiber as reinforcement in concrete structure. For example, fiber-reinforcement in SCC has in practice showed greater loadbearing capacity than corresponding structural elements from ordinary vibrated concrete (Löfgren, 2005).

An important factor regarding fiber-reinforced concrete is that cross-sections exposed to moment and/or axial force with fiber-reinforcement alone have significantly poorer ductility than traditional reinforced cross-sections. It is therefore required to supplement with conventional reinforcement or prestressing reinforcement which can transmit the tensile forces from moments and axial forces (Kanstad, 2020).

4.3 Types of fiber

There are several different types of fibers that are used to improve the properties of concrete and cementitious composites, i.e. the ductility or toughness. Fibers are produced in different sizes and shapes, and produced by either steel, synthetics, glass, or natural materials (Löfgren, 2005). Today, steel fiber is most used. However, the use of different composite fiber with documented properties and technical approval is increasing.

All fibers used in concrete must be tested and documented. Requirements for documentation and declaration from the fiber producer must be in accordance with the following standards

- NS-EN 14889-1 Fiber for Betong – Del 1: Stålfibere – Definisjonskrav, krav og samsvar
- NS-EN 14889-2 Fiber for Betong – Del 2: Definisjon, krav og samsvar

(Kanstad, 2020)

4.4 Fiber geometry and fiber orientation

The geometry of individual fibers varies, and the cross-section can be circular, quadratic, rectangular, triangular, flat, or polygonal (Löfgren, 2005).

The orientation of the fibers plays an important role for the mechanical performance of fiber-reinforced concrete. Casting method, equipment, geometry of the cross-section and the properties of the concrete are factors that influence the orientation and distribution of the fiber-reinforcement in the concrete (Døssland, 2008).

Through several experiments, it has been verified that the fiber-reinforcement tends to orient itself perpendicular to the flow direction of the SCC. For solid concrete structures, the fiber orientation is mainly spatially oriented (approximately isotropic). The fiber tends to orient itself parallel to the cast, which leads to a more 2-dimensional fiber orientation for constructions with small thickness in relation to the fiber length, i.e. plates and walls. The same effect will cause the fiber to orient in a longitudinal direction for small beams and column cross-sections (Kanstad, 2020).

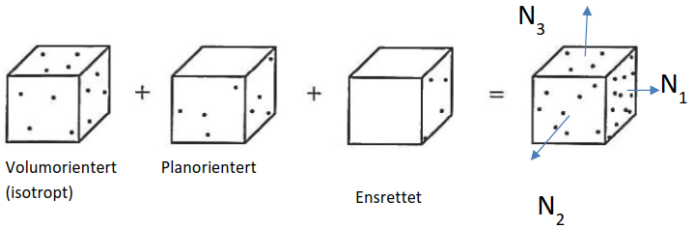

Figure 7 Combinations of fiber orientation (Kanstad, 2020)

If the fiber is oriented and distributed as intended, acceptable safety of load-bearing structures can be achieved with supplement of ordinary reinforcement, or in certain cases without ordinary reinforcement. This distribution can only be achieved by accurate execution and control. Therefore concrete mixing, transport and casting requires extended control according to NS-EN 13670, supplemented by requirement from NB38 (Kanstad, 2020).

4.5 Material properties

4.5.1 Behavior in compression

Generally, the compressive relations that are valid for plain concrete also apply to FRC (fib, Model Code Volume 1, 2010).

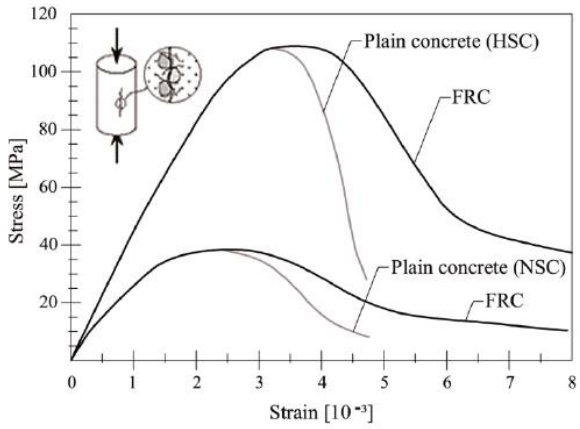

Figure 8 Main differences between plain and fiber-reinforced concrete having both normal and high strength under uniaxial compression (fib, Model Code Volume 1, 2010)

4.5.2 Behavior in tension

Fibers are active as soon as micro-cracks are formed in the concrete. The main advantage of adding fibers to concrete is that they generate a post-cracking residual tensile strength in combination with a large tensile strain. Due to this, the fiber-reinforced concrete is characterized by substantial ductility and toughness (fib, Model Code Volume 1, 2010).

With regard to the behavior in tension, various test methods are possible. Bending tests can be carried out aiming at determining the load-deflection relation, and the results can be used for deriving the stress-crack width relations by inverse analysis, performing equilibrium calculations for numerous crack openings (fib, Model Code Volume 1, 2010). This is shown in Figure 9.

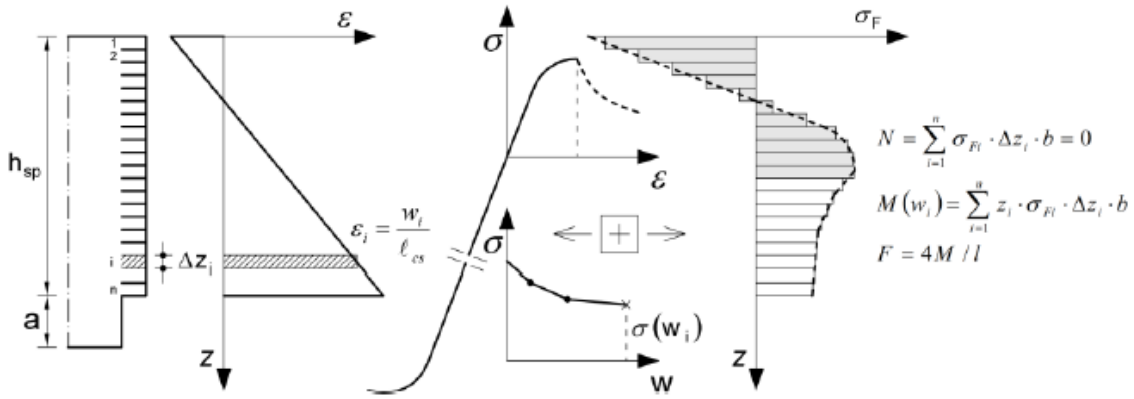

Figure 9 Inverse analysis of beam in bending performed to obtain stress-crack opening relation (fib, Model Code Volume 1, 2010)

Nominal values of the material properties can be determined by performing a 3-point bending test according to EN 14651. The diagram of the applied force versus the deformation shall be produced. The deformation is generally expressed in terms of Crack Mouth Opening Displacement (fib, Model Code Volume 1, 2010).

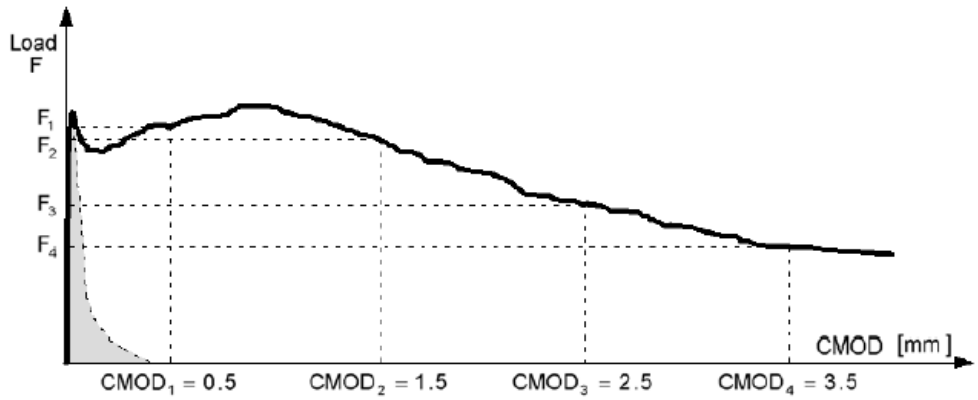

Figure 10 Typical load F - CMOD curve for plain concrete and FRC (fib, Model Code Volume 1, 2010)

4.5.3 Residual tensile strength ($f_{R,i}$) – testing

The residual tensile strength for fiber-reinforced concrete is a material parameter that is determined from the bending moment in standardized test-beams at given crack-widths in the bottom of a beam under the assumption of linear stress distribution over the cross-

section height. This does not match the actual stress distribution after cracking, and due to this, the parameter is often characterized as a fictive strength and is not used direct when designing.

FRC should have a relatively stable residual tensile strength with increasing crack width. This residual tensile strength can be greater or less than the tensile strength of the concrete, depending on factors such as the amount of fiber and the tensile strength of the fiber (Kanstad, 2020).

The provision of residual tensile strength shall be in accordance with NS-EN 14651, and can be determined from measured load or moment at given deflection for standard beam-test

$$f_{R,i} = 6M_{Ri}/bh^2 \quad (4.0)$$

where $M_{Ri} = f_{R,i} \cdot L/4$

Here, linear stress distribution over the cross section is used, or modulus of section for uncracked cross-section. Because it is easier to measure the deflection rather than the crack opening, NS-EN gives the following expression for the interaction between the two

CMOD=(δ-0,04)/0,85

Characteristic values are thereafter determined as

$$f_{Rk,i} = f_{Rk,i} - k \cdot s \quad (4.1)$$

where

s is the standard deviation from the testing

k=1,7 when the testing method is according to NB38 section 2.5.3

The following strength parameters will be known from the testing:

$F_{ct,L}f_{ctk,L}$ = mean and characteristic residual tensile strength at first cracking or at crack width = 0,05mm at hardening behavior

$f_{R,1}f_{Rk,1}$ = mean and characteristic residual tensile strength at 0,5mm crack width

$f_{R,2}f_{Rk,2}$ = mean and characteristic residual tensile strength at 1,5mm crack width

$f_{R,3}f_{Rk,3}$ = mean and characteristic residual tensile strength at 2,5mm crack width

$f_{R,4}f_{Rk,4}$ = mean and characteristic residual tensile strength at 3,5mm crack width

The characteristic values $f_{Rk,1}$ and $f_{Rk,3}$ is used to classify the residual tensile strength class in accordance with NB 38 chapter 2 (Kanstad, 2020).

4.5.4 Residual tensile strength ($f_{R,i}$) – theoretical values

The uniaxial effective characteristic value for residual tensile strength with a given volume for fiber can be decided theoretical in combination with the given concrete. This is given by

$$F_{Ftu,ef} = \eta_0 \, v_f \, \sigma_{fk,mid}$$

where

v_f =volume of fiber

$\sigma_{fk,mid}$ = Characteristic value for mean stress in all fibers crossing the crack in random directions. This parameter is strongly dependent of fiber type and concrete quality and must be determined from relevant tests.

η_0 =Capacity factor

(Kanstad, 2020)

4.5.5 Classification

To classify the post-cracking strength of fiber-reinforced concrete, a linear elastic behavior can be assumed. This is done by considering the characteristic flexural residual strength values that are significant for serviceability ($f_{Rk,1}$) and ultimate ($f_{Rk,1}$) conditions (fib, Model Code Volume 1, 2010).

The strength interval is defined by two subsequent numbers, given in Mpa, thereafter, letters correspond to the residual strength ratios. The designer has to specify the residual strength class and the f_{R3k}/f_{R1k} as well as the material of the fiber (fib, Model Code Volume 1, 2010)

Strength internals:

1.0, 1.5, 2.0, 2.5, 3.0, 4.0, 5.0, 6.0, 7.0, 8.0, … [MPa]

A	$0,5 \leq F_{R3K}/F_{R1K} < 0,7$
B	$0,7 \leq f_{R3k}/f_{R1k} < 0,9$
C	$0,9 \leq f_{R3k}/f_{R1k} < 1,1$
D	$1,1 \leq f_{R3k}/f_{R1k} < 1,3$
E	$1,3 \leq f_{R3k}/f_{R1k}$

Table 1 Residual strength ratios (fib, Model Code Volume 1, 2010)

4.6 Shear properties of FCR

According to (Löfgren, 2005) the principal action responsible for transferring shear stresses across a crack in plain concrete is often explained as aggregate interlock and friction at the crack faces. For FRC at low and moderate fiber dosages the cracking strength is not affected, but as soon as the matrix cracks, the fibers are activated and starts to be pulled out. This results in a significant tougher behavior.

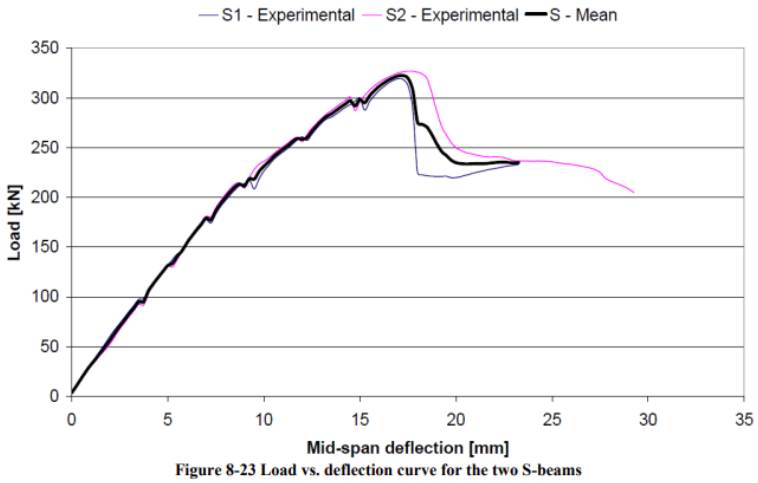

Figure 8-23 Load vs. deflection curve for the two S-beams

Figure 11 Load VS deflection curve (Sandbakk, 2011)

Figure 11 shows the load vs deflection curve for two beams with FRC tested for shear failure. Here, the largest shear force V_E was 161,5kN, and the calculated shear resistance without the fiber contribution was 48,8kN. This means that the fiber contribution was about 70% for the shear resistance. However, it should be noted that shear resistance for plane concrete is encumbered with uncertainty (Sandbakk, 2011).

4.7 Calculation method according to NB38

According to NB38, residual strength class may be determined by finding the moment or the design shear force, and thereafter turn the formula to find the dimensioning residual tensile strength.

Finding the design residual tensile strength based on the design moment

$$f_{Ftud} = \frac{M_{Ed}}{0.4 \cdot b \cdot h^2} \tag{4.2}$$

Where b is the width of cross section

h is the height of the cross section

Design residual tensile strength based on the design shear force is given by

$$f_{Ftud} = \frac{\tau_{Ed} - \eta_c \cdot \tau_{Rdc}}{\eta_F} \tag{4.3}$$

The residual tensile strength can be replaced with

$$f_{Ftud} = \frac{f_{Ftu,ef}}{\gamma_{SF}} \tag{4.4}$$

Where γ_{SF} is the material factor based on whether the fiber is determined from test data with or by testing according to NS-EN.

The effective residual tensile strength is given by

$$f_{Ftu,ef} = f_{Ftsk} \cdot k_0 \quad (4.5a)$$

$$f_{Fts,ef} = f_{Ftuk} \cdot k_0 \quad (4.5b)$$

Where k_0 is the fiber orientation factor

Characteristic residual tensile strength in ULS and SLS

$$f_{Ftuk} = f_{R.3kbe} \cdot 0.37 \quad (4.6a)$$

$$f_{Ftsk} = f_{R.1kbe} \cdot 0.45 \quad (4.6b)$$

Both equations are based on two different tension distributions, where f_{Ftuk} is based on a linear elastic behavior of $f_{R.3k}$, while f_{Ftsk} is based on a constant stress distribution in the tensile zone (Kanstad, 2020).

$$f_{R.3kbe} = min(f_{R.3k,} 0.6 \cdot f_{R.3m}) \quad (4.7a)$$

$$f_{R.1kbe} = min(f_{R.1k,} 0.6 \cdot f_{R.1m}) \quad (4.7b)$$

Where $f_{R.3k}$ and $f_{R.1k}$ are the residual flexural tensile strength

$f_{R.3m}$ and $f_{R.1m}$ are the mean values based on the residual strength class and test results.

To avoid favorable results from bending tests, an upper limit for characteristic residual tensile strength is set to 60%, although an average coefficient of variation from 15-30% can be expected from the beam test (Kanstad, 2020).

4.8 Fiber content and documentation

The concrete manufacturer shall document the residual strength class and ductility class. The residual flexural strength is determined as a characteristic value based on a minimum of 6 test pieces per fiber quantity. Each result will be reported as mean values, standard deviation and as a characteristic value. This can be done in two ways: Either by testing the actual concrete and fiber intended for the given project, where the concrete is manufactured at the factory and the fiber is added according to procedure.

Alternatively, documentation can be based on experimental data and results from concrete with same strength and amount of fiber, but different raw materials/additives and production equipment. This means that the specified concrete class may not necessarily be “valid”, as the concrete can achieve higher strength class. For example, if the concrete meets requirement of B45, then it is treated accordingly (Kanstad, 2020).

The following figure shows an example of determinating the necessary fiber content to obtain specified characteristic residual flexural tensile strength by interpolation between documented test results (Kanstad, 2020).

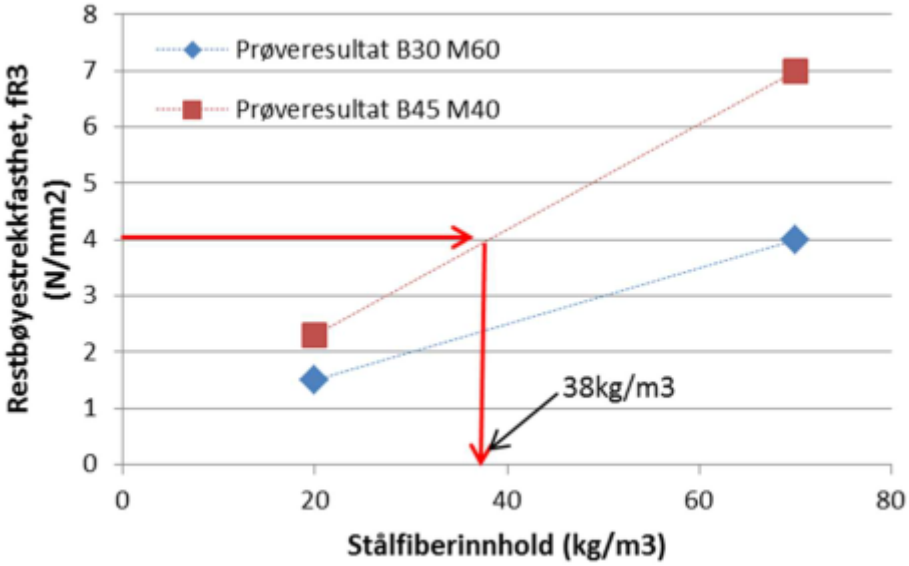

Figure 12 Residual tensile strength and steel fiber content (Kanstad, 2020)

5 Punching shear in flat slabs

5.1 General

Punching shear resistance of prestressed slabs with fiber reinforcement depends not only on effects of particular factors, such as concrete strength, trajectory of tendons, slab dimensions or fiber volume, but also on their cross-interaction (Long Nguyen-Mihn, 2012).

Punching shear can result from a concentrated load applied on a relatively small area of the structure, and in flat slabs punching shear failures normally develop around supported areas such as columns, capitals, or walls. In other cases, as for instance foundation slabs, transfer slabs or deck slabs of bridges, punching failures can also develop around loaded areas (fib, Model Code Volume 2, 2010).

Current formulas for punching shear resistance of post-tensioned flat slabs are based on empirical approach and the punching shear capacity of slabs is calculated as the sum of the punching shear resistance of conventional steel reinforced concrete flat slab and of the resistance contribution of prestressing (Long Nguyen-Mihn, 2012).

5.2 One-way shear and two-way shear

In the design of slabs, the strength in shear frequently controls the thickness of a member, especially in the vicinity of a concentrated load or column. Shear failure may occur on one of two different types of failure surfaces: One-way shear (beam-type shear) and two-way shear (punching shear). A slab that experience beam-type shear acts as a wide beam, and the shear failure occurs across the entire width of the member. This is illustrated in Figure 13a). The critical section for this type of shear failure is usually assumed to be located at a distance d from the face of the column. This type of shear is often critical for footings, but rarely cause concern in the design of floor slabs (Ranzi, 2018).

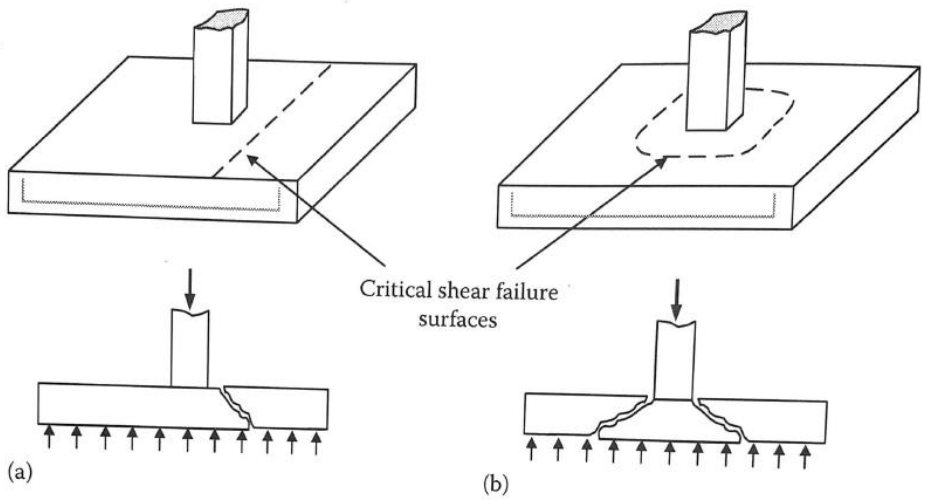

Figure 13 Types of shear failure. a) Beam-type shear b) Punching shear (Ranzi, 2018)

The other type of shear failure may occur in the vicinity of a concentrated load or column, and the failure may occur on a surface that forms a truncated cone or pyramid. This type of failure is called punching shear and is illustrated in Figure 13b). The critical section for punching shear failure is assumed to be perpendicular to the plane of the slab.

6 Shear and moment transfer at column-slab connections

6.1 The Strip Model

The Strip Model for slab punching shear describes an internal distribution for the transfer of vertical load between a two-way slab and a column and may be considered an extension of the Strip Method of Design. The Strip Method allows a designer to define a load distribution that rigorously satisfies equilibrium at all points in a slab and to reinforce the slab for the bending moments (that are the consequence of that load distribution).

The Strip Model divides the slab into radial strips and plate quadrants. This is shown in Figure 14 under.

No load can reach the column without passing through one of the radial strips, and within each strip, shear is carried to the column by arching action. This is illustrated as a curved arch, with maximum slope at the face of the column. The quadrants of a two-way slab are fundamentally slender flexural elements. This means that the shear transfer across the boundary between a strip and its adjacent quadrant of plate is through the two-plate equivalent of beam action.

(Carlos E.Ospina, 2017)

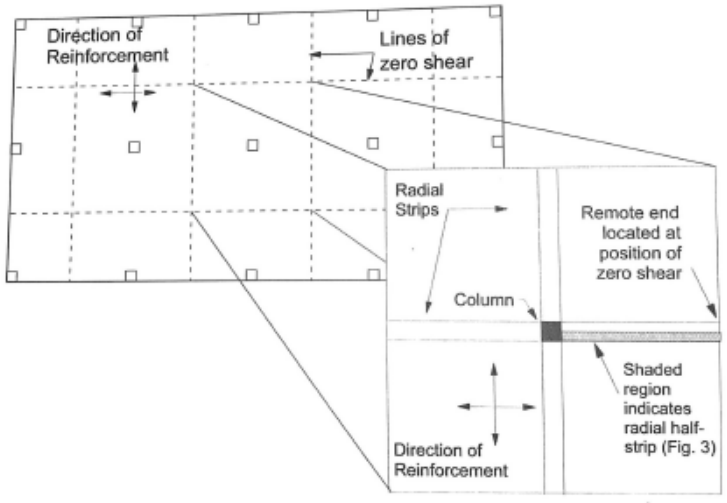

Figure 14 Geometry of Strip Model (Carlos E.Ospina, 2017)

6.2 Critical shear crack theory

The Critical Shear Crack Theory for shear was first developed in the 1980's as a model for calculating the shear strength of planar members. The theory was aimed at one-way slabs and beams without transverse reinforcement and to two-way slabs supported on columns.

The Critical Shear Crack Theory is based on the assumption that the shear strength is governed by the development of a critical shear crack that disturbs the shear transfer actions and thus limits the strength of the member.

In a slender one-way member without transverse reinforcement, the critical shear crack first opens for low load levels. This is followed by a combined opening and sliding of the crack as soon the crack develops with a lower inclination towards the load introduction region. Such sliding is important to activate aggregate interlocking and to transfer shear forces across the critical shear crack.

The comparison between the measured crack kinematics and similar displacement paths representing loss of aggregate interlocking shows that before failure, the shear force can be carried across the critical shear crack only in some regions. From this simple observation it can be inferred that the shear capacity of a cracked member depends upon the position of the critical shear crack with respect to the theoretical strut carrying shear, the opening of the critical shear crack and the roughness of the crack.

(Aurelio Muttoni A. P., 2018)

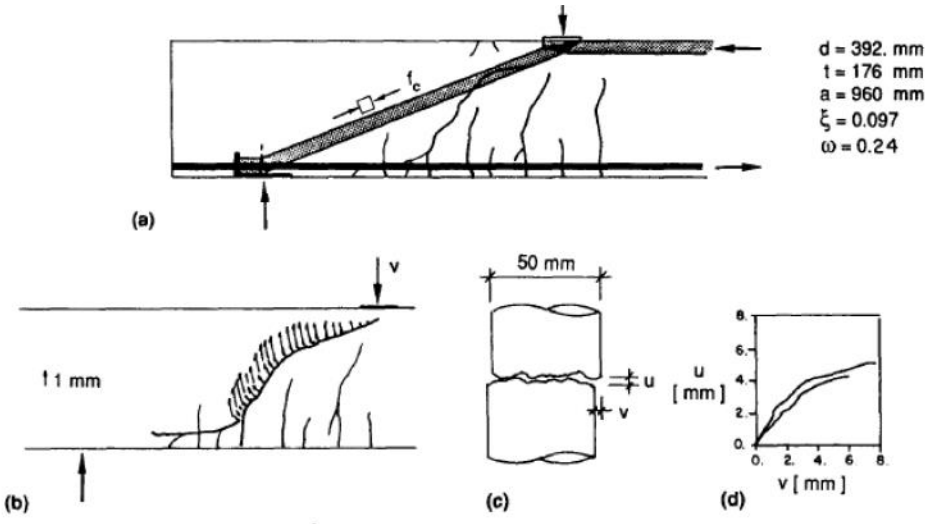

Figure 15 a) Observed crack pattern in a shear test with a/d = 2.45 and theoretical strut representing arching actions; b) measured crack kinematics c) and d) crack kinematics in a concrete element in case of loss of aggregate interlock (Aurelio Muttoni A. P., 2018)

6.2.1 Slabs without transverse reinforcement

Two-way slabs develop first cracking associated to radial bending moments in the supported area. This cracking is followed by the development of radial cracks associated to tangential bending moments. Due to the presence of shear forces, tangential cracks develop in an inclined manner and may disturb the inclined compression struts carrying shear (Aurelio Muttoni A. P., 2018).

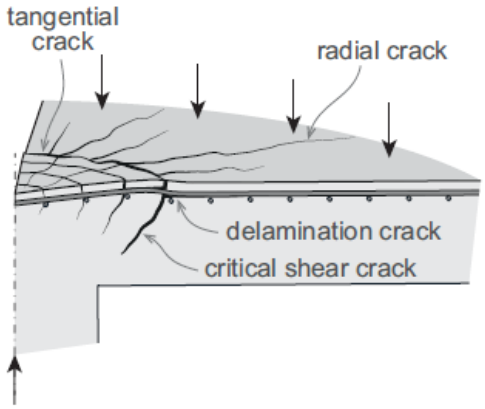

Figure 16 Cracking development in a slab-column connection (Aurelio Muttoni A. P., 2018)

6.3 Slabs supported on interior columns

The structural response of reinforced concrete slabs supported on interior columns was investigated experimentally by Kinnunen and Nylander. Here, test specimens consisting of circular slab portions supported on circular columns were placed in the center and loaded along the circumference. Kinnunen and Nylander observed two main failure modes: yielding of the flexural reinforcement at small reinforcement ratios (failure in bending) and failure of the slab along a conical crack within which a concrete plug was punched (Ericsson, 2010).

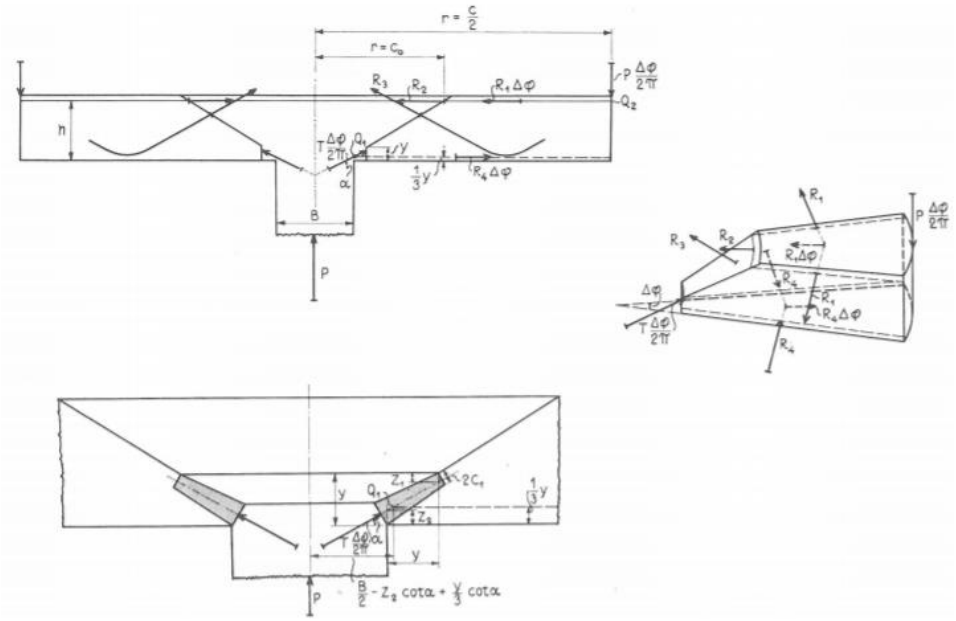

Figure 17 Mechanical model of Kinnunen and Nylander (Ericsson, 2010)

Initially tangential cracks (flexural cracks) were encountered on the top surface of the slab above the column, due to the hogging moments. Crack propagation continued with the formation of radial cracks starting from the tangential cracks.

Thereafter additional tangential cracks were formed outside the circumference of the column, and after further loading the latter tangential cracks deviated from their original vertical direction into an inclined course towards the column face on the bottom surface of the slab.

With the increase of vertical displacements, the cracking extended to the edge of the column. Finally, the shear crack either coincided with or was located outside the outermost tangential crack that was observed before failure.

Based on their experiments, Kinnunen and Nylander developed a model describing the punching mechanism. This is illustrated in Figure 17, where the slab is divided in several parts bounded by the propagated shear cracks and the radial cracks. From the column to the bottom of the shear crack, an imaginary compressed conical shell is developed that carries the outer portion of the slab. During the tests they discovered that the outer portion could be regarded as a rigid body because it behaved accordingly. When a load is applied to the slab portion, it is believed to rotate around a center of rotation placed at the root of the shear crack.

The punching shear failure criterion is related to the tangential strain at the bottom of the slab. The conical shell is subjected to compression in all three directions, resulting in an increased concrete compressive strength. During loading the compressive, tangential strain at the bottom of the slab increases until the internal concrete bond in the transverse direction is impaired. When the maximum value is reached, the enhanced effect decreases and there is a loss of strength.

The model proposed by Kinnunen and Nylander has constituted the foundation for many researchers who have proposed modified models.

(Ericsson, 2010).

6.4 Slabs supported on edge columns

An experimental study was done by Anderson (1966) on punching shear in slabs supported on edge columns. Here, three cases were studied in order to compare different structural solutions. This included

- Specimen *I-a*. This simulated a slab between two floor levels supported on square columns. The columns were then relatively stiff compared to the slab
- Specimen *I-b* was a slab supported by underlying square columns on pinned supports
- Specimen *I-c* resembled specimen *I-a* apart from the employment of a rectangular column.

By the use of a rectangular column, Andersson could study the influence of the eccentricity on the punching capacity.

Specimens *I-a* and *I-c* experienced shear failure, and both specimens had a similar crack pattern. This is illustrated in Figure 18 below (Ericsson, 2010).

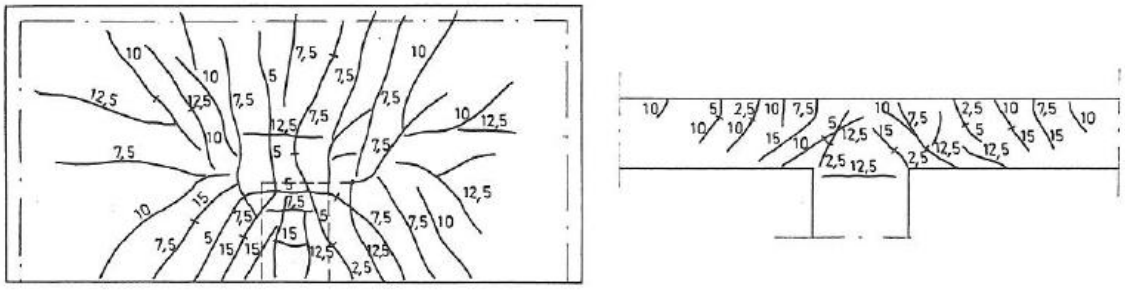

Figure 18 Crack patterns of specimen I-c (Ericsson, 2010)

During loading, radial and tangential cracks developed at the top part of the slab, and inclined cracks occurred along the column supported edge, believed to be caused by torsional moments. Rupture appeared when a shear crack reached the bottom of the slab in vicinity of the column face parallel to the edge. At failure, the inclined cracks along the edge were wide in specimen *I-a.* This indicated that the failure might have started as a torsional-shear failure. The cracks that caused failure (approximate positions) are illustrated in Figure 19 (Ericsson, 2010).

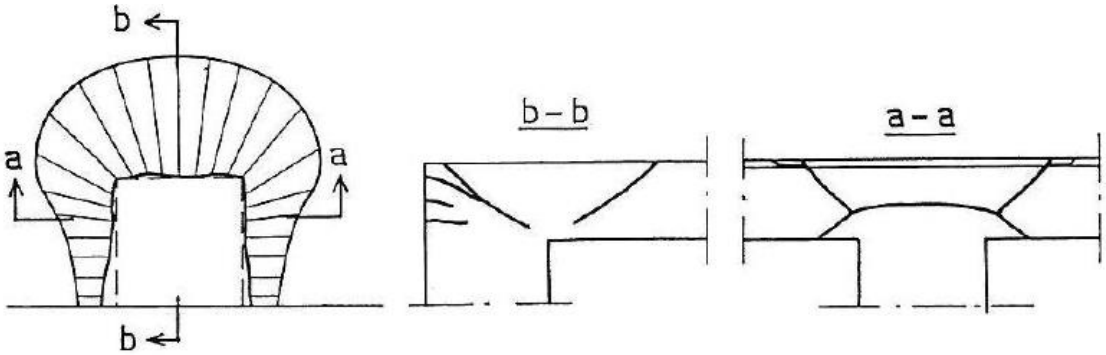

Figure 19 Approximate positions of the cracks that caused failure of test slab 1-a (Ericsson, 2010)

6.5 Slabs supported on corner columns

During the 1970's, the Royal Institute of Technology in Stockholm carried out two sets of experiments on corner supported concrete slabs, both conducted by Ingvarsson. The test specimens from the first set consisted of square concrete slabs supported on square columns. The observed crack propagation was similar for all the specimens tested. Cracking was initiated by flexural cracks at the bottom face of the slabs in the span, and with increased loading flexural cracks were also observed at the top faces above the columns. In addition, inclined cracks along the edges near the columns were formed, which was believed to be caused by torsional moments. For the specimens that failed in shear, shear cracks propagated just prior to the load increment that caused the rupture (Ericsson, 2010).
It was observed that the behavior at failure for several of the specimens differed

from the observations from by Kinnunen and Nylander. While corner supported slabs experienced tensile strains in the tangential direction, the centrically supported slab had compressive strains in the same direction. In the radial direction reverse strains were observed. According to Ingvarsson, the difference in the structural behavior indicated that corner supported slabs are prone to shear failure rather than punching shear, similar to the behavior of beams. This is illustrated in Figure 20 below (Ericsson, 2010).

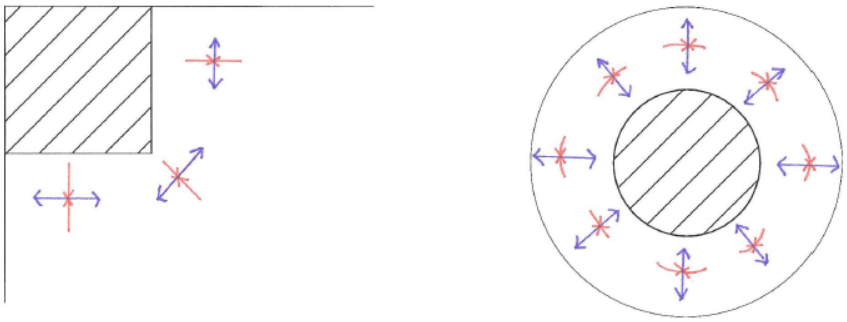

Figure 20 Reverse directions of strains were observed on the bottom surfaces near the columns between slabs supported on corners and interiorly (Ericsson, 2010)

6.6 Observations on punching shear

Failure due to punching seems to be caused by the shear crack from the top surface reaching the compressed region and causing the capacity provided by the compressive zone to cease. This is regardless of the position of the column.

In all experiments the failure mode has been related to measured strains, although comparing the reported strains from the different experiments is complex and most likely not reliable. This is because the strain's dependency on crack propagation, other events in adjacent regions and the inaccuracy of the monitoring equipment (Ericsson, 2010).

7 Punching shear resistance in accordance with code requirements

The following sections presents the code requirements for estimation of punching shear resistance according to Eurocode 2 (current and proposed provisions), the American Building Code 318-19 and FIB's Model Code. The last section presents a comparison of parameters affecting the resistance in prEN 1992-1-1 and EN 1992-1-1.

7.1 Punching shear resistance estimation based on EN 1992-1-1 Section 6.4

This section presents the current design provisions in Eurocode 2. All equations and illustrations are obtained from EN 1992-1.1.

7.1.1 Checks

The following checks should be carried out:

At the column perimeter, or the parameter of the loaded area, the maximum punching shear stress should not be exceeded:

$$v_{Ed} \leq v_{Rd,max} \tag{7.0}$$

where $V_{Rd,max}$ is the design value of the maximum punching shear resistance, and V_{Ed} is the maximum shear stress.

The value of $V_{Rd,max}$ is given by the Norwegian National Annex and is set equal to:

$$V_{Rd,max} = 0{,}4 \cdot v \cdot f_{cd} \tag{7.1}$$

where v is a factor determined as:

$$v = 0{,}6 \cdot \left(1 - \frac{f_{ck}}{250}\right)$$

Punching shear reinforcement is not necessary if the following expression is obtained

$$v_{Ed} \leq v_{Rd,c} \tag{7.2}$$

where $V_{Rd,c}$ is the design value of the punching shear resistance of a slab without shear reinforcement. If this condition is not satisfied, shear reinforcement is required and should be designed in accordance with section 6.4.5 in EN 1992-1-1.

7.1.2 Effective depth, d_{eff}

The effective depth of a slab is assumed to constant and may normally be taken as:

$$d_{eff} = \frac{d_{y+}\, d_z}{2} \tag{7.3}$$

7.1.3 Load distribution and basic control perimeter

The basic control perimeter u_1 may be taken to be at distance 2d from the loaded area and should be constructed so as to minimize its length.
(Norsk Standard, 2008)

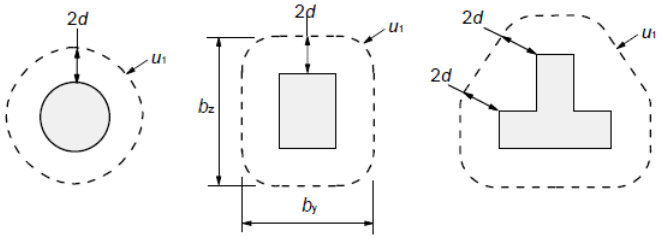

Figure 21 Typical basic control perimeters around loaded areas (Norsk Standard, 2008)

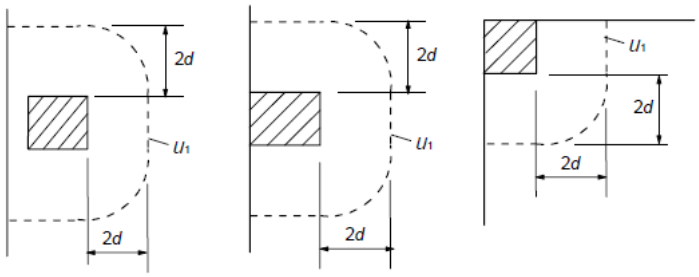

Figure 22 Basic control perimeters for loaded areas close to or at edge or corner (Norsk Standard, 2008)

7.1.4 Maximum shear stress

$$v_{Ed} = \beta \cdot \frac{V_{Ed}}{u_i \cdot d} \tag{7.4}$$

Where *d* is the mean effective depth of the slab, according to equation 7.3 above.

7.1.5 Factor β

Due to asymmetrical load, different spans, or boundary conditions there will always be a moment transfer from the plate to the column, which will affect the shear stress distribution around the critical control section. The β-value considers the unbalanced moment, at the same time as it takes into account the geometry. The design shear stress along the control section is therefore increased by multiplying by this value (Sørensen, 2013).

$$\beta = 1 + k \cdot \frac{M_{Ed}}{V_{Ed}} \cdot \frac{u_1}{W_1} \tag{7.5}$$

where

k is a coefficient dependent on the ratio between the column dimensions c_1 and c_2: its value is a function of the proportions of the unbalanced moment transmitted by uneven shear and by bending and torsion. It should be noted that the β-value varies depending on different cases. Calculations of β-values is attached in Appendix B.

$\frac{M_{Ed}}{V_{Ed}}$ is the eccentricity of the load

u_1 is the length of the basic control perimeter

W_1 corresponds to a distribution of shear and is a function of the basic control perimeter *u*1. (Norsk Standard, 2008)

7.1.6 Punching shear resistance of slabs without shear reinforcement

$$v_{Rd,c} = C_{Rd,c}k(100\rho_l \cdot f_{ck})^{1/3} + k_1\sigma_{cp} \geq (v_{min} + k_1\sigma_{cp}) \quad (7.6)$$

where

$$k = 1 + \sqrt{\frac{200}{d}} \leq 2{,}0$$

$$\rho_l = \sqrt{\rho_{l_y} + \rho_{l_z}} \leq 0{,}02$$

where ρ_{ly}, ρ_{lz} represents the bonded tension steel in y- and z- directions respectively. ρ_{ly} and ρ_{lz} should be calculated as mean values taking into account a slab width equal to the column width plus *3d* each side.

$$\sigma_{cp} = \frac{(\sigma_{cy} + \sigma_{cz})}{2}$$

where σ_{cy} and σ_{cz} are the normal stresses in the critical section in y- and z-direction.

$\sigma_{c,y} = \frac{N_{Ed,y}}{A_{c,y}}$ and $\sigma_{c,z} = \frac{N_{Ed,z}}{A_{c,z}}$

where $N_{Ed,y}$ and $N_{Ed,z}$ are the longitudinal forces the full bay for internal column and the longitudinal force across the control section for edge columns. The force may be from a load or prestressing acting. A_c is the area of concrete according to the definition of N_{Ed}.

7.1.7 Punching shear resistance of slabs with shear reinforcement

$$v_{Rd,cs} = 0{,}75 \cdot v_{Rd,c} + 1{,}5\left(\frac{d}{s_r}\right) \cdot A_{sw} \cdot f_{ywd,ef} \cdot \left(\frac{1}{u_1 \cdot d}\right) \cdot sin\alpha \leq k_{max} \cdot V_{Rd,c} \quad (7.7)$$

where

A_{sw} is the area of one perimeter of the shear reinforcement around the column.

S_r is the radial spacing of perimeters of shear reinforcement.

$F_{ywd,ef}$ is the effective design strength of the punching shear reinforcement, according to $f_{ywd,ef} = 250 + 0{,}25 \cdot d \leq f_{ywd}$

d is the mean value of the effective depths on the orthogonal directions.

α is the angle between the shear reinforcement and the plane slab. For stirrups the angle between the reinforcement and the slab will be 90 degrees, and therefore $sin\alpha$ will be 1.

The punching shear stress should not exceed the design value of the maximum punching shear resistance

$$v_{Ed} = \frac{\beta \cdot V_{Ed}}{u_0 \cdot d} \leq V_{Rd,max} \quad (7.8)$$

where u_0 is the length of column periphery and *d* is the mean of the effective depths in the orthogonal directions (Norsk Standard, 2008).

7.2 Punching shear resistance estimation based on prEN Section 8.4 and L.8.4

This section presents the design provisions from the Eurocode 2 that currently is under preparation. The new provisions for punching shear design of prEN 1992-1-1:2018 are based on *fib* Model Code 2010, which has a pre-normative character. All equations and illustrations are obtained from prEN 1992-1.1.

7.2.1 Checks

The punching shear resistance shall be verified according to the following procedure.

Detailed verification of the punching shear resistance may be omitted, provided that the following condition is satisfied outside the control perimeter.

$$\tau_{Ed} \leq \tau_{Rdc,min} \tag{7.9}$$

Punching shear reinforcement may be omitted when the following condition is satisfied

$$\tau_{Ed} \leq \tau_{Rd,c} \tag{7.10}$$

For slabs requiring punching shear reinforcement, the following conditions should be satisfied

$$\tau_{Ed} \leq \tau_{Rd,max} \tag{7.11}$$

The punching shear reinforcement should be provided to satisfy the following condition

$$\tau_{Ed} \leq \tau_{Rd,cs} \tag{7.12}$$

7.2.2 Effective depth, d_v

The effective depth of a slab should be taken as the distance from the supporting area to the average level of the reinforcement layers

$$d_v = \frac{d_{vx+}\, d_{vy}}{2} \tag{7.13}$$

7.2.3 The control perimeter

The control perimeter may normally be taken at a distance 0,5 d_v from the face of the supporting area and should be constructed so as to minimize its length, $b_{0,5}$.

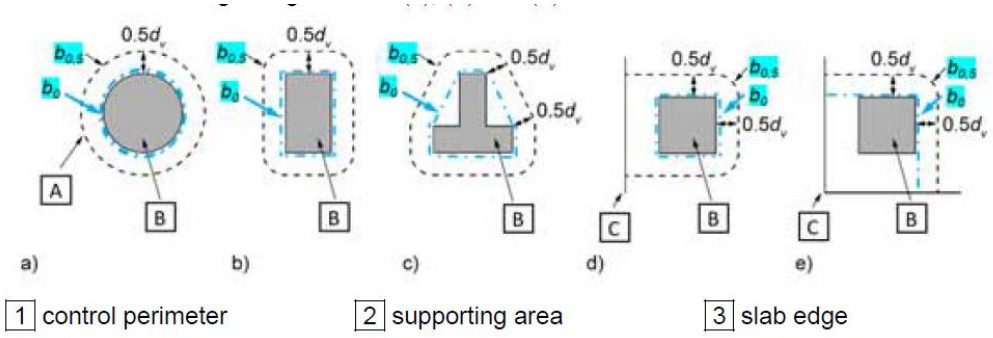

Figure 23 Typical control perimeters $b_{0,5}$ and perimeters b_0 around supporting areas (Aurelio Muttoni F. F.-R., 2020)

(Aurelio Muttoni F. F.-R., 2020)

The effect of concentration of the punching shear forces at the corners of large supporting areas may be taken into account by reducing the control perimeter. This is done by assuming that the length of its straight segments does not exceed 3_{dv} for each edge.

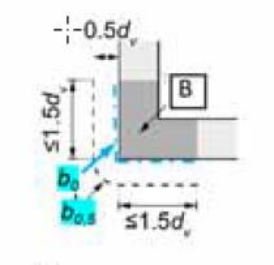

Figure 24 Length of the control section for a corner wall (Aurelio Muttoni F. F.-R., 2020)

7.2.4 Design shear stress

The design shear stress may be calculated as

$$\tau_{Ed} = \beta_e \cdot \frac{V_{Ed}}{b_{0,5} \cdot d_v} \qquad (7.14)$$

7.2.5 Factor β_e

Beta is a coefficient accounting for concentrations of the shear forces. The approximated values for internal, edge and corner columns may be used only if all following conditions are fulfilled:

- The lateral stability does not depend on frame action of slabs and columns
- The adjacent spans do not differ in length more than 25 %
- The slab is only under uniformly distributed loads
- The moment transferred to the edge and corner columns are not larger than $M_{td,max} = 0{,}25 b_e \cdot d^2 \cdot f_{cd}$

Otherwise, the refined values should be adopted. Refined values are given by:

$$\beta_e = 1 + 1{,}1 \cdot \frac{e_b}{b_b} \qquad (7.15)$$

The approximated values are given by:

$\beta_e = 1.15$ for internal coloumns
$\beta_e = 1.4$ for edge columns
$\beta_e = 1.5$ for corner columns

Where

e_b is the component of the eccentricity of the resultant of shear forces with respect to the centroid of the control perimeter which may be simplified replacing parts of circles by corners and where the straight segments are not limited to $3d_v$.

b_b is the geometric mean of the minimum and maximum overall widths of the control perimeter.
(Aurelio Muttoni F. F.-R., 2020)

7.2.6 Punching shear resistance of slabs without shear reinforcement

The design punching shear stress resistance shall be calculated as follows:

$$\tau_{Rd.c} = \frac{0,6}{\gamma_v} \cdot k_{pb}(100 \cdot \rho_l \cdot f_{ck} \cdot \frac{d_{dg}}{d_v})^{\frac{1}{3}} \leq \frac{0,6}{\gamma_v} \cdot \sqrt{f_{ck}} \quad (7.16)$$

Where

$\rho_l = \sqrt{\rho_{l_y} + \rho_{l_z}}$ are the reinforcement ratios of bonded flexural reinforcement in the x- and y-directions respectively.

d_{dg} is a size parameter describing the failure zone roughness, which depends on the concrete type and its aggregate properties.

k_{pb} is the punching shear gradient, can be calculated as:

$$1 \leq 3.6\sqrt{1 - \frac{b_0}{b_{0.5}}} \leq 2.5$$

γ_v is a partial factor for shear and punching resistance without shear reinforcement.

7.2.7 Punching shear resistance of slabs with shear reinforcement

Where shear reinforcement is required, it should be calculated in accordance to:

$$\tau_{Rd.cs} = \eta_c \cdot \tau_{Rd.c} + \eta_s \cdot \rho_w \cdot f_{ywd} \geq \rho_w \cdot f_{ywd} \quad (7.17)$$

Where

$\rho_w = \frac{A_{sw}}{s_r \cdot s_t}$

$\eta_s = \frac{d_v}{150 \cdot \phi_v} + \left(15 \cdot \frac{d_{dg}}{d_v}\right)^{\frac{1}{2}} \cdot \left(\frac{1}{\eta_c \cdot k_{pb}}\right)^{\frac{3}{2}} \leq 0.8$

7.2.8 Punching shear resistance of FRC slabs without shear reinforcement

The design punching shear stress resistance of FRC slabs with flexural reinforcement should be calculated as follows:

$$\tau_{Rd,cF} = \eta_c \cdot \tau_{Rd,c} + \eta_F \cdot f_{Ftud} \geq \eta_c \cdot \tau_{Rdc,min} + f_{Ftud} \quad (7.18)$$

Where

$\eta_c = \frac{\tau_{Rd.c}}{\tau_{Ed}} \leq 1$ and $\eta_F = 1,0$

7.2.9 Punching shear resistance of FRC slabs with shear reinforcement

Where shear reinforcement is required in FRC slabs with flexural reinforcement:

$$\tau_{Rd,cs} = \eta_c \cdot \tau_{Rd,c} + \eta_s \cdot \rho_w \cdot f_{ywd} + \eta_F \cdot f_{Ftud} \geq \rho_w \cdot f_{ywd} + \eta_F \cdot f_{Ftud} \quad (7.19)$$

(Aurelio Muttoni F. F.-R., 2020)

7.3 Punching shear resistance estimation based on ACI 318-19

This section presents the design provisions given in ACI 318-19. All equations and illustrations are obtained from ACI 318-19.

7.3.1 General

ACI differentiate between one-way and two-way shear strength, but due to the scope of thesis only two-way shear strength will be presented in the following sections.

7.3.2 Two-way shear strength

Two-way shear strength is calculated in accordance with chapter 22.6, which provide requirements for determining nominal shear strength, either with shear reinforcement or without shear reinforcement.

Nominal shear strength for two-way members without shear reinforcement shall be calculated by:

$$V_n = V_c \tag{7.20}$$

Nominal shear strength for two-way members with shear reinforcement shall be calculated by

$$V_n = V_c + V_s \tag{7.21}$$

7.3.3 Effective depth, *d*

According to (ACI Committee 318, 2019), the calculation of V_c and for V_s for two-way shear, *d,* shall be the average of the effective depths in the two orthogonal directions. For prestressed, two-way members, *d*, need not to be taken less than 0,8h.

7.3.4 Limiting material strengths

ACI 318-19 concern the limitation of concrete strength. Because there are limited test data on the two-way shear strength of high-strength concrete slabs, two-way slabs constructed with concretes that have compressive strengths greater than 70 MPa is limited $\sqrt{f_c'}$ to 8.3 MPa for the calculation of shear strength. Also, the upper limit of 420 MPa on the value of f_{yt} used in design is intended to control cracking.

7.3.5 Critical section for two-way members

According to ACI 318 critical sections shall be located so that the perimeter b_0 is a minimum but do not need to be closer than *d*/2 to (a) and (b)

(a) Edges or corners of columns, concentrated loads, or reaction areas
(b) Changes in slab or footing thickness, such as edges of capitals, drop panels, or shear caps.
(ACI Committee 318, 2019)

For square or rectangular columns, concentrated loads, or reaction areas, critical sections for two-way shear in accordance with (a) and (b) shall be permitted to be defined assuming straight sides.

For a circular or regular polygon-shaped column, critical sections for two-way shear in accordance with (a) and (b) shall be permitted to be defined assuming a square column of equivalent area.

For two-way members reinforced with headed shear reinforcement or single- or multi-leg stirrups, a critical section with perimeter b_o located d/2 beyond the outermost peripheral line of shear reinforcement shall also be considered. The shape of this critical section shall be a polygon selected to minimize b_0 (ACI Committee 318, 2019).

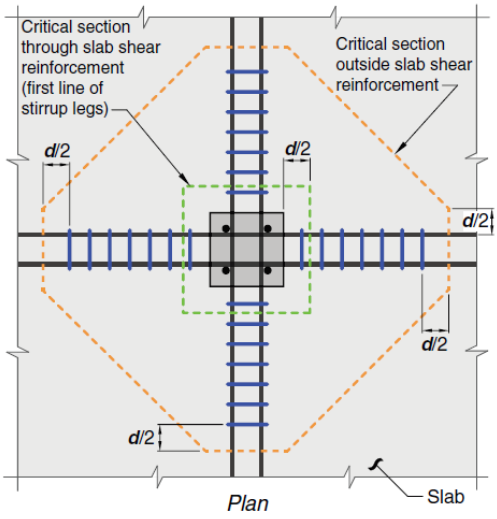

Figure 25 Critical sections for two-way shear in slab with shear reinforcement at interior column (ACI Committee 318, 2019)

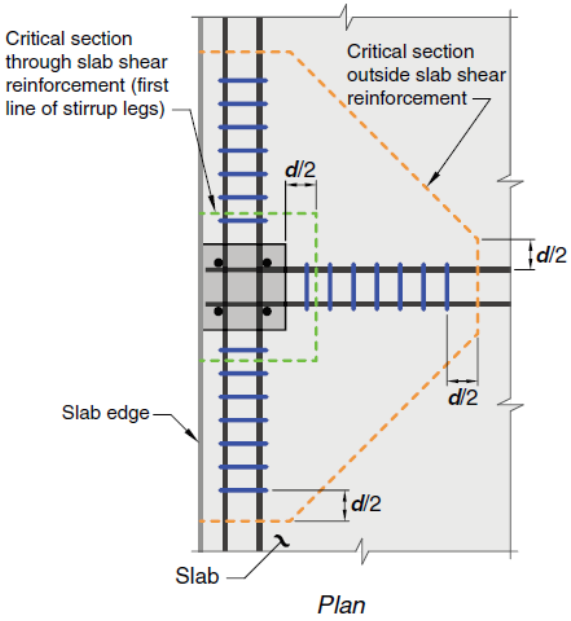

Figure 26 Critical sections for two-way shear in slab with shear reinforcement at edge column (ACI Committee 318, 2019)

7.3.6 Beta-value

For shapes other than rectangular, β is taken to be the ratio of the longest overall dimension of the effective loaded area to the largest overall perpendicular dimension of the effective loaded area, as illustrated for an L-shaped reaction area in Figure 27. The effective loaded area is that area totally enclosing the actual loaded area, for which the perimeter is a minimum (ACI Committee 318, 2019).

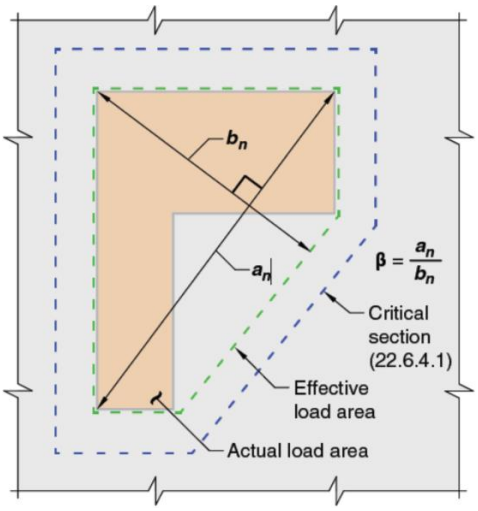

Figure 27 Value of β for a nonrectangular loaded area (ACI Committee 318, 2019)

7.3.7 Two-way shear strength without shear reinforcement

For members of uniform thickness without shear reinforcement, it is sufficient to check shear using one section. For slabs with changes in thickness or with shear reinforcement, it is necessary to check shear at multiple sections as defined in (a) and (b). For columns near an edge or corner, the critical perimeter may extend to the edge of the slab (ACI Committee 318, 2019).

v_c		
Least of (a), (b), and (c):	$0.33\lambda_s\lambda\sqrt{f'_c}$	(a)
	$\left(0.17+\frac{0.33}{\beta}\right)\lambda_s\lambda\sqrt{f'_c}$	(b)
	$\left(0.17+\frac{0.083\alpha_s d}{b_o}\right)\lambda_s\lambda\sqrt{f'_c}$	(c)

Notes:

(i) λ_s is the size effect factor given in 22.5.5.1.3.

(ii) β is the ratio of long to short sides of the column, concentrated load, or reaction area.

(iii) α_s is given in 22.6.5.3.

Figure 28 Vc for two-way members without shear reinforcement (ACI Committee 318, 2019)

7.3.8 Two-way shear strength with shear reinforcement

According to (ACI Committee 318, 2019) experimental evidence indicates that the measured concrete shear strength of two-way members without shear reinforcement does not increase in direct proportion with member depth. This phenomenon is referred to as the "size effect." The modification factor λs accounts for the dependence of two-way shear strength of slabs on effective depth (ACI Committee 318, 2019).

Type of shear reinforcement	Critical sections	v_c		
Stirrups	All	$0.17\lambda_s\lambda\sqrt{f'_c}$		(a)
Headed shear stud reinforcement	According to 22.6.4.1	Least of (b), (c), and (d):	$0.25\lambda_s\lambda\sqrt{f'_c}$	(b)
			$0.17\left(1+\frac{2}{\beta}\right)\lambda_s\lambda\sqrt{f'_c}$	(c)
			$0.083\left(2+\frac{\alpha_s d}{b_o}\right)\lambda_s\lambda\sqrt{f'_c}$	(d)
	According to 22.6.4.2		$0.17\lambda_s\lambda\sqrt{f'_c}$	(e)

Notes:

(i) λ_s is the size effect factor given in 22.5.5.1.3.

(ii) β is the ratio of long to short sides of the column, concentrated load, or reaction area.

(iii) α_s is given in 22.6.5.3.

Figure 29 Vc for two-way members with shear reinforcement (ACI Committee 318, 2019)

7.4 Punching shear resistance estimation based on FIB's Model Code

This section presents the design provisions from FIB's Model Code. All equations and illustrations are obtained FIB's Model Code Volume 2.

7.4.1 Checks

The following conditions must be satisfied when designing a slab structure.

The punching shear resistance is calculated as

$$V_{Rd} = V_{Rd,c} + V_{Rd,s} \geq V_{Ed} \tag{7.22}$$

where

V_{Rd} is the shear resistance

$V_{Rd,c}$ is the design shear resistance attributed to the concrete

$V_{Rd,s}$ is design shear resistance provided by shear reinforcement

V_{Ed} is the design shear force

(fib, Model Code Volume 2, 2010)

7.4.2 Shear-resisting effective depth, d_v

The shear-resisting effective depth of the slab is the distance from the centroid of the reinforcement layers to the supported area (fib, Model Code Volume 2, 2010).

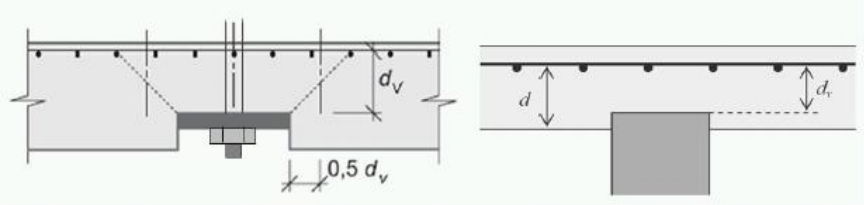

Figure 30 Effective depth of the slab considering support penetration (dv) and effective depth for bending calculations (d) (fib, Model Code Volume 2, 2010)

7.4.3 The basic control perimeter b_1

The basic control perimeter *b*1 may normally be taken at a distance 0.5 dv from the supported area and should be determined in order to minimize its length. The length of the control perimeter is limited by slab edges (fib, Model Code Volume 2, 2010).

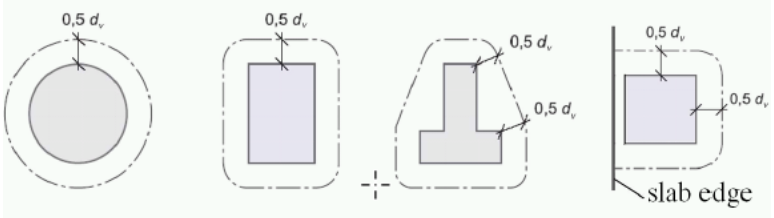

Figure 31 Basic control perimeters around supported areas (fib, Model Code Volume 2, 2010)

7.4.4 Design shear force

Contribution of point loads applied within a distance of d<a_v≤2d from the face of the support to the design shear force V_{Ed} may be reduced by the factor:

$$\beta = \frac{a_v}{2 \cdot d} \tag{7.23}$$

Where *d* is the mean effective depth of the slab

$$z=0{,}9 \cdot d$$

$$z = \frac{z_e^2 A_s + z_p^2 A_p}{z_s A_s + z_p A_p} \tag{7.24}$$

7.4.5 Members without shear reinforcement

Shear resistance of a slab without shear reinforcement:

$$V_{Rd,c} = k_v \cdot \frac{\sqrt{f_{ck}}}{\gamma_c} \cdot z \cdot b_w \tag{7.25}$$

$\sqrt{f_{ck}}$ shall not be greater than 8MPa

7.4.6 Members with shear reinforcement

$$V_{Rd,s} = \frac{A_{sw}}{s_w} \cdot z \cdot f_{ywd} \cdot (cot\theta + cot\alpha) \cdot sin\alpha \tag{7.26}$$

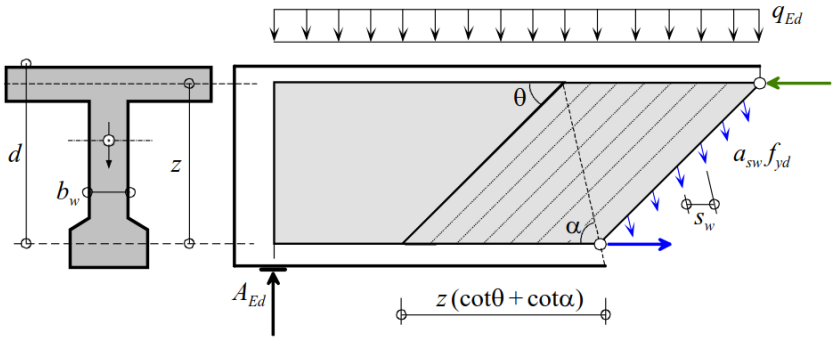

Figure 32 Geometry and definitions (fib, Model Code Volume 2, 2010)

(fib, Model Code Volume 2, 2010)

7.4.7 Punching shear resistance of FRC slabs without shear reinforcement

For slab elements without conventional reinforcement with predominantly bending actions, the strength verification can be done with reference to the resisting moment, M_{Rd}, evaluated by considering a rigid plastic relationship

$$M_{Rd} = \frac{f_{Ftud} \cdot t^2}{2} \tag{7.27}$$

When a linear analysis is performed, the max. principal moment should be lower than M_{Rd}. When a limit analysis is performed, M_{Rd} can be regarded as the reference value.

Shear in fiber-reinforced slabs without reinforcement or prestressing is not regarded as dominant unless significant load concentrations occur close to the support.

(fib, Model Code Volume 2, 2010)

7.4.8 Punching shear resistance of FRC slabs with shear reinforcement

$$V_{Rd} = V_{Rd,F} + V_{Rd,s} \tag{7.28}$$

$$V_{Rd,F} = V_{Rd,c} + V_{Rd,f} \tag{7.29}$$

$$V_{Rd,f} = \frac{f_{Ftuk}}{\gamma_F} \cdot b_0 \cdot d_v \tag{7.30}$$

f_{Ftuk} is the characteristic value of the ultimate residual tensile strength for FRC, calculated taking into account w_u = 1,5 mm [MPa];

b_0 is the shear resisting control perimeter

d_v is the shear resisting effective depth

(fib, Model Code Volume 2, 2010)

8 Comparison of punching shear resistance models in prEN 1992-1-1 and EN 1992-1-1

The following sections presents a comparison in some of the parameters of the current and proposed version of Eurocode 2. This also include the background for some of the changes made in prEN 1992-1-1.

8.1 Background for the changes in prEN 1992-1-1

Punching design was one of the chapters that collected more systematic review comments of the current EC2. Many reasons supported an in-depth review of this section, mostly to address scientific and design concerns, as well as to enhance the ease-of-use. Numerous works criticizing the consistency of the method for punching shear design according to EN 1992-1-1 have been published in the scientific literature.

One of the critics were that the verification of punching shear resistance according to EN 1992-1-1 is different for slabs and footings. The control section is defined at 2.0*d* for slabs, while an iteration is required for footings to search the control section that minimizes the resistance. If the location of the control perimeter at 2.0*d* for flat slabs is not physically consistent with experimental observations the iteration required for the case of footings is not suitable for practice.

In addition, a re-definition of the control section consistent with the experimental observations, equal for both cases and without any iterative procedure is also recommended.

Recent works have shown that the size effect law included in the current approach does not describe the corresponding phenomenon suitably. The current approach may underestimate the effect of the size of the member and overestimate the punching resistance for large size members. Recent comparisons of the current approach against datasets of experimental tests confirm this.

The size-effect law should be corrected in the next generation of EC2. The current approach does not consider any slenderness effect. Recent works assessing the performance of the current approach against datasets of experimental tests have shown that slab slenderness plays a role in the punching resistance. Including this parameter in the design method should be considered for the next generation of EN 1992-1-1.

A recently performed comparison between the design method of EC2 and a dataset of experimental tests suggests that the punching strength of slabs with shear reinforcement may be overestimated by the current approach.
(Aurelio Muttoni F. F.-R., 2020)

Some works on the topic questioned the validity of the calculation of the effective stress in the shear reinforcement only as a function of the effective depth, while others discussed on the general validity of the verification of the concrete struts at the face of the supported area. This latter verification can underestimate the punching strength in some cases and overestimate in others. For these reasons, a complete revision of the design of transverse reinforcement is recommended for the next generation of EC2 (Aurelio Muttoni A. P., 2018).

8.2 Critical control section

In EN 1992-1-1, the basic control perimeter u_1 may normally be taken at a distance 2d from the loaded area and should be constructed so as to minimize its length, while in prEN 1992-1-1, the control perimeter may normally be taken at a distance 0,5 d_v from the face of the supporting area (Norsk Standard, 2008).

8.3 D_{lower}/k_2

D_{lower} is a parameter from prEN 1992-1-1 included in the formula for d_{dg} and describes the aggregate size. A higher value of d_{lower} will result in an increased roughness in the failure zone and therefore a better ability to transfer loads.

According to prEN 1992-1-1 d_{dg} is a size parameter describing the failure zone roughness. This depends on the concrete type and its aggregate properties (Aurelio Muttoni F. F.-R., 2020).

K_2 is a factor from NS-EN 1992-1-1 included in the formula $C_{Rd.c}$. The values for k_2 is given in the Norwegian National Annex and only two values are given. If the aggregate size is less than 16mm, 0,15 shall be used. However, if the aggregate size is equal or greater than 16mm the value 0,18 shall be used (Norsk Standard, 2008).

8.4 KPB

K_{pb} is a shear gradient for the strength enhancement for punching due to the shear field gradient in the control section. The coefficient also represents a smooth transition between one- and two-way shear, where the value tends to be 1 at very large supported areas. The punching shear resistance in these areas tends to act as a one-way slab. By decreasing the supported area, the enhancement coefficient will increase. This value has a limit between 1 and 2.5. An upper limit is required to avoid excessive shear resistance over small supported areas (Aurelio Muttoni A. P., 2018).

8.5 RC ratio

The reinforcement ratio affects the resistance in the same manner for the proposed and current version, but it has no upper limit in the proposal. Consequently, reinforcement ratios exceeding 2% contributes to larger resistance in the proposal.

FEM ANALYSIS

9 Modelling and analysis of flat slab in FEM-Design software and ADAPT

9.1 FEM-Design

FEM-Design is an advanced modeling software for FEM-analysis and design of load-bearing concrete, steel, timber, and foundation structures according to Eurocode with NA. The working environment is based on the familiar CAD tools that make the model creation and structure editing simple and intuitive. The program is ideal for all types of construction tasks from single element design to global stability analysis of large structures and makes it a practical tool for structural engineers (StruSoft, 2021).

9.2 ADAPT builder

ADAPT-Floor Pro is a three-dimensional finite element software for analysis and design of concrete and post-tensioned floor and foundation systems. This software provides a powerful and easy to use tool for the analysis of all types of slab systems. Unlike other 2D diaphragm-based slab design programs, ADAPT-Floor Pro's true 3D FEM analysis provides the most accurate results even for the most complex transfer and waffle slabs. Its Dynamic Rebar Design (DRD)™ module gives structural engineers complete control over the design and placement of mild reinforcement, leading to optimized designs. Extensive import and export capabilities further streamline the design process through to the creation of structural drawings (ADAPT, 2021).

9.3 Modelling of flat slab in FEM-Design software and ADAPT

When comparing the punching shear resistance in FEM-Design and ADAPT the structrual response (i.e, deflections and stresses) was compared. Although the objectives of the study only included the structural behavior related to punching shear, a review of the results, e.g. moments and deflections, were performed. The reports from both the softwares are attached in Appendix A.

Both analysis were performed as a linear elastic FE analysis. Although concrete is a non-linear and nonhomogeneous material, linear elastic material behavior is often considered during design. According to NS EN 1992-1, non-linear analysis is to be preferred, but due to all the load combinations it is not often used in design practice.

9.3.1 Material properties

The following table presents the material properties for the FE analysis.

Material	Properties
Characteristic compressive strength	35MPa
Characteristic yield strength of rebar	500MPa
Cross-sectional area	150mm^2
Characteristic yield strength	1860MPa

Table 2 Material properties

9.3.2 Boundary conditions

For both FEM-Design and ADAPT a hinged connection was selected between the columns and slabs. That is, the flat slab is not designed to transfer moment from the columns.

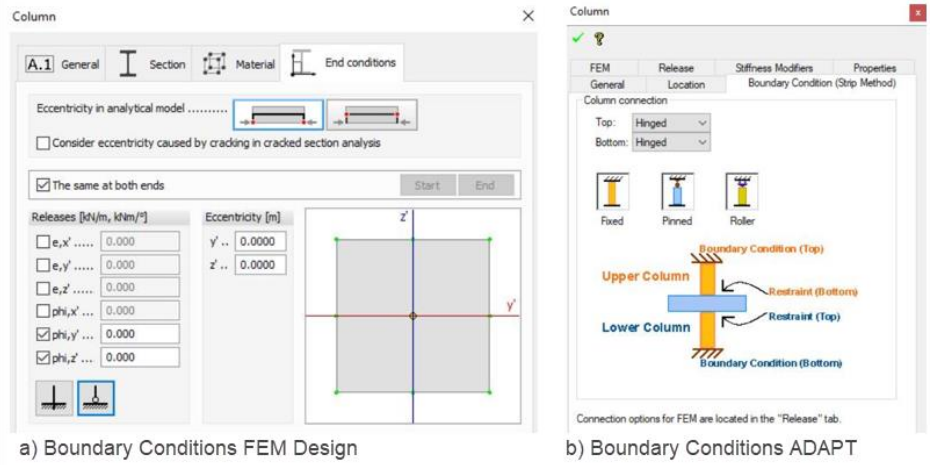

Figure 33 Boundary Conditions in FEM-Design and ADAPT

9.3.3 Tendon profile

In FEM-Design the software does not include options for tendon profiles, and the cables are modelled as parabolic. This is considered a more realistic tendon profile.

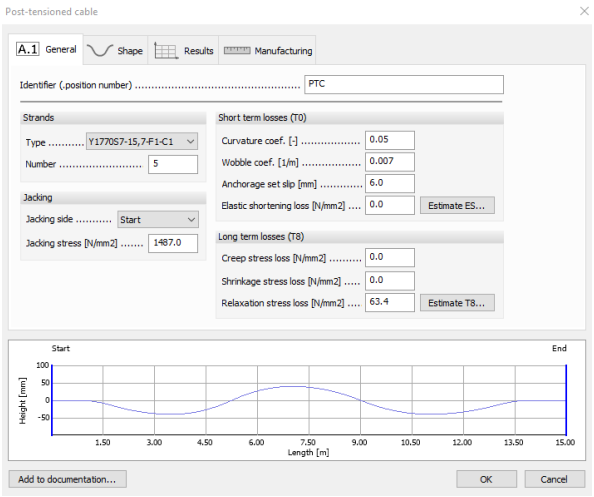

Figure 34 Tendon profile in FEM-Design

In ADAPT, the Software includes different options for the tendon profile, e.g. a harped profile, which is considered an idealized tendon profile. Due to the comparison between FEM-Design and ADAPT, a parabolic profile was chosen.

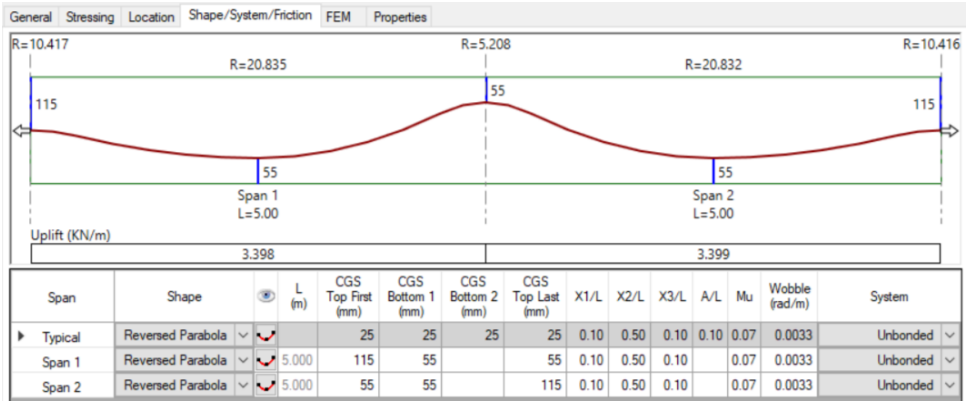

Span	Shape	L (m)	CGS Top First (mm)	CGS Bottom 1 (mm)	CGS Bottom 2 (mm)	CGS Top Last (mm)	X1/L	X2/L	X3/L	A/L	Mu	Wobble (rad/m)	System
Typical	Reversed Parabola		25	25	25	25	0.10	0.50	0.10	0.10	0.07	0.0033	Unbonded
Span 1	Reversed Parabola	5.000	115	55		55	0.10	0.50	0.10		0.07	0.0033	Unbonded
Span 2	Reversed Parabola	5.000	55	55		115	0.10	0.50	0.10		0.07	0.0033	Unbonded

Figure 35 Tendon profile in ADAPT

9.3.4 Tendon layouts

There are several possible arrangements of the tendons, and ideally the tendons should be distributed between the column lines and the span, the same way that the moment is distributed (Sørensen, 2013). In this study, the distributed cables were placed in x-direction c/c 500mm, and the banded cables were placed c/c 140mm over the columns in y-direction. The column strip in the mid span were given 5 cables, and the two column strips at the end of the slab were given 3 cables.

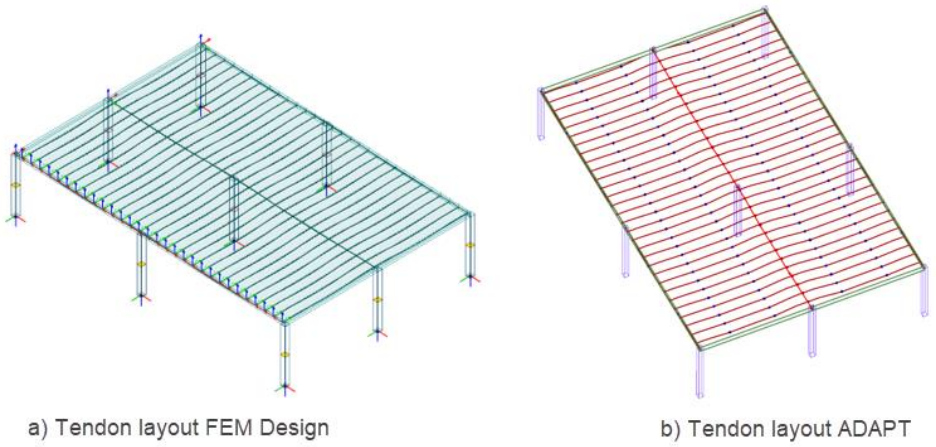

Figure 36 Tendon layouts for FEM-Design and ADAPT

9.4 Peak smoothing in FEM-Design software vs ADAPT

As an effect of the mesh refinement the results are converging to the theoretical solution. The problem is due to that certain places get infinite inner forces according to the theory, so the inner forces increase each time by refining the mesh. These places could be point supports, end points of edge supports, vertices of surface supports, point loads etc. (StruSoft, 2021)

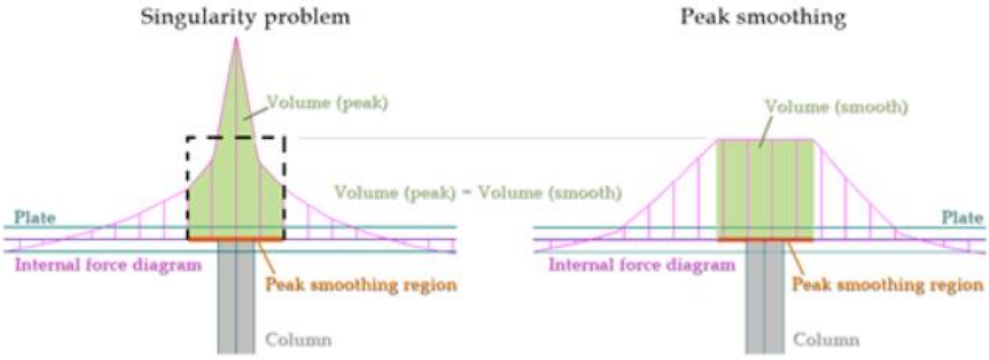

Figure 37 Peak smoothing (StruSoft, 2021)

In practice, the singularity problem usually occurs at supports because they heavily influence the inner forces, e.g. negative moments, in ratio. There are three known possibilities to solve the above-mentioned problem, which is either choosing an optimal finite element size at singularity places, a more realistic and precise model definition or peak smoothing (StruSoft, 2021). FEM-Design describes how the program calculates peak-smoothing, and the following sections describes the background theory and procedure regarding this. ADAPT on the other hand, does not per this date, have a technical report regarding singularity problems. This is therefore not reviewed in this study.

9.4.1 FEM-Design

FEM-Design defines peak smoothing regions to solve the possible singularity problems. These regions are the active zones in the environment of the singularity, where the inner forces change substantially as a result of mesh refinement.

Peak smoothing regions can be generated automatically by the mesh generator or calculation processes. The automatic generation always results circular peak smoothing regions with center points placed in the location of the singularity. Automatic generation of peak smoothing regions can be set and controlled at the general settings of mesh generation. The radius of the circular regions is calculated from the following formula:

$$\mathrm{r} = \frac{t}{2} + \mathrm{f} \cdot \mathrm{v} \tag{9.0}$$

where *t* is the characteristic geometric parameter of the object that causes singularity, *v* is the thickness of the planar element in the considered place, and *f* is a factor set manually. The default value is 0.5, which means 45 degrees angle of projection starts from the connection and ends in the calculation plane of the related planar element.

(StruSoft, 2021)

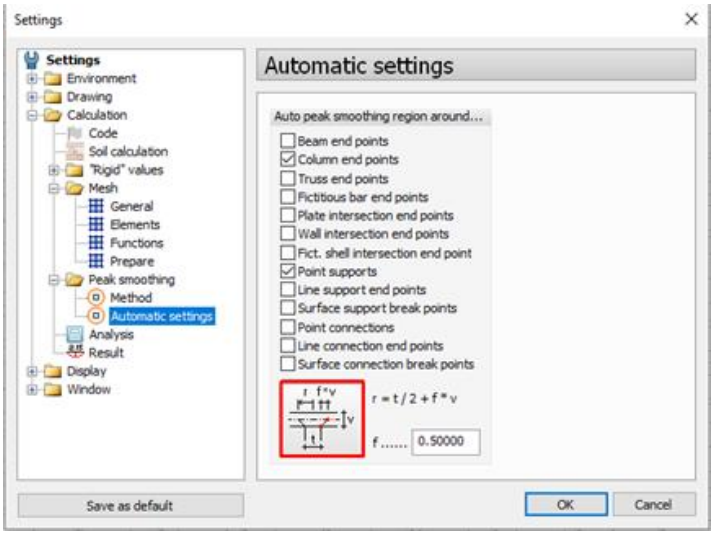

Figure 38 Settings of automatic peak smoothing generation (StruSoft, 2021)

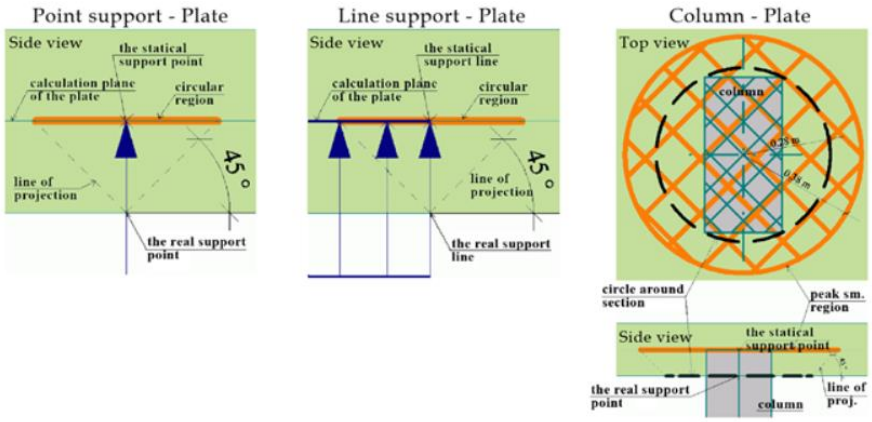

Figure 39 Examples for peak smoothing regions by different element-plate connection (StruSoft, 2021)

In FEM-Design, the steps of the peak smoothing algorithm are the followings during calculations (inner forces):

- Select the peak smoothing method for moments, normal and shear forces under Settings/Calculation/Peak smoothing/Method
- The program creates peak smoothing regions and/or checks the predefined active zones.
- Allow peak smoothing algorithm for internal force and stress calculations. It is not enough to generate peak smoothing regions, so you have to confirm the smoothing process in the calculate dialog before starting any analysis (and design) calculations.
- The program calculates a constant value for cutting the peaks according to volume calculations of inner diagrams above the peak smoothing regions. That means, the volume at the final constant result value is equal with the volume derived from the peak (singularity) value above the same peak smoothing region.

It is important to select the correct peak smoothing method because it has a great effect to the results (StruSoft, 2021).

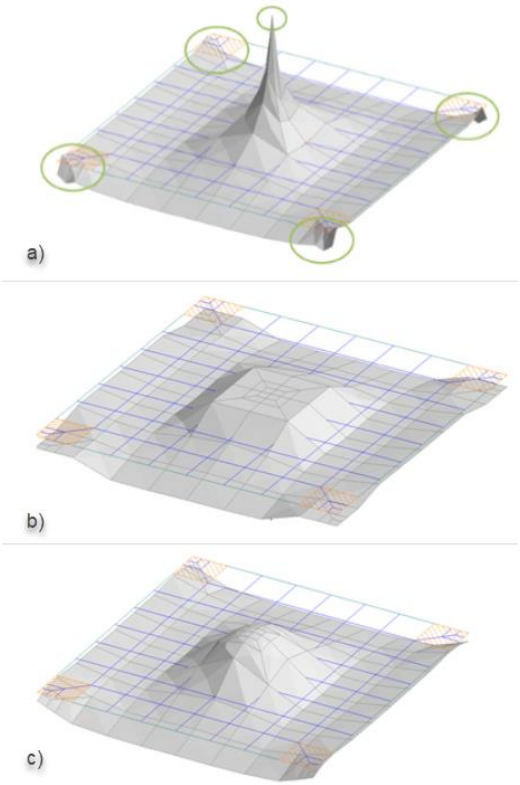

Figure 40 a) No peak smoothing b) Use of constant shape function c) Use of higher order shape functions (StruSoft, 2021)

PARAMETRIC STUDY

The following sections presents the results from a parametric study of a flat slab. In this study, the punching shear resistance around different critical control sections was controlled, and then compared with results from ADAPT and FEM-Design. The study also looked at the correlation between the design shear force and the punching shear resistance.

The calculations were done in accordance with prEN-1992-1-1 and EN 1992-1-1. It should be noted that all the formulas from EN-1992-1-1 was performed in accordance with the Norwegian National Annex. For complete calculations see Appendix A.

10 General

For the parametric study a rectangular flat slab spanning 15m x 10m directly supported on columns was analyzed. The support conditions for all columns were hinged. The slab thickness was set to 230mm, with a concrete strength of B35. The basis of the thickness was to see if it was possible to design a slab that was slimmer “than usual”.

The structural loads considered besides the self-weight of the slab, and the loads due to prestressing, was a distributed live load of 2kN/m^2 and an additional dead load of 1 kN/m^2.

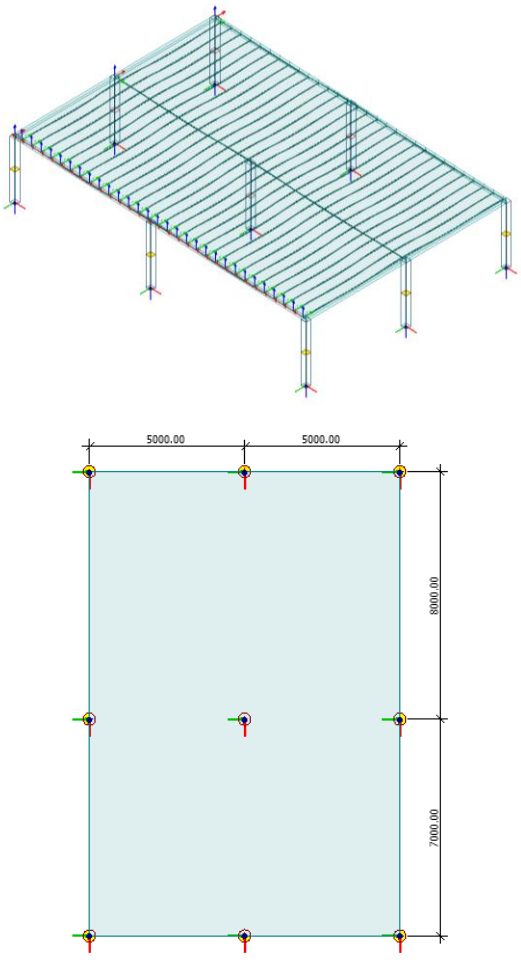

Figure 41 Geometry of the flat slab

The study was performed with square columns, including interior, edge, and corner columns for the following cases:

- Without shear reinforcement
- With post-tensioning
- With fiber reinforcement
- With shear reinforcement
- With PT, fiber, and shear reinforcement

In every case, a set of parameters were varied (one at a time, while others stayed constant). The starting values are presented in Table 3 below.

	Inner column	Edge column	Corner column
B [mm]	250	250	250
F_{CK} [MPa]	35	35	35
ρ	0.0031	0.0031	0.0031
D_{DG} [mm]	32	32	32
E_X [mm]	40	40	40
E_Y [mm]	55	55	55

Table 3 Starting values

It should be noted that initially the thesis was intended to investigate columns with different geometry, e.g. square, rectangular, and circular columns. However, it was discovered at an early stage that this parameter was not a govern parameter.

In EN 1992-1-1 there is no difference between circular and rectangular columns regarding the punching shear resistance, while there was an insignificant difference between in prEN 1992-1-1 because of the control perimeter. Due to this, different geometry for the columns is not included in this study.

To calculate the punching shear resistance, the design shear- and moment values was implemented from FEM-Design on the prerequisites presented initially in this chapter. They are presented in Table 4 under.

	Inner column	Edge column	Corner column
V_{ED} (KN)	643	206	85
$M_{ED,X}$ (KNM)	103	16	15
$M_{ED,Y}$ (KNM)	126	96	17

Table 4 Design values

10.1 Without shear reinforcement

Figure 42-44 shows the difference in the punching shear resistance in the flat slab at increased characteristic compressive strength, column size and slab thickness. According to the formulas in EN 1992-1-1, the column placement does not affect the shear resistance.

prEN-1992-1-1 considers the control perimeter, which gives a different punching shear resistance depending on where the column is located. Complete calculations are given in Appendix A.

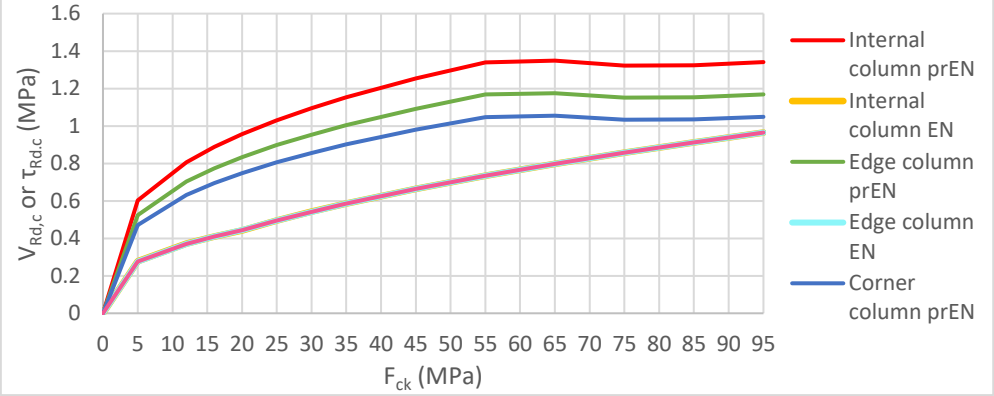

Figure 42 Punching shear resistance without shear reinforcement for different characteristic compressive strengths

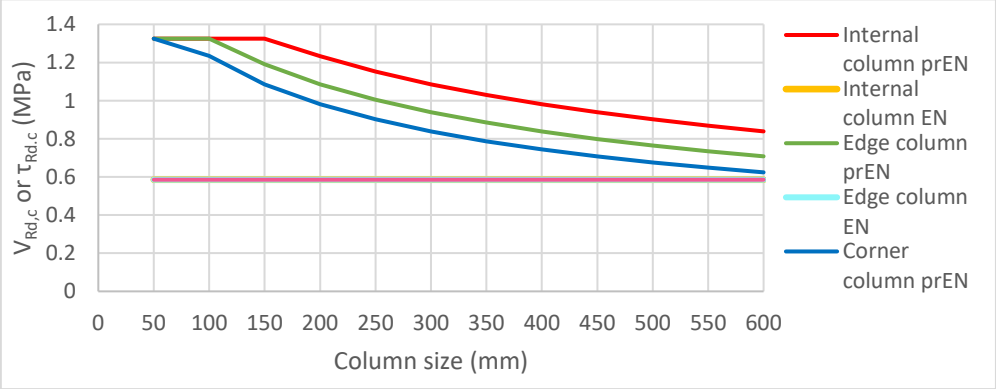

Figure 43 Punching shear resistance for different column sizes

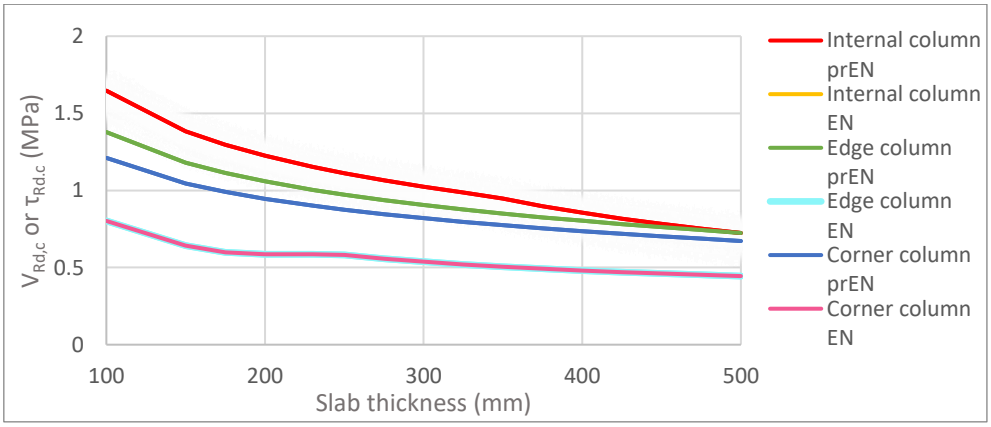

Figure 44 Punching shear resistance with different slab thickness

Figure 45 presents the varied parameters D_{lower} and k. D_{lower} is a parameter from prEN 1992-1-1 included in the formula for d_{dg}, while k is a factor from EN 1992-1-1. The results show that the aggregate size affects the punching shear resistance in prEN 1992-1-1, but in EN 1992-1-1 there are only two options for aggregate size, and therefore only two values are possible.

Complete calculations are given in Appendix A.

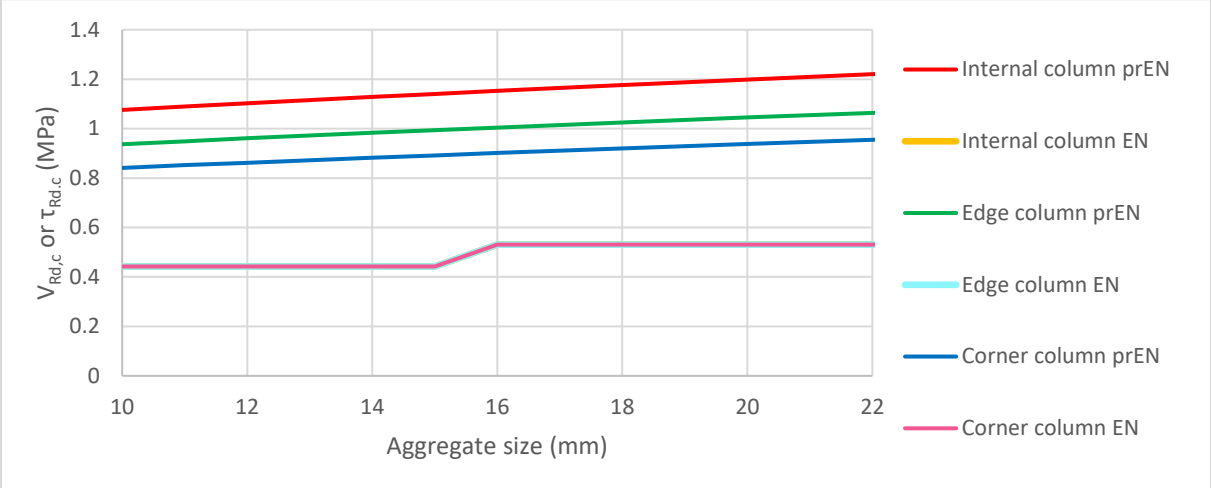

Figure 45 Punching shear resistance for different aggregates

The last varied parameter was the reinforcement ratio. EN 1992-1-1 has a limit for the reinforcement ratio at 0,02, while prEN 1992-1-1 does not include an upper limit. However, the shear resistance formula in preEN 1992-1-1 includes a maximum limit, which is reached at a higher reinforcement ratio.

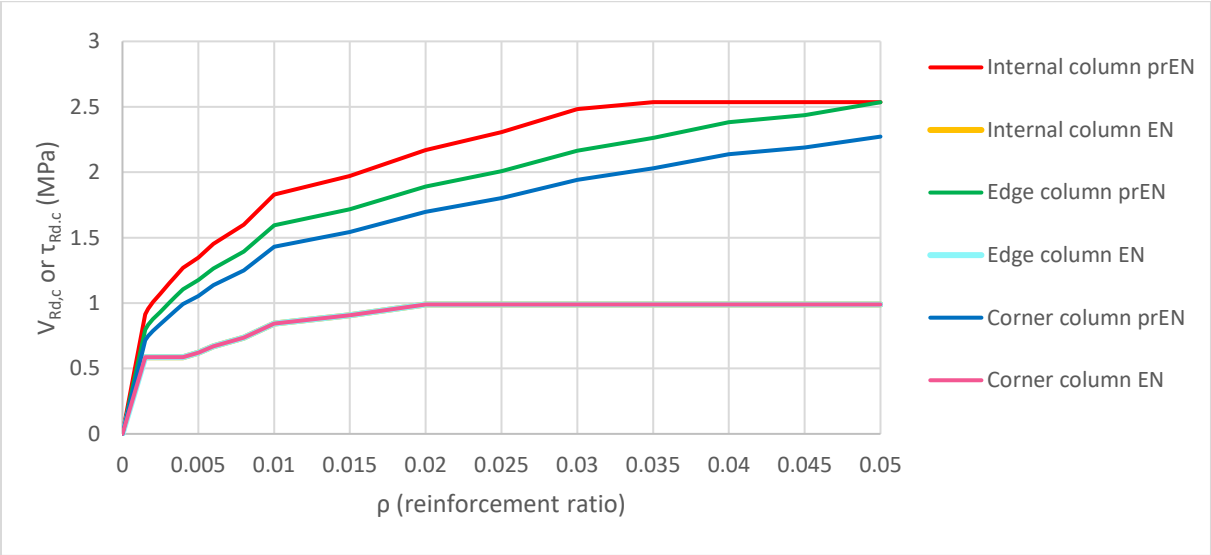

Figure 46 Punching shear resistance for different reinforcement ratios

10.2 With post-tensioned tendons

In the case with post-tensioned mono strands, the following parameters were varied for square columns:

- f_{ck} [Mpa] Characteristic compressive strength
- P_{mt} [kN] Jacking force
- e_p [mm] Cable eccentricity

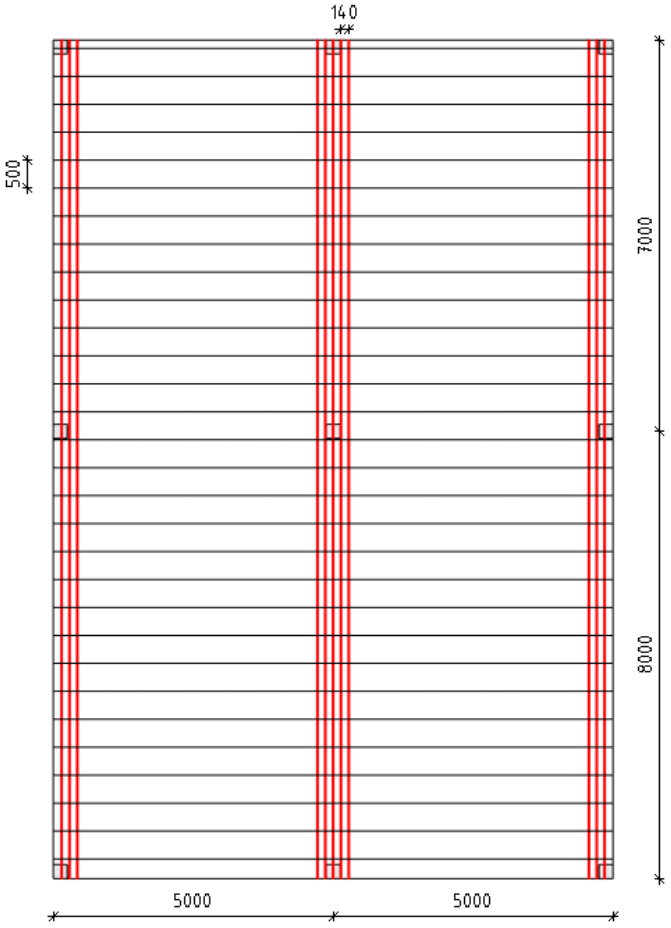

Figure 47 Tendon layout

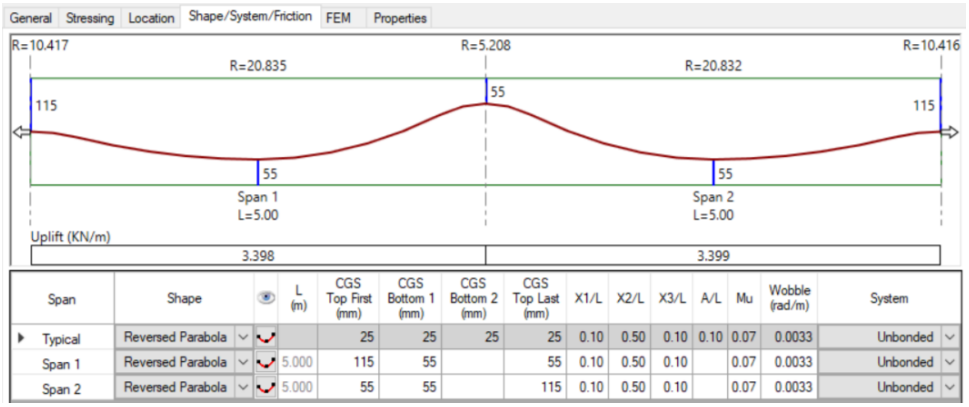

Span	Shape		L (m)	CGS Top First (mm)	CGS Bottom 1 (mm)	CGS Bottom 2 (mm)	CGS Top Last (mm)	X1/L	X2/L	X3/L	A/L	Mu	Wobble (rad/m)	System
Typical	Reversed Parabola			25	25	25	25	0.10	0.50	0.10	0.10	0.07	0.0033	Unbonded
Span 1	Reversed Parabola		5.000	115	55		55	0.10	0.50	0.10		0.07	0.0033	Unbonded
Span 2	Reversed Parabola		5.000	55	55		115	0.10	0.50	0.10		0.07	0.0033	Unbonded

Figure 48 Tendon profile in ADAPT

The following figures shows the punching shear resistance with and without PT for internal, edge and corner columns. The values are based on calculations with a jacking force of 178kN with 5 concentrated cables for internal columns, 3 concentrated cables for edge and corner columns, and distributed cables with distance of 500mm. Complete calculations are given in Appendix A.

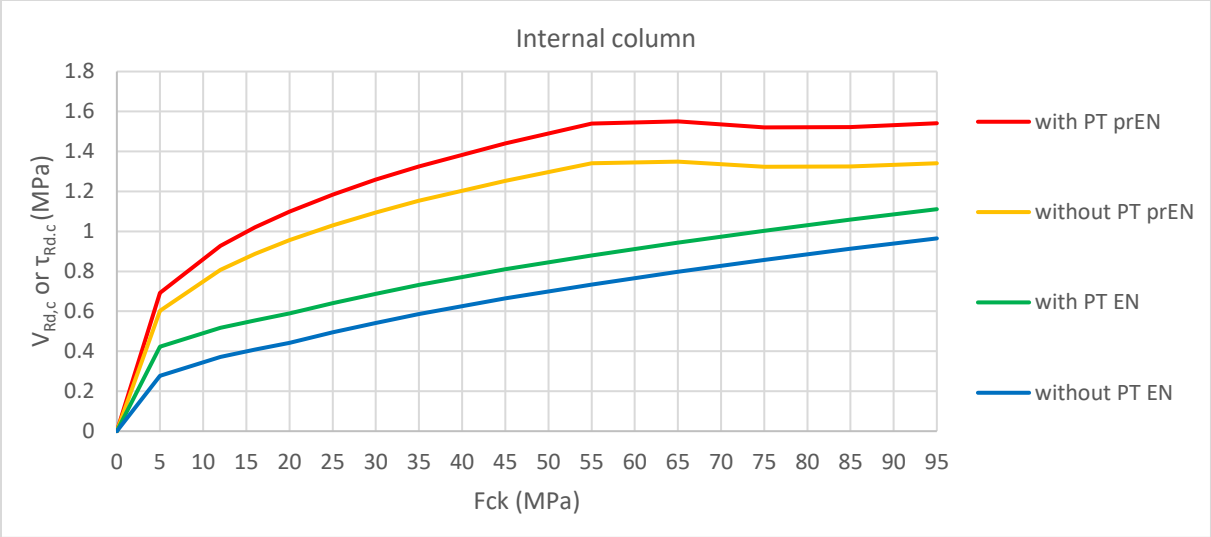

Figure 49 Punching shear resistance for different characteristic compressive strengths

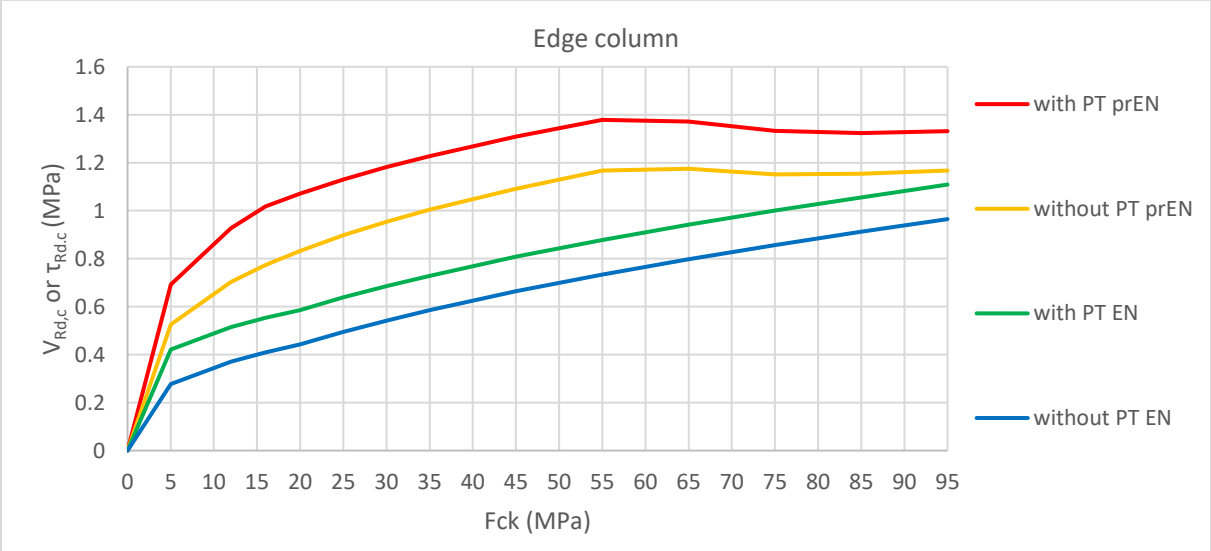

Figure 50 Punching shear resistance for different characteristic compressive strengths

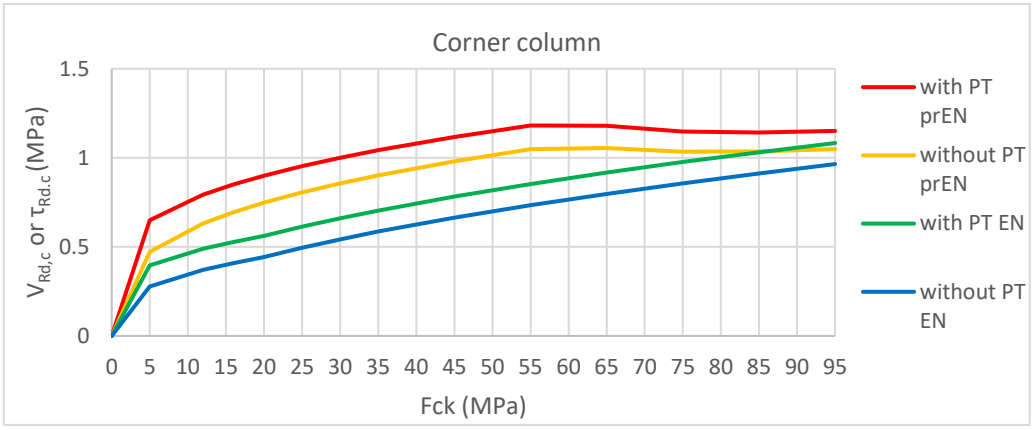

Figure 51 Punching shear resistance for different characteristic compressive strengths

Figure 52 shows the punching shear resistance when increasing the jacking force. According to prEN 1992-1-1 the shear resistance reaches a limit due to factor k_{pb}, while EN 1992-1-1 does not have this limitation.

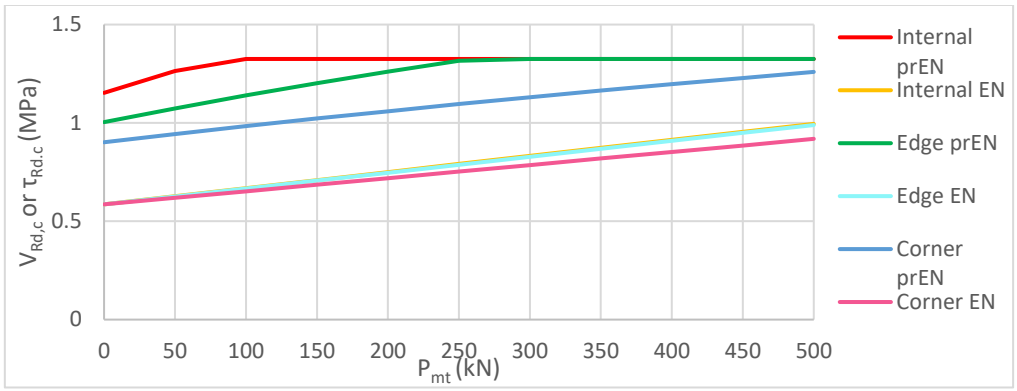

Figure 52 punching shear resistance with increasing jacking force

Figure 53 shows the punching shear resistance when changing the eccentricity on the PT-cables in the section. To show the difference, factor k_{pb} was not taken into account. However, if k_{pb} was considered, the result for internal and edge column would have been constant due to the upper limitation of k_{pb}.

Corner columns are not included because the strands do not provide an uplifting force due to their centric placement in the cross-section. The formula in EN 1992 do not include the profile tendon, and all results will be constant.

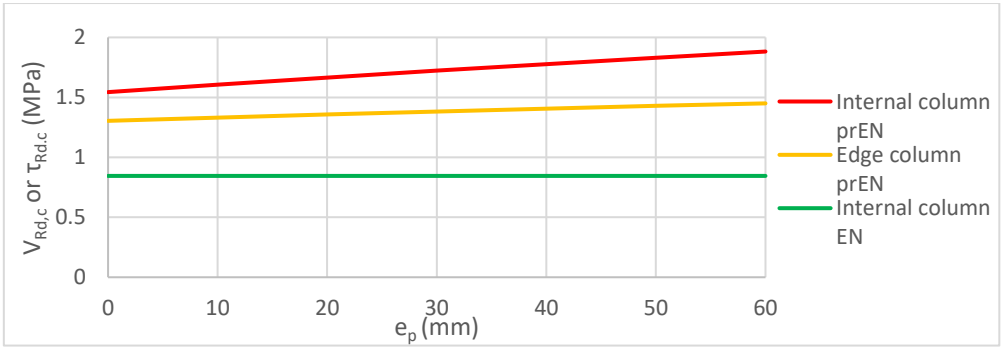

Figure 53 punching shear resistance due to eccentricity on the PT-cables in the section

10.3 Fiber-reinforcement

In the case of fiber reinforcement, the following parameters were varied:

- f_{ck} [Mpa] Characteristic compressive strength
- D [mm] Thickness of the slab
- f_{Ftud} Residual tensile strength

Figure 54 shows the punching shear resistance with and without FRC for different locations of the columns. The same amount of FRC was used in the different cases, which gives the corner and edge column a higher resistance due to a lower design shear force. Here class R5.0d is used. Complete calculations are given in Appendix A.

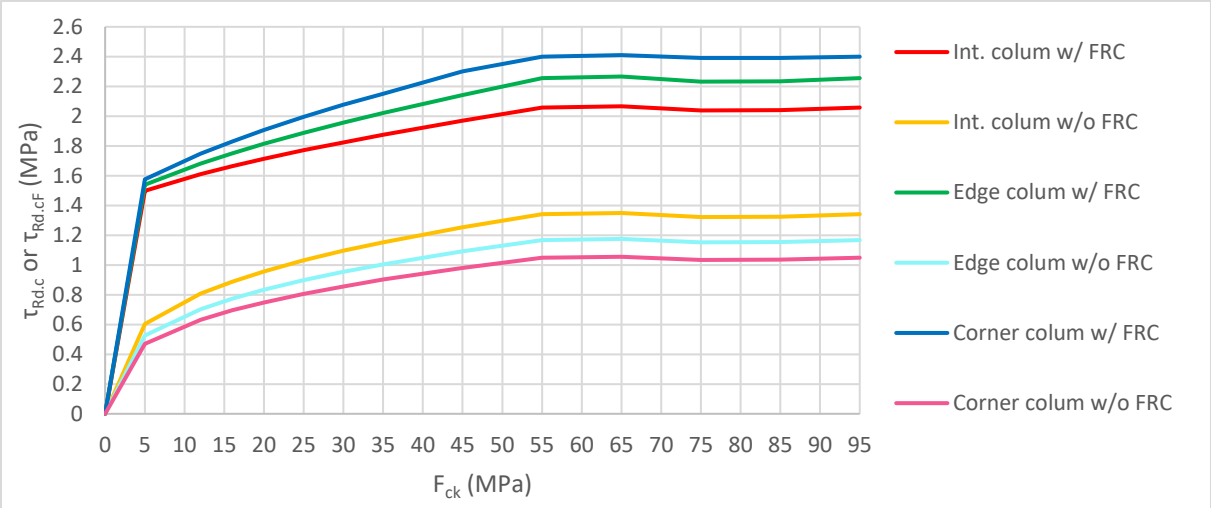

Figure 54 Punching shear resistance with and without FRC for different characteristic compressive strengths

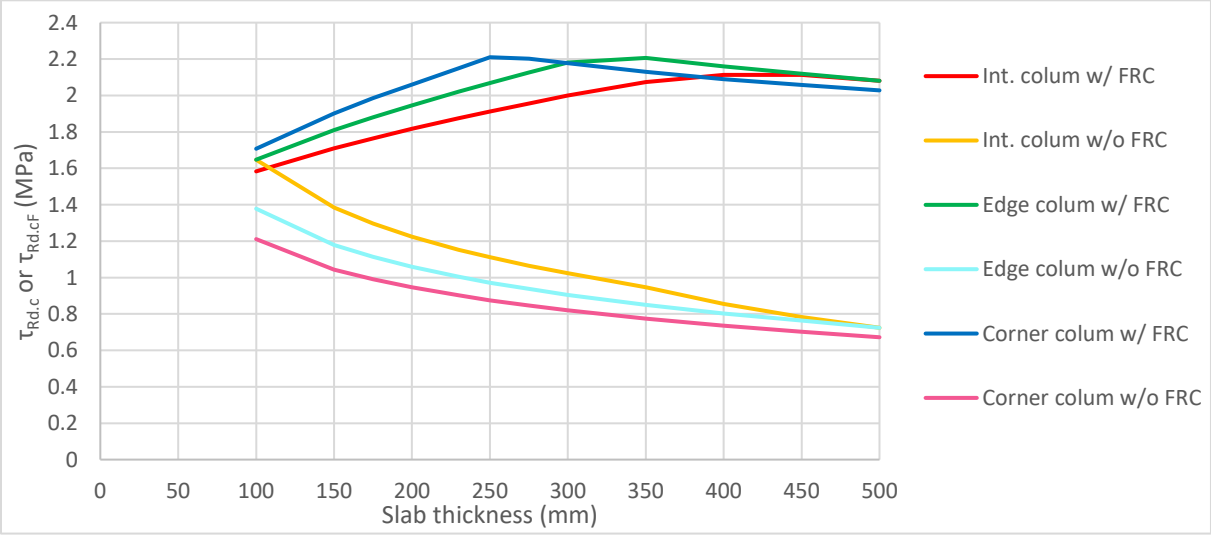

Figure 55 Punching shear resistance with and without FCR for different slab thickness

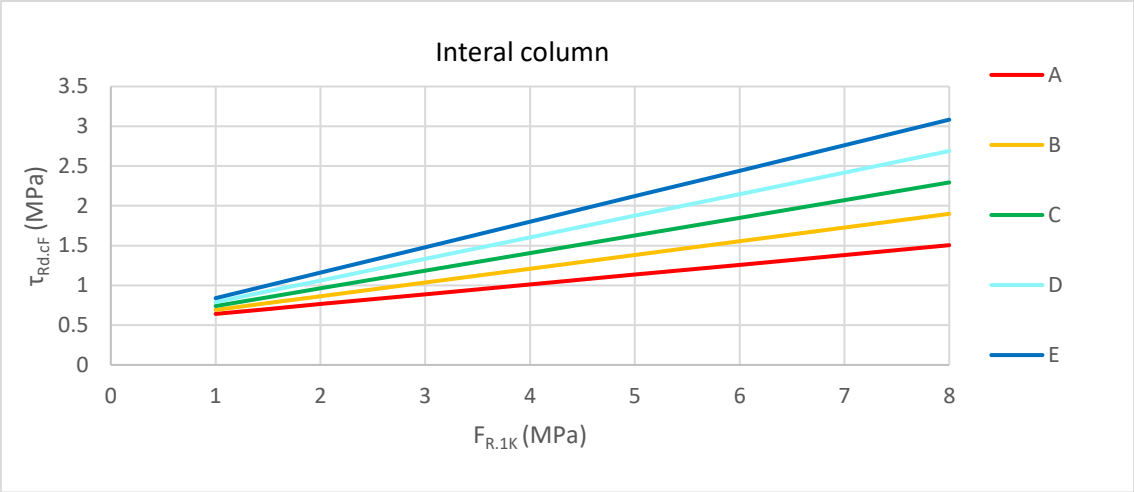

Figure 56 Punching shear resistance for different residual tensile strength classes

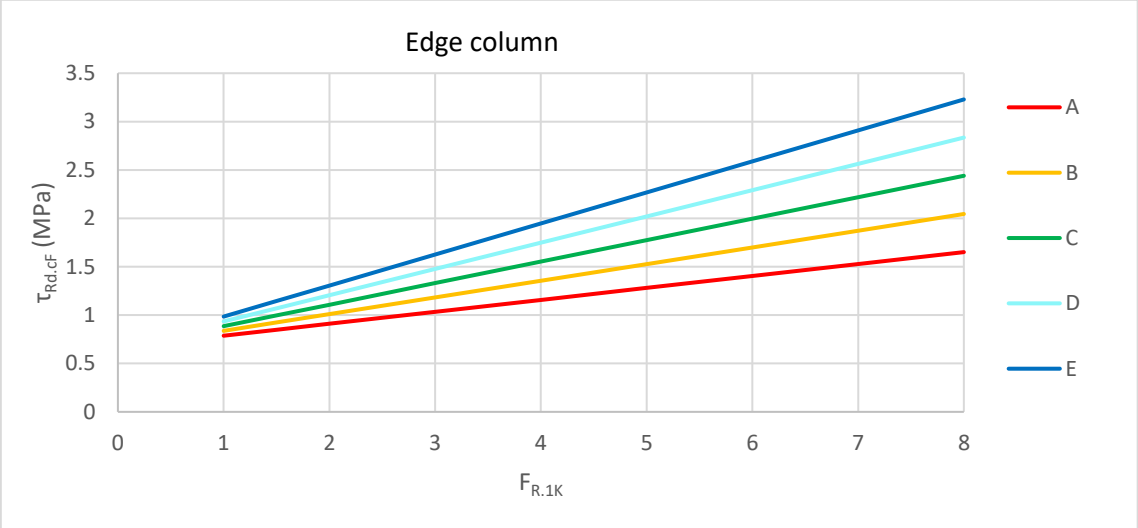

Figure 57 Punching shear resistance for different residual tensile strength classes

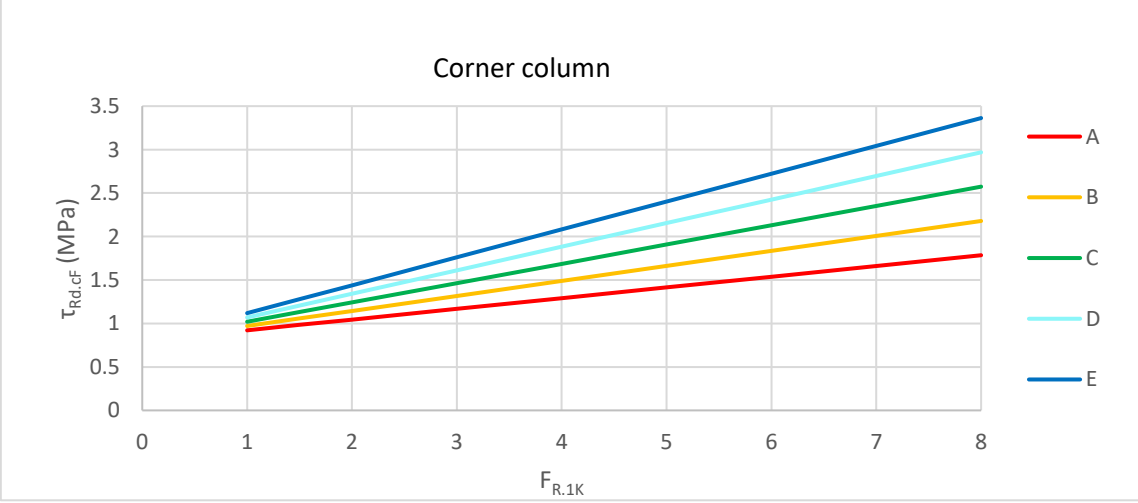

Figure 58 Punching shear resistance for different residual tensile strength classes

10.4 Shear reinforcement

In the case with shear reinforcement, only stirrups were used as shear reinforcement. The following parameters were varied

- f_{ck} [Mpa] Characteristic compressive strength
- A_{sw} [mm^2] Area of shear reinforcement

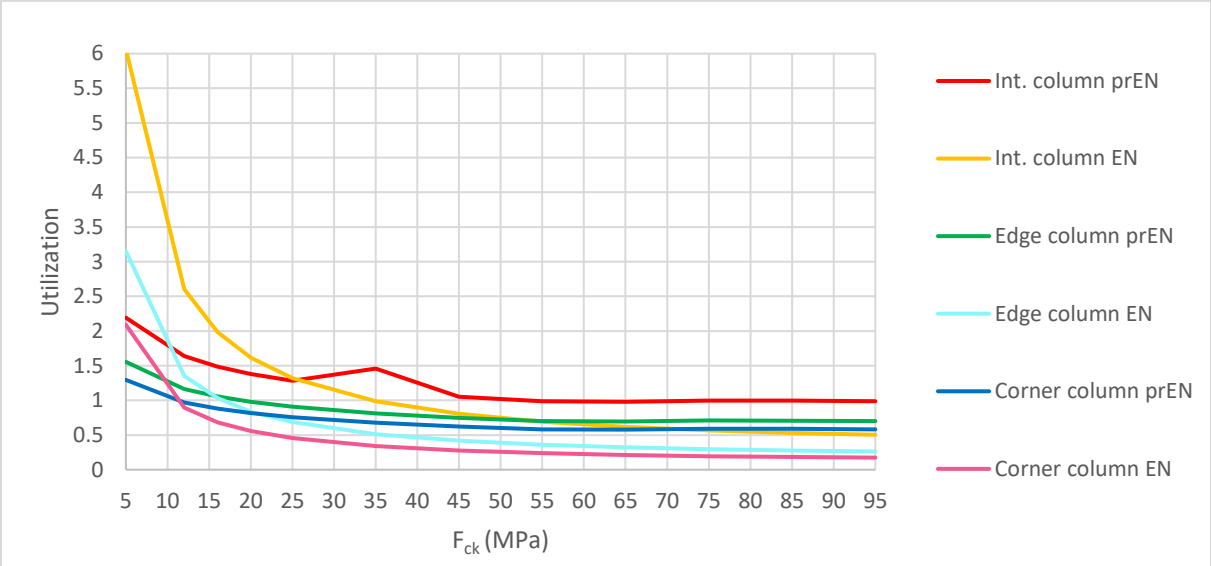

Figure 59 Utilization of shear capacity relative to designed shear force

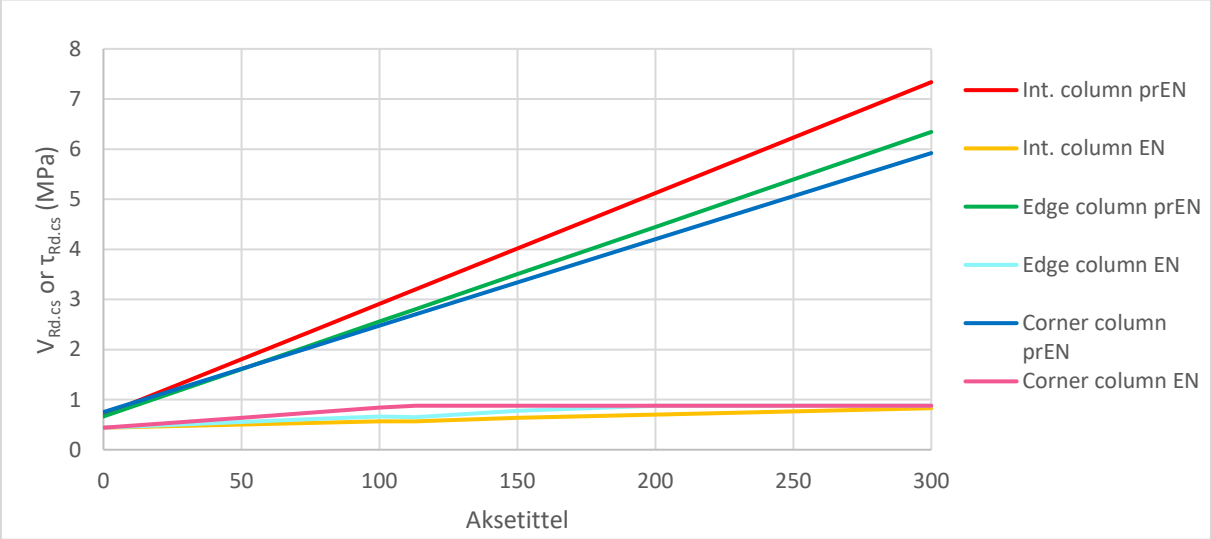

Figure 60 Punching shear resistance for increased shear reinforcement

10.5 PT, Fiber-reinforcement and shear reinforcement

In this case, stirrups were used as shear reinforcement, mono strands were used for prestressing and steel fiber was used for the fiber reinforcement.

- f_{ck} [Mpa] Characteristic compressive strength
- A_{sw} [mm^2] Area of shear reinforcement

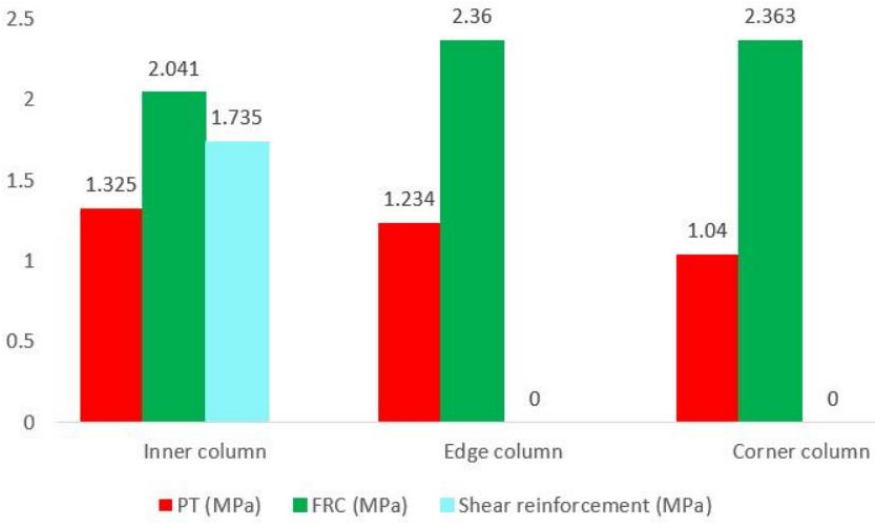

Figure 61 Contributions from PT, fiber reinforcement and shear reinforcement

10.6 Design shear force

Figure 62 to 64 shows the changes in the design shear force while increasing the characteristic compressive strength, slab thickness and column size. Complete calculations are given in Appendix A.

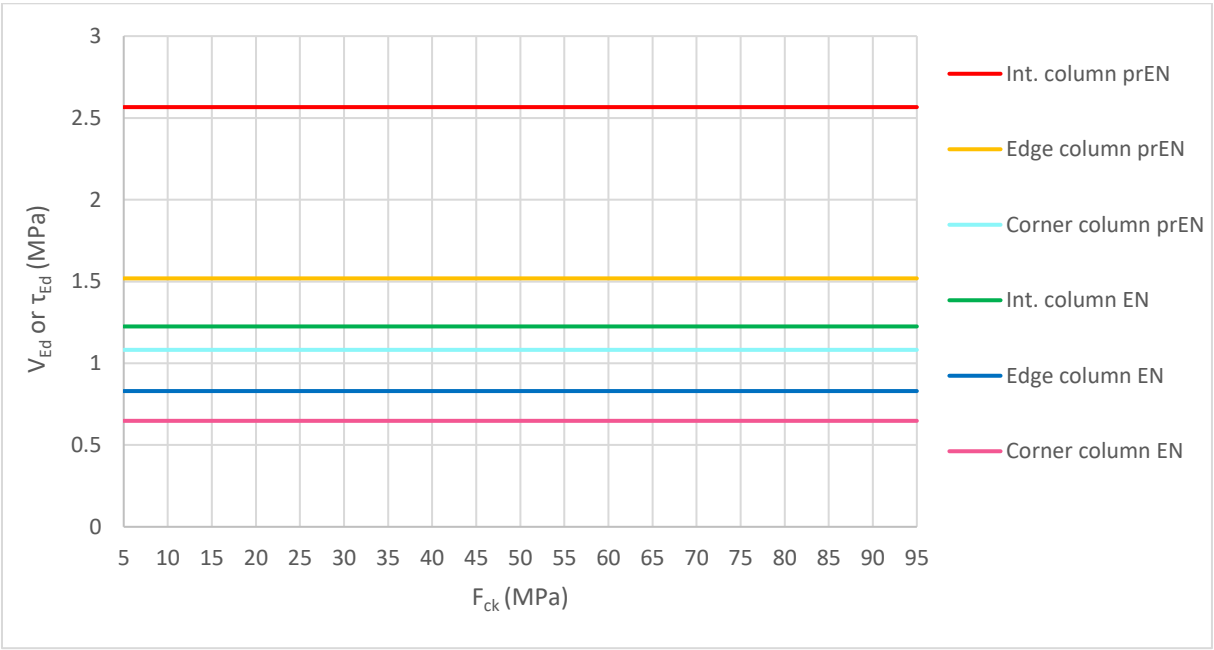

Figure 62 Design shear force relative to different characteristic compressive strengths

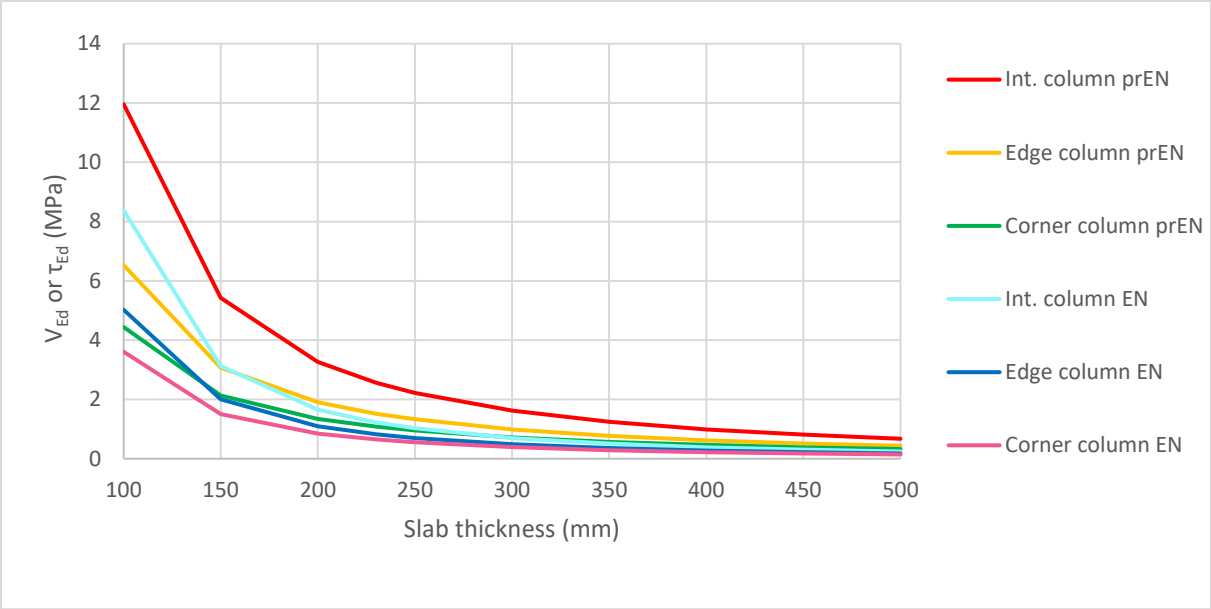

Figure 63 Design shear force for different slab thickness

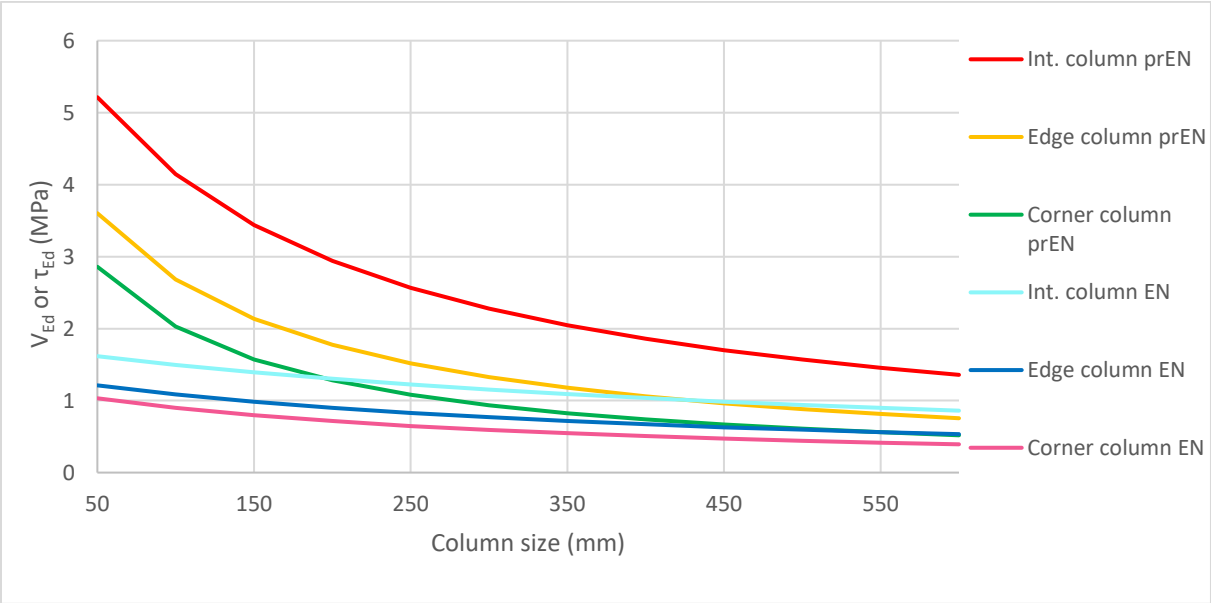

Figure 64 Design shear force for different column sizes

10.7 Results from FEM-Design

The following tables show the results from the FEM-Design analysis with and without post-tensioned tendons. An example of the detailed results is given below.

Reports are given in Appendix A.

	Internal column	Edge column	Corner column
V (kN)	630	202	76
V_{ed} (MPa)	1.2	0.93	0.76
$V_{rd,c}$ (MPa)	0.71	0.68	0.86
$V_{rd,max}$ (MPa)	4.09	4.09	4.09
Σ_{CP}	1.24	0.98	2.75
U_1	3296	1648	824
B	1.15	1.4	1.5

Table 5 Results from FEM-Design analysis with post-tensioned tendons

	Internal column	Edge column	Corner column
V (kN)	644	200	76
V_{Ed} (MPa)	1.23	0.94	0.75
$V_{Rd,c}$ (MPa)	0.59	0.59	0.59
$V_{Rd,max}$ (MPa)	4.09	4.09	4.09
σ_{cp}	0	0	0
u_1	3296	1648	824
β	1.15	1.4	1.5

Table 6 Results from FEM-Design analysis without post-tensioned tendons

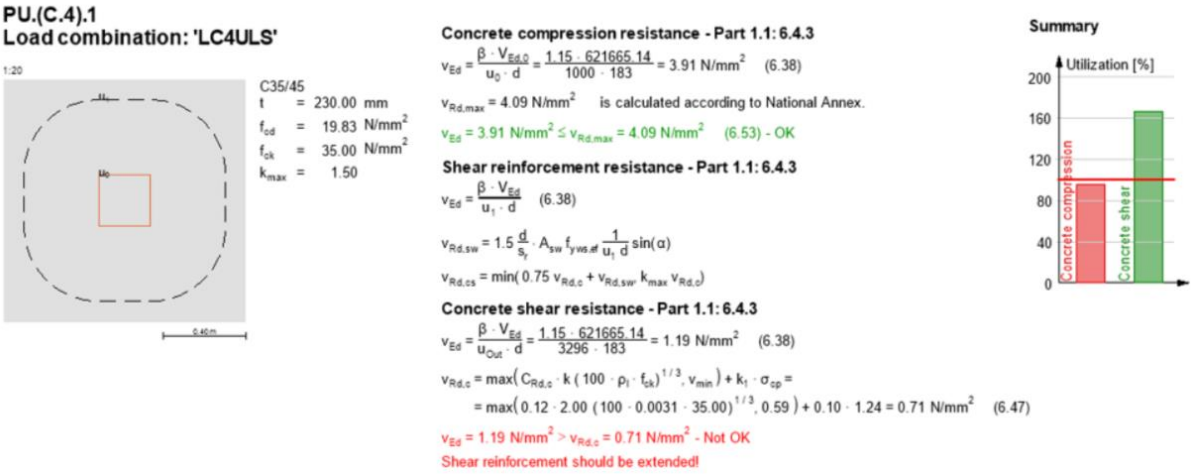

Figure 65 Detailed result of internal column from FEM-Design

10.8 Results from ADAPT

	Internal column	Edge column	Corner column
V (kN)	550	211	80
V_{Ed} (MPa)	1.97	0.426	0.76
$V_{Rd.c}$ (MPa)	0.672	0.672	0.672
u_1	3296	1648	824
β	1.15	1.4	1.5

Table 7 Results from ADAPT analysis with post-tensioned tendons

DISCUSSION

11 Parametric study

The following sections discusses the different cases from the parametric study and the parameters that were varied.

11.1 Without shear reinforcement

In the case without shear reinforcement the following parameters were varied: characteristic compressive strength, column size, thickness of the slab, factors related to aggregate size and reinforcement ratio. The first parameter, the compressive strength, resulted in an increased shear resistance with increased compressive strength, as would be expected. It is however important to note that the all the values from the results cannot be considered as realistic due to the practical aspects. For a normal concrete flat slab, the concrete quality will usually be between B30 and B45, both due to costs and structural behavior. This should be taken into account when the results are studied. The interesting aspect here were the observation on the placement of the columns. According to EN 1992-1-1 the placement of the columns did not affect the punching shear resistance, while in the prEN 1992-1-1 there was a difference due to the control perimeter. All values from EN 1992-1-1 were below minimum value.

The next parameter, column size, showed that the punching shear resistance decreased while increasing the column size according to prEN 1992-1-1, but the column size did not affect the resistance according to EN 1992-1-1. The observation that the resistance is lower with a larger column size is perhaps a contradicting one, but because the factor k_{pb} is included in prEN 1992-1-1, the punching shear resistance will decrease the lower this value is. The value of k_{pb} is a shear gradient enhancement coefficient that is depended on the size of the column, and if the column size increases, the k_{pb} will decrease.

Thereafter different thicknesses of the slab were varied. The results show that the changes in the slab thickness decreased the punching shear resistance. It could be expected that a thicker member would have a higher punching shear resistance, but due to the nature of the formula, the resistance will in fact decrease when the value for d_v increases.

The parameters D_{lower} and k were also studied. D_{lower} is a parameter from prEN 1992-1-1 included in the formula for d_{dg}, while k is a factor from EN 1992-1-1. The results shows that the aggregate affects the punching shear resistance in prEN 1992-1-1, but in EN 1992-1-1 there are only two options for aggregate size, and therefore only two values are possible.

Last, the studied parameter was the reinforcement ratio. EN 1992-1-1 has a limit for reinforcement ratio at 0,02, while the maximum value according to prEN 1992-1-1 is reached at a higher reinforcement ratio. Although the results show that the punching shear resistance were increased with higher reinforcement ratios, other factors like design

guidelines for reinforcement, adequate spacing for casting and other practical aspects should also be implemented in the design.

11.2 Prestressing

In the case with post-tensioned mono strands, the following parameters were varied for circular and square columns: characteristic compressive strength, jacking force and cable eccentricity. The results showed that there was an increased resistance with increased compressive strength, as would be expected also in this case. However, it is important to note that all the values from the results cannot be considered as realistic due to the practical aspects.

Regarding the jacking force, the results showed that according to prEN 1992-1-1 there is a limit due to factor k_{pb}, while EN 1992-1-1 does not have this limitation. However, there are limiting factors that will prevent the jacking force of reaching a very high value, e.g. bursting of concrete.

The parameter that affected the punching shear resistance the least, was changing the eccentricity on the PT-cables in the section.

11.3 Fiber reinforcement

In the of case fiber reinforcement, the following parameters were varied: characteristic compressive strength, column size, thickness of the slab and residual tensile strength.

The results showed that there was an increased resistance with increased compressive strength, as would be expected also in this case. The limitations regarding the concrete strengths will also apply for this case.

One of the main observations was the development in shear resistance according to prEN 1992-1-1 when considering the slab thickness. The results showed that the punching shear resistance increased with FRC if the slab thickness increased, and without FRC the resistance decreased with an increased slab thickness.

11.4 With shear reinforcement

In the case without shear reinforcement the following parameters were varied: characteristic compressive strength and area of shear reinforcement. This particular case is maybe the one that is of least interest. This is because in the design, the shear reinforcement is chosen on the basis of the lack of residual shear resistance. That is, e.g. if the fiber reinforcement provides sufficient punching shear resistance, shear reinforcement will not be required.

11.5 Fiber-reinforcement with PT and shear reinforcement

The study showed that the fiber reinforcement had the greatest contribution to the punching shear resistance according to the proposed provisions in Eurocode 2. The shear reinforcement had the second greatest contribution, although this contribution will vary.

The purpose of the shear reinforcement is to account for the residual shear capacity and depending on the contribution from the fiber-reinforcement, post-tensioning and shear force, this value will therefore be different depending on the given case. If the contribution is e.g. sufficiently high from the fiber, the required amount of shear reinforcement will be lower/not required, because there will be a higher capacity in the slab to withstand the shear force.

12 Results from ADAPT and FEM-Design

One of the limitations when comparing the parametric study is that neither ADAPT or FEM-Design have implemented the design guidelines from prEN 1992-1-1. Therefore, the comparison between the hand calculations in Mathcad was only performed in accordance with EN 1992-1-1. In addition, the fiber-reinforcement was not included in the FE analysis because neither ADAPT or FEM-Design have implemented this in their software.

When comparing and validating the results from the analysis in FEM-Design and ADAPT, it was shown that deflections were lower with post-tensioned tendons, which is an expected result, and helps to validate the given results. The same observations were seen for other structural responses, e.g. moments in the flat slab.

When comparing the analysis, FEM-Design estimated higher stresses over the columns compared with the estimated stresses from ADAPT. There could be several reasons for this, such as how ADAPT calculates the full width of the column strips. Other govern parameters could be that ADAPT does not include the Norwegian National Annex, and that the input for the tendons are slightly different.

As an effect of the mesh refinement the results in a FE analysis converges to the theoretical solution. The problem is due to that certain places get infinite inner forces according to the theory, so the inner forces increase each time by refining the mesh. In practice, the singularity problem usually occurs at supports because they heavily influence the inner forces, e.g. negative moments, in ratio. This can, as discussed in Chapter 9, be solved with peak smoothing. However, when reviewing the results from the analysis there were no observations regarding singularity problems in the mesh, and no particularly high stress values in neither FEM-Design nor ADAPT. This is because the slab has a simplified geometry with no openings or discontinuity. Due to this, no measures were taken regarding singularity.

13 Comparison of parameters in prEN 1992-1-1 and EN 1992-1-1

Punching shear design was one of the chapters that had scientific and design concerns, and numerous works criticizing the consistency of the method for punching shear design according to EN 1992-1-1 have been published in the scientific literature. The following sections discusses some of the parameters and the changes that were implemented in the proposed provisions.

13.1 Critical control section

In EN 1992-1-1, the critical control section is set to be 2d from the column face, while the critical control section in the proposed provisions is decreased to 0.5d. This change has resulted in a higher design shear force in prEN 1992-1-1. The reason for the increased design shear force is due to a smaller critical control section, and therefore the distribution of the shear force will occur over a smaller area.

13.2 Beta value β

One of the most difficult procedures in prEN 1992-1-1 is how to calculate the coefficients β, accounting for concentrations of the shear forces. The approximated coefficients have remained the same, but the refined ones have changed. The implemented changes have resulted in a more conservative design shear force.

13.3 D_{lower}/k_2

D_{lower} is a parameter from prEN 1992-1-1 included in the formula for d_{dg} and describes the aggregate size. From the results it is observed that the punching shear resistance increases at higher values of d_{lower}. This is because a higher value of d_{lower} will provide a larger roughness in the failure zone.

EN 1992-1-1 accounts for the aggregate size in the factor k_2 which is included in the formula $C_{Rd.c}$. The values for k_2 is given in the Norwegian National Annex and only two values are possible, depending on the aggregate size. Therefore, the results only give two different values, hence increasing the aggregate size will not contribute to increased punching shear resistance. In prEN 1992-1-1 the results show that by increasing the aggregate size, the punching shear resistance will also increase. However, there is a given upper limit that states that d_{lower} cannot exceed 24mm. The factor k_2 is therefore not considered a govern parameter, and the factor d_{lower} is considered to have a relatively small contribution to the punching shear resistance.

According to prEN 1992-1-1 d_{dg} is a size parameter describing the failure zone roughness. This depends on the concrete type and its aggregate properties (Aurelio Muttoni F. F.-R., 2020).

K_2 is a factor from NS-EN 1992-1-1 included in the formula $C_{Rd.c}$. The values for k_2 is given in the Norwegian National Annex and only two values are given. If the aggregate size is less than 16mm, 0,15 shall be used. However, if the aggregate size is equal or greater than 16mm the value 0,18 shall be used (Norsk Standard, 2008).

13.4 KPB

K_{pb} is a shear gradient for the strength enhancement for punching due to the shear field gradient in the control section. This parameter was a new addition in prEN 1992-1-1 and is included in the punching shear resistance formula. The formula for K_{pb} includes the relationship between the reduced critical control section and the critical control section. Furthermore, the formula has limitation where the value can only be between 1 and 2.5.

For a slab with axial compression k_{pb} is multiplied with the pre-stressing forces and because k_{pb} has an upper limit, the stresses provided by the pre-stressing cannot exceed a certain value. In other words, k_{pb} ensures that the contribution from the pre-stressing is not fully utilized. If k_{pb} did not have an upper limit, the shear resistance would be significantly increased due to the full contribution from the pre-stressing.

CONCLUSION

Calculations performed in Mathcad have been performed in order to assess the structural behavior with respect to punching shear resistance of post-tensioned flat slabs with fiber-reinforcement. The study showed that the fiber-reinforcement had the greatest contribution to the punching shear resistance according to the proposed provisions in Eurocode 2. The shear reinforcement had the second greatest contribution, although this contribution will vary. The purpose of the shear reinforcement is to account for the residual shear capacity and depending on the contribution from the fiber reinforcement, post-tensioning and shear force, this value will therefore be different depending on the given case.

The study also showed that the punching shear resistance was lower for EN-1992-1-1 compared to prEN 1992-1-1. However, the proposed version will give a lower capacity because the design shear force is increased due to the decreased critical control section. This was observed for e.g. the slab thickness, where a thicker slab did not increase the resistance.

The results show that the aggregate affects the punching shear resistance in prEN 1992-1-1, but in EN 1992-1-1 there are only two options for aggregate size, and therefore only two values are possible.

The reinforcement ratio affects the resistance in the same manner for the proposed and current version, but it has no upper limit in the proposal. Consequently, reinforcement ratios exceeding 2% contributes to larger resistance in the proposal.

The punching shear resistance in post-tensioned flat slabs with fiber-reinforced is complex due to several reasons. The first being that the interaction between the different contributions are somehow intricate, and each contribution is governed by many parameters and factors. Due to this, it is important to understand the totality in the punching shear resistance in addition to the separate contributions.

When the design of a flat slab is performed, many factors play a role, and isolating the different parameters and factors can be somehow difficult because of the dependency between them. There is also another important aspect, which include the practical and economical aspects of the design. In theory, punching shear resistance can be increased through huge amounts of fiber, a very high concrete quality or very much conventional reinforcement. Due to budgets, reinforcement design guidelines and other limiting factors, it is important to keep in mind that a structural solution should also meet other demands than the punching shear resistance.

SUGGESTIONS FOR FURTHER WORK

When investigating the punching shear resistance in post-tensioned flat slabs with fiber-reinforcement, more case studies are suggested with the advantage of the relation to reality. The interaction between the different contributions to the punching shear resistance is complex theoretically, and more studies should be conducted to confirm the theoretical trends and observations. Especially for the contribution from the fiber reinforcement, beam tests should be done in order to get exact input values.

Another aspect of this subject that would be interesting to investigate are flat slabs with drop panels and footings. Often one of the solutions to increase the shear resistance is to use drop panels, and because the calculations are slightly different it would be of great advantage to investigate this more. In addition, the punching shear resistance around slab openings should also be studied. This is described thorough in prEN 1992-1-1.

Furthermore, the thesis only investigated the contribution from prestressing from unbonded tendons, and not bonded tendons. Both prEN 1992-1-1 and EN 1992-1-1 presents a different calculation method regarding bonded systems, and a comparison of the two would be beneficial in order to decide which structural solution is better in different cases.

Last, it is suggested to study other, and more complex load cases.

REFERENCES

ACI Committee 318. (2019). *Building Code Requirements for Structural Concrete (ACI 318-19).* Farmington Hills, MI: American Concrete Institute.

ADAPT. (2021, Mai 06). *Adapt Solutions*. Retrieved from Adapt Solutions: https://adaptsolutions.wordpress.com/adapt-builder/

Aurelio Muttoni, A. P. (2018). *PT-SC2-T1 D3BG - Background documents to prEN 1992-1-1.* Karlsruhe Institute of Technology.

Aurelio Muttoni, F. F.-R. (2020). *Updated Draft by SC2/WG1/CDG prEN 1992-1-1-D7 Working File (Rev. 7) 2020-11-16 AFTER SC2 FOR CEN-ENQUIRY.* Norsk Standard.

Carlos E.Ospina, D. M. (2017). *Punching shear of structural concrete slabs.* Philadelphia: fib.

Døssland, Å. (2008). *Fibre Reinforcement in Load Carrying Concrete Structures .* Trondheim: NTNU.

Ericsson, F. (2010). *Punching Shear in Reinforced Concrete - Slabs Supported on Edge Steel Columns.* Gøteborg: CHALMERS UNIVERSITY OF TECHNOLOGY.

fib, I. F. (2010). *Model Code Volume 1.* International Federation for Structural Concrete (fib).

fib, I. F. (2010). *Model Code Volume 2.* International Federation for Structural Concrete (fib).

G.Nawy, E. (2003). *PRESTRESSED CONCRETE A fundamental Approach.* New Jersey: Pearson.

Kanstad, T. (2020). *NB 38 Fiberarmert betong i bærende konstruksjoner.* Oslo: Norsk betongforening.

Long Nguyen-Mihn, M. R.-N.-P. (2012). Punching shear resistance of post-tensioned steel fiber reinforced concrete.

Löfgren, I. (2005). *Fibre-reinforced Concrete for Industrial Construction.* Göteborg: Chalmers University of Technology.

Norsk Standard. (2008). *Prosjektering av betongkonstruksjoner.* Oslo: Standard Norge.

Ranzi, R. I. (2018). *Design of prestressed conrete to Eurocode 2.* Boca Raton: CRC Press.

Sandbakk, S. (2011). *Fibre Reinforced Concrete: Evaluation of test methods and material development.* Trondheim: NTNU.

Sivertsen, M., & Tøsti, A. B. (2015). *Etteroppspent og fiberarmert flatedekke.* Trondheim: NTNU.

StruSoft. (2021, Juni 25.04.21). *FEM design*. Retrieved from https://strusoft.com/products/fem-design: https://strusoft.com/products/fem-design

Sørensen, S. I. (2013). *BETONGKONSTRUKSJONER Beregning og dimensjonering etter Eurocode 2.* Trondheim: Fagbokforlaget.

The concrete society . (2005). *Post-tensioned concrete floors: Design handbook Technical report No. 43.* Surrey: The concrete society .

Gjennomlokking - Innvendig søyle - EN

KONSTANTE PARAMETERE:

$\alpha_{cc} := 0.85$	En koeffisient som tar hensyn til virkninger av langtidslast på trykkfastheten samt ugunstige virkninger som er en følge av måten lasten påføres.	NA.3.1.6
$\gamma_c := 1.5$	Materialkoeffisient for betong	Tabell NA 2.1N
$\gamma_s := 1.15$	Materialkoeffisient for stål	Tabell NA 2.1N

TVERRSNITT DEKKE:

$d := 230\ mm$	Tverrsnittykkelse	
$c_{min} := 25\ mm$	Minste overdekning	NA.4.4N
$\Delta c_{dev} := 10\ mm$	Største tillatte negative avvik	NA.4.4.1.3
$c_{nom} := c_{min} + \Delta c_{dev} = 35\ mm$	Nominell overdekning	EN 4.4.1.1 (4.1)
$\varnothing_x := 12\ mm$	Stangdiameter i x-retning	
$\varnothing_y := 12\ mm$	Stangdiameter i y-retning	
$a_{s.x} := 200\ mm$	Senteravstand mellom slakkarmering	
$a_{s.y} := 200\ mm$	Senteravstand mellom slakkarmering	
$d_v := d - c_{nom} - \frac{\varnothing_x + \varnothing_y}{2} = 183\ mm$	Effektiv tverrsnittykkelse	EN 6.4.2 (6.32)

GEOMETRI SØYLE:

$b_x := 250\ mm$	Bredde x-retning på søyle
$b_y := 250\ mm$	Bredde y-retning på søyle

KRITISK KONTROLLSNITT:

$u_1 := 2 \cdot (b_x + b_y) + \pi \cdot 4\ d_v = 3299.646\ mm$	Omkrets av kritisk kontrollsnitt	EN 6.4.3 Figur 6.13
$u_0 := 2 \cdot (b_x + b_y) = 1000\ mm$	Omkrets redusert kritisk kontrollsnitt	EN 6.4.3 Figur 6.13

Gjennomlokking - Innvendig søyle - EN

BETONG:

$\begin{bmatrix} f_{ck} \\ f_{cd} \end{bmatrix} :=$ Fasthetsklasse: B35

$f_{ck} = 35\ \mathbf{MPa}$	Karakteristisk sylindertrykkfasthet	EN Tabell 3.1
$f_{cd} = 19.833\ \mathbf{MPa}$	Dimensjonerende betongtrykkfasthet	EN 3.1.6

ARMERING:

$\begin{bmatrix} f_{yk} \\ f_{yd} \end{bmatrix} :=$ Kamstål : B500NC

$f_{yk} = 500\ \mathbf{MPa}$	Karakteristisk strekkfasthet
$f_{yd} = 434.78\ \mathbf{MPa}$	Dimensjonerende strekkfasthet

---

LASTER:

$v_{Ed} := 643\ \mathbf{kN}$

DIMENSJONERENDE SKJÆRKRAFT, V_{Ed}:

$\beta := 1.15$	Beta-verdi for innvendig søyle	EN 6.4.3 Fig. 6.21N
$V_{Ed} := \beta \cdot \frac{v_{Ed}}{u_1 \cdot d_v} = 1.225\ \mathbf{MPa}$		EN 6.4.3 (6.38)

SPENNKABLER:

INFO:
Konsentrete kabler: 5 stk. over midt støtte i y-retning, c/c 140mm
Fordelte kabler: spenner i x-retning med c/c 500mm

$b_{s.x1} := 5000\ mm$ Lengde påvirket område av spennkabler i x-retning

$b_{s.y1} := 7500\ mm$ Lengde påvirket område av spennkabler i y-retning

$n_{y.1} := 5$ Antall konsentrerte kabler over spennet i y-retning

$n_{x.1} := \frac{b_{s.y1}}{500\ mm} = 15$ Antall fordelte kabler over spennet i x-retning

$P_{mt} := 178\ kN$ Oppspenningskraft med tap

$P_{mt.y1} := P_{mt} \cdot n_{y.1} = 890\ kN$

$P_{mt.x1} := P_{mt} \cdot n_{x.1} = 2670\ kN$

$\sigma_{cp.y} := \frac{P_{mt.y1}}{b_{s.x1} \cdot d} = 0.774\ MPa$ Spenning i tverrsnittet i y-retning EN 6.4.4

$\sigma_{cp.x} := \frac{P_{mt.x1}}{b_{s.y1} \cdot d} = 1.548\ MPa$ Spenning i tverrsnittet i x-retning EN 6.4.4

DIMENSJONERENDE SKJÆRKAPASITET, V_{Rdc}:

$k_2 := 0.18$ Tilslag med kornstørrelse lik eller større enn 16mm NA.6.4.4

$C_{Rd.c} := \frac{k_2}{\gamma_c} = 0.12$ Faktor NA.6.4.4(1)

$k := min\left(1 + \sqrt{\frac{200}{\frac{d_v}{mm}}}, 2\right) = 2$ Verdi av fordeling av det ubalanserte momentet overført EN 6.4.4

$b_{s.x} := b_x + 2 \cdot (3 \cdot d_v) = 1.348\ m$ Slakkarmering i platebredde 3dv til hver siden av søyle i x- og y-retning EN 6.4.4

$b_{s.y} := b_y + 2 \cdot (3 \cdot d_v) = 1.348\ m$

$A_{sl.x} := \pi \cdot \frac{\phi_x^{\ 2}}{4} \cdot \frac{b_{s.x}}{a_{s.x}} = 762.276\ mm^2$ Armerings areal innenfor platebredden 3dv til hver side av søyle EN 6.4.4

$A_{sl.y} := \pi \cdot \frac{\phi_x^{\ 2}}{4} \cdot \frac{b_{s.y}}{a_{s.y}} = 762.276\ mm^2$

$\rho_{l.x} := \frac{A_{sl.x}}{b_{s.x} \cdot d_v} = 0.00309$ Armeringsforhold i x-retning EN 6.4.4

$\rho_{l.y} := \frac{A_{sl.y}}{b_{s.y} \cdot d_v} = 0.00309$ Armeringsforhold i y-retning EN 6.4.4

$\rho_l := min\left(\sqrt{\rho_{l.x} \cdot \rho_{l.y}}, 0.02\right) = 0.00309$ EN 6.4.4

$k_1 := 0.1$ NA.6.4.4

$\sigma_{cp} := \frac{\sigma_{cp.x} + \sigma_{cp.y}}{2} = 1.161\ MPa$ Spenning i tverrsnittet fra spennkabler EN 6.4.4

$V_{min} := 0.035 \cdot k^{\frac{3}{2}} \cdot f_{ck}^{\frac{1}{2}} \cdot MPa^{\frac{1}{2}} = 0.586\ MPa$ NA.6.3N

$V_{Rd.c} := \max\left(C_{Rd.c} \cdot k \cdot \left(100 \cdot \rho_l \cdot f_{ck}\right)^{\frac{1}{3}} \cdot MPa^{\frac{2}{3}} + k_1 \cdot \sigma_{cp}, V_{min} + k_1 \cdot \sigma_{cp}\right) = 0.702\ MPa$ 6.4.4 (6.47)

$V_{Rd.c} \geq V_{Ed} = 0$ Behov for skjærarmering

SKJÆRARMERING, $V_{Rd.cs}$:

$v := 0.6 \cdot \left(1 - \frac{f_{ck}}{250\ MPa}\right)$ EN (6.6N)

$V_{Rd.max} := 0.4 \cdot v \cdot f_{cd} = 4.094\ MPa$ Maks skjærkraft

$V_{Ed1} := \frac{\beta \cdot v_{Ed}}{u_0 \cdot d_v} = 4.041\ MPa$

EN 6.4.5 (6.53)

$V_{Ed1} \leq V_{Rd.max} = 1$

$u_{out} := \frac{\beta \cdot v_{Ed}}{V_{Rd.c} \cdot d_v} = 5758.057\ mm$ Ytre kontrollperimeter EN 6.4.5 (6.54)

$d_{out} := \frac{u_{out} - 2 \cdot \left(b_x + b_y\right)}{2 \cdot \pi} = 757.268\ mm$ Avstand fra søyleliv til uout.

$s_0 := 60\ mm$ $s_0 \geq 0.3 \cdot d_v = 1$ Avstand fra søyleliv til første bøyle EN 9.4.3 Fig 9.10a

$s_{r.max} := 0.75 \cdot d_v = 137.25\ mm$ Radiell avstand mellom skjærarm. utover EN 9.4.3 Fig 9.10a

$s_r := 130\ mm$

$n_s := \frac{d_{out} - k \cdot d_v - s_0}{s_r} = 2.548$ Antall bøyler i et snitt fra søyleliv og ut til kontrollsnitt det er behov for skjærarmering

$1.5 \cdot d_v = 274.5\ mm$ Tangentiell avstand innenfor kontrollsnittet EN 9.4.3 (1)

$2 \cdot d_v = 366\ mm$ Tangentiell avstand utenfor kontrollsnittet EN 9.4.3 (1)

$s_{t.max} := 1.5 \cdot d_v = 274.5\ mm$ Tangentiell avstand innenfor kontrollsnittet EN 6.4.5 Fig 6.22

$n_t := \frac{u_1}{s_{t.max}} = 12.021$

$n_t := 12$

$s_t := \frac{u_1}{n_t} = 274.97\ mm$ Tangentiell avstand innenfor kontrollsnittet

$f_{ywd} := \frac{f_{yk}}{\gamma_s} = 434.783\ MPa$

$f_{ywd.ef} := min\left(250\ MPa + 0.25 \cdot d_v \cdot \frac{N}{mm^3}\right) = 295.75\ MPa$ EN 6.4.5(6.52)

$A_{sw} := \frac{\left(V_{Ed} - 0.75 \cdot V_{Rd.c}\right) \cdot s_r \cdot u_1}{1.5 \cdot f_{ywd.ef}} = 675.185\ mm^2$ Areal av skjærarmering langs omkretsen av et snitt EN 6.4.5

$A_{sw.min} := \frac{0.08 \cdot \sqrt{f_{ck}} \cdot MPa^{\frac{1}{2}} \cdot \left(s_r \cdot s_t\right)}{1.5 \cdot f_{yk}} = 22.558\ mm^2$ Min. arm av en armeringsstang EN 9.4.3 (9.11)

$\phi_v := \sqrt{\frac{A_{sw} \cdot 4}{n_t \cdot \pi}} = 8.464\ mm$ Diameter behov rundt kontrollsnitt

$\phi_v := 10\ mm$

$A_{sw} := n_t \cdot \frac{\pi \cdot \phi_v^{\ 2}}{4} = 942.478\ mm^2$

$\rho_{sw} := \frac{\pi \cdot \phi_v^{\ 2}}{4\ s_r \cdot s_t} = 0.0022$ Armeringsforhold

$V_{Rd.cs} := 0.75 \cdot V_{Rd.c} + 1.5 \cdot \frac{d}{s_r} \cdot A_{sw} \cdot f_{ywd.ef} \cdot \left(\frac{1}{u_1 \cdot d_v}\right) = 1.751\ MPa$ EN 6.4.5(6.52)

$k_{max} := 1.5$

$k_{max} \cdot V_{Rd.c} = 1.053\ MPa$

$V_{Rd.cs} \le k_{max} \cdot V_{Rd.c} = 0$ Ikke OK! EN 6.4.5(6.52)

$V_{Rd.cs} \ge V_{Ed} = 1$

Gjennomlokking - Rand søyle - EN

Disclaimer: Beregningsmetodene som presenteres her er tiltenkt å bli lest i sammenheng med NS-EN 1992-1-1 og det norske nasjonale tillegget, NA.

KONSTANTE PARAMETERE:

$\alpha_{cc} := 0.85$	En koeffisient som tar hensyn til virkninger av langtidslast på trykkfastheten samt ugunstige virkninger som er en følge av måten lasten påføres.	NA.3.1.6
$\gamma_c := 1.5$	Materialkoeffisient for betong	Tabell NA 2.1N
$\gamma_s := 1.15$	Materialkoeffisient for stål	Tabell NA 2.1N

TVERRSNITT DEKKE:

$d := 230\ mm$	Tverrsnittykkelse	
$c_{min} := 25\ mm$	Minste overdekning	NA.4.4N
$\Delta c_{dev} := 10\ mm$	Største tillatte negative avvik	NA.4.4.1.3
$c_{nom} := c_{min} + \Delta c_{dev} = 35\ mm$	Nominell overdekning	EN 4.4.1.1 (4.1)
$\varnothing_x := 12\ mm$	Stangdiameter i x-retning	
$\varnothing_y := 12\ mm$	Stangdiameter i y-retning	
$a_{s.x} := 200\ mm$	Senteravstand mellom slakkarmering	
$a_{s.y} := 200\ mm$	Senteravstand mellom slakkarmering	
$d_v := d - c_{nom} - \frac{\varnothing_x + \varnothing_y}{2} = 183\ mm$	Effektiv tverrsnittykkelse	EN 6.4.2 (6.32)

GEOMETRI SØYLE:

$b_x := 250\ mm$	Bredde x-retning på søyle	
$b_y := 250\ mm$	Bredde y-retning på søyle	

KRITISK KONTROLLSNITT:

$u_1 := 2 \cdot b_x + b_y + \frac{\pi \cdot 4\ d_v}{2} = 1899.823\ mm$	Omkrets av kritisk kontrollsnitt	EN 6.4.3 Figur 6.13
$u_0 := 2 \cdot b_x + b_y = 750\ mm$	Omkrets redusert kritisk kontrollsnitt	EN 6.4.3 Figur 6.13

Gjennomlokking - Rand søyle - EN

BETONG:

$\begin{bmatrix} f_{ck} \\ f_{cd} \end{bmatrix} :=$ Fasthetsklasse: B35

$f_{ck} = 35\ \mathbf{MPa}$	Karakteristisk sylindertrykkfasthet	EN Tabell 3.1
$f_{cd} = 19.833\ \mathbf{MPa}$	Dimensjonerende betongtrykkfasthet	EN 3.1.6

ARMERING:

$\begin{bmatrix} f_{yk} \\ f_{yd} \end{bmatrix} :=$ Kamstål : B500NC

$f_{yk} = 500\ \mathbf{MPa}$	Karakteristisk strekkfasthet
$f_{yd} = 434.78\ \mathbf{MPa}$	Dimensjonerende strekkfasthet

---

LASTER:

$v_{Ed} := 206\ \mathbf{kN}$

DIMENSJONERENDE SKJÆRKRAFT, V_{Ed}:

$\beta := 1.4$	Beta-verdi for innvendig søyle	EN 6.4.3 Fig. 6.21N
$V_{Ed} := \beta \cdot \frac{v_{Ed}}{u_1 \cdot d_v} = 0.83\ \mathbf{MPa}$		EN 6.4.3 (6.38)

SPENNKABLER:

INFO:
Konsentrerte kabler: 3 stk. over støtte på rand, c/c 140mm
Fordelte kabler: spenner i x-retning med c/c 500mm

$b_{s.x1} := 2500\ mm - 150\ mm = 2350\ mm$ Lengde påvirket område av spennkabler i x-retning

$b_{s.y1} := 7500\ mm$ Lengde påvirket område av spennkabler i y-retning

$n_y := 3$ Antall konsentrerte kabler over spennet i y-retning

$n_x := \frac{b_{s.y1}}{500\ mm} = 15$ Antall fordelte kabler over spennet i x-retning

$P_{mt} := 178\ kN$ Oppspenningskraft med tap

$P_{mt.y} := P_{mt} \cdot n_y = 534\ kN$

$P_{mt.x} := P_{mt} \cdot n_x = 2670\ kN$

$\sigma_{cp.y} := \frac{P_{mt.y}}{b_{s.x1} \cdot d} = 0.988\ MPa$ Spenning i tverrsnittet i y-retning EN 6.4.4

$\sigma_{cp.x} := \frac{P_{mt.x}}{b_{s.y1} \cdot d} = 1.548\ MPa$ Spenning i tverrsnittet i x-retning EN 6.4.4

DIMENSJONERENDE SKJÆRKAPASITET, V_{Rdc}:

$k_2 := 0.18$ Tilslag med kornstørrelse lik eller større enn 16mm NA.6.4.4

$C_{Rd.c} := \frac{k_2}{\gamma_c} = 0.12$ Faktor NA.6.4.4(1)

$k := min\left(1 + \sqrt{\frac{200}{\frac{d_v}{mm}}}, 2\right) = 2$ Verdi av fordeling av det ubalanserte momentet overført EN 6.4.4

$b_{s.x} := \left(3 \cdot d_v\right) + b_x = 799\ mm$ Slakkarmering i platebredde 3dv til hver siden av søyle i x- og y-retning EN 6.4.4

$b_{s.y} := 3 \cdot b_y = 750\ mm$

$A_{sl.x} := \pi \cdot \frac{\phi_x^{\,2}}{4} \cdot \frac{b_{s.x}}{a_{s.x}} = 451.824\ mm^2$ Armerings areal innenfor platebredden 3dv til hver side av søyle EN 6.4.4

$A_{sl.y} := \pi \cdot \frac{\phi_x^{\,2}}{4} \cdot \frac{b_{s.y}}{a_{s.y}} = 424.115\ mm^2$

$\rho_{l.x} := \frac{A_{sl.x}}{b_{s.x} \cdot d_v} = 0.00309$	Armeringsforhold i x-retning	EN 6.4.4
$\rho_{l.y} := \frac{A_{sl.y}}{b_{s.y} \cdot d_v} = 0.00309$	Armeringsforhold i y-retning	EN 6.4.4
$\rho_l := min\left(\sqrt{\rho_{l.x} \cdot \rho_{l.y}}, 0.02\right) = 0.00309$		EN 6.4.4
$k_1 := 0.1$		NA.6.4.4
$\sigma_{cp} := \frac{\sigma_{cp.x} + \sigma_{cp.y}}{2} = 1.268\ MPa$	Spenning i tverrsnittet fra spennkabler	EN 6.4.4

$V_{min} := 0.035 \cdot k^{\frac{3}{2}} \cdot f_{ck}^{\frac{1}{2}} \cdot MPa^{\frac{1}{2}} = 0.586\ MPa$ NA.6.3N

$V_{Rd.c} := \max\left(C_{Rd.c} \cdot k \cdot \left(100 \cdot \rho_l \cdot f_{ck}\right)^{\frac{1}{3}} \cdot MPa^{\frac{2}{3}} + k_1 \cdot \sigma_{cp}, V_{min} + k_1 \cdot \sigma_{cp}\right) = 0.712\ MPa$ 6.4.4 (6.47)

$V_{Rd.c} \geq V_{Ed} = 0$ Behov for skjærarmering

SKJÆRARMERING, $V_{Rd.cs}$:

$$v := 0.6 \cdot \left(1 - \frac{f_{ck}}{250\ MPa}\right)$$ EN (6.6N)

$V_{Rd.max} := 0.4 \cdot v \cdot f_{cd} = 4.094\ MPa$ Maks skjærkraft

$$V_{Ed1} := \frac{\beta \cdot v_{Ed}}{u_0 \cdot d_v} = 2.101\ MPa$$

EN 6.4.5 (6.53)

$V_{Ed1} \le V_{Rd.max} = 1$

$$u_{out} := \frac{\beta \cdot v_{Ed}}{V_{Rd.c} \cdot d_v} = 2212.017\ mm$$ Ytre kontrollperimeter EN 6.4.5 (6.54)

$$d_{out} := \frac{\left(u_{out} - 2 \cdot b_x - b_y\right)}{\pi} = 465.375\ mm$$ Avstand fra søyleliv til uout.

$s_0 := 60\ mm$ $s_0 \ge 0.3 \cdot d_v = 1$ Avstand fra søyleliv til første bøyle EN 9.4.3 Fig 9.10a

$s_{r.max} := 0.75 \cdot d_v = 137.25\ mm$ Radiell avstand mellom skjærarm. utover EN 9.4.3 Fig 9.10a

$s_r := 130\ mm$

$$n_s := \frac{d_{out} - k \cdot d_v - s_0}{s_r} = 0.303$$ Antall bøyler i et snitt fra søyleliv og ut til kontrollsnitt det er behov for skjærarmering

$1.5 \cdot d_v = 274.5\ mm$ Tangentiell avstand innenfor kontrollsnittet EN 9.4.3 (1)

$2 \cdot d_v = 366\ mm$ Tangentiell avstand utenfor kontrollsnittet EN 9.4.3 (1)

$s_{t.max} := 1.5 \cdot d_v = 274.5\ mm$ Tangentiell avstand innenfor kontrollsnittet EN 6.4.5 Fig 6.22

$$n_t := \frac{u_1}{s_{t.max}} = 6.921$$

$n_t := 7$

$$s_t := \frac{u_1}{n_t} = 271.403\ mm$$ Tangentiell avstand innenfor kontrollsnittet

$$f_{ywd} := \frac{f_{yk}}{\gamma_s} = 434.783\ MPa$$

$$f_{ywd.ef} := min\left(250\ MPa + 0.25 \cdot d_v \cdot \frac{N}{mm^3}\right) = 295.75\ MPa$$ EN 6.4.5(6.52)

$$A_{sw} := \frac{\left(V_{Ed} - 0.75 \cdot V_{Rd.c}\right) \cdot s_r \cdot u_1}{1.5 \cdot f_{ywd.ef}} = 164.339\ mm^2$$

Areal av skjærarmering langs omkretsen av et snitt

EN 6.4.5

$$A_{sw.min} := \frac{0.08 \cdot \sqrt{f_{ck}} \cdot MPa^{\frac{1}{2}} \cdot \left(s_r \cdot s_t\right)}{1.5 \cdot f_{yk}} = 22.265\ mm^2$$

Min. arm av en armeringsstang

EN 9.4.3 (9.11)

$$\phi_v := \sqrt{\frac{A_{sw} \cdot 4}{n_t \cdot \pi}} = 5.467\ mm$$

Diameter behov rundt kontrollsnitt

$$\phi_v := 8\ mm$$

$$A_{sw} := n_t \cdot \frac{\pi \cdot \phi_v^{\,2}}{4} = 351.858\ mm^2$$

$$\rho_{sw} := \frac{\pi \cdot \phi_v^{\,2}}{4\ s_r \cdot s_t} = 0.00142$$

Armeringsforhold

$$V_{Rd.cs} := 0.75 \cdot V_{Rd.c} + 1.5 \cdot \frac{d}{s_r} \cdot A_{sw} \cdot f_{ywd.ef} \cdot \left(\frac{1}{u_1 \cdot d_v}\right) = 1.329\ MPa$$

EN 6.4.5(6.52)

$$k_{max} := 1.5$$

$$k_{max} \cdot V_{Rd.c} = 1.069\ MPa$$

$$V_{Rd.cs} \le k_{max} \cdot V_{Rd.c} = 0$$

EN 6.4.5(6.52)

$$V_{Rd.cs} \ge V_{Ed} = 1$$

Gjennomlokking - Hjørne søyle - EN

Disclaimer: Beregningsmetodene som presenteres her er tiltenkt å bli lest i sammenheng med NS-EN 1992-1-1 og det norske nasjonale tillegget, NA.

KONSTANTE PARAMETERE:

$\alpha_{cc} := 0.85$	En koeffisient som tar hensyn til virkninger av langtidslast på trykkfastheten samt ugunstige virkninger som er en følge av måten lasten påføres.	NA.3.1.6
$\gamma_c := 1.5$	Materialkoeffisient for betong	Tabell NA 2.1N
$\gamma_s := 1.15$	Materialkoeffisient for stål	Tabell NA 2.1N

TVERRSNITT DEKKE:

$d := 230\ mm$	Tverrsnittykkelse	
$c_{min} := 25\ mm$	Minste overdekning	NA.4.4N
$\Delta c_{dev} := 10\ mm$	Største tillatte negative avvik	NA.4.4.1.3
$c_{nom} := c_{min} + \Delta c_{dev} = 35\ mm$	Nominell overdekning	EN 4.4.1.1 (4.1)
$\varnothing_x := 12\ mm$	Stangdiameter i x-retning	
$\varnothing_y := 12\ mm$	Stangdiameter i y-retning	
$a_{s.x} := 200\ mm$	Senteravstand mellom slakkarmering	
$a_{s.y} := 200\ mm$	Senteravstand mellom slakkarmering	
$d_v := d - c_{nom} - \frac{\varnothing_x + \varnothing_y}{2} = 183\ mm$	Effektiv tverrsnittykkelse	EN 6.4.2 (6.32)

GEOMETRI SØYLE:

$b_x := 250\ mm$	Bredde x-retning på søyle	
$b_y := 250\ mm$	Bredde y-retning på søyle	

KRITISK KONTROLLSNITT:

KRITISK KONTROLLSNITT:

$u_1 := b_x + b_y + \frac{\pi \cdot 4\ d_v}{4} = 1074.911\ mm$	Omkrets av kritisk kontrollsnitt	EN 6.4.3 Figur 6.13
$u_0 := b_x + b_y = 500\ mm$	Omkrets redusert kritisk kontrollsnitt	EN 6.4.3 Figur 6.13

BETONG:

$\begin{bmatrix} f_{ck} \\ f_{cd} \end{bmatrix} :=$ Fasthetsklasse: B35

$f_{ck} = 35\ \mathbf{MPa}$	Karakteristisk sylindertrykkfasthet	EN Tabell 3.1
$f_{cd} = 19.833\ \mathbf{MPa}$	Dimensjonerende betongtrykkfasthet	EN 3.1.6

ARMERING:

$\begin{bmatrix} f_{yk} \\ f_{yd} \end{bmatrix} :=$ Kamstål : B500NC

$f_{yk} = 500\ \mathbf{MPa}$	Karakteristisk strekkfasthet
$f_{yd} = 434.78\ \mathbf{MPa}$	Dimensjonerende strekkfasthet

---

LASTER:

$v_{Ed} := 85\ \mathbf{kN}$

DIMENSJONERENDE SKJÆRKRAFT, V_{Ed}:

$\beta := 1.5$	Beta-verdi for innvendig søyle	EN 6.4.3 Fig. 6.21N
$V_{Ed} := \beta \cdot \frac{v_{Ed}}{u_1 \cdot d_v} = 0.648\ \mathbf{MPa}$		EN 6.4.3 (6.38)

SPENNKABLER:

INFO:
Konsentrerte kabler: 3 stk. over støtte på rand, c/c 140mm
Fordelte kabler: spenner i x-retning med c/c 500mm

$b_{s.x1} := 2500\ mm - 150\ mm = 2350\ mm$ Lengde påvirket område av spennkabler i x-retning

$b_{s.y1} := 4000\ mm - 150\ mm = 3850\ mm$ Lengde påvirket område av spennkabler i y-retning

$n_y := 3$ Antall konsentrerte kabler over spennet i y-retning

$n_x := \frac{b_{s.y1}}{500\ mm} = 7.7$ Antall fordelte kabler over spennet i x-retning

$P_{mt} := 178\ kN$ Oppspenningskraft med tap

$P_{mt.y} := P_{mt} \cdot n_y = 534\ kN$

$P_{mt.x} := P_{mt} \cdot n_x = 1370.6\ kN$

$\sigma_{cp.y} := \frac{P_{mt.y}}{b_{s.x1} \cdot d} = 0.988\ MPa$ Spenning i tverrsnittet i y-retning EN 6.4.4

$\sigma_{cp.x} := \frac{P_{mt.x}}{b_{s.y1} \cdot d} = 1.548\ MPa$ Spenning i tverrsnittet i x-retning EN 6.4.4

DIMENSJONERENDE SKJÆRKAPASITET, V_{Rdc}:

$k_2 := 0.18$ Tilslag med kornstørrelse lik eller større enn 16mm NA.6.4.4

$C_{Rd.c} := \frac{k_2}{\gamma_c} = 0.12$ Faktor NA.6.4.4(1)

$k := min\left(1 + \sqrt{\frac{200}{\frac{d_v}{mm}}}, 2\right) = 2$ Verdi av fordeling av det ubalanserte momentet overført EN 6.4.4

$b_{s.x} := b_x + (3 \cdot d_v) = 0.799\ m$ Slakkarmering i platebredde 3dv til hver siden av søyle i x- og y-retning EN 6.4.4

$b_{s.y} := b_y + (3 \cdot d_v) = 0.799\ m$

$A_{sl.x} := \pi \cdot \frac{\phi_x^{\,2}}{4} \cdot \frac{b_{s.x}}{a_{s.x}} = 451.824\ mm^2$ Armerings areal innenfor platebredden 3dv til hver side av søyle EN 6.4.4

$A_{sl.y} := \pi \cdot \frac{\phi_x^{\,2}}{4} \cdot \frac{b_{s.y}}{a_{s.y}} = 451.824\ mm^2$

$\rho_{l.x} := \frac{A_{sl.x}}{b_{s.x} \cdot d_v} = 0.00309$	Armeringsforhold i x-retning	EN 6.4.4
$\rho_{l.y} := \frac{A_{sl.y}}{b_{s.y} \cdot d_v} = 0.00309$	Armeringsforhold i y-retning	EN 6.4.4
$\rho_l := min\left(\sqrt{\rho_{l.x} \cdot \rho_{l.y}}, 0.02\right) = 0.00309$		EN 6.4.4
$k_1 := 0.1$		NA.6.4.4
$\sigma_{cp} := \frac{\sigma_{cp.x} + \sigma_{cp.y}}{2} = 1.268\ MPa$	Spenning i tverrsnittet fra spennkabler	EN 6.4.4

$V_{min} := 0.035 \cdot k^{\frac{3}{2}} \cdot f_{ck}^{\frac{1}{2}} \cdot \mathbf{MPa}^{\frac{1}{2}} = 0.586\ \mathbf{MPa}$ NA.6.3N

$V_{Rd.c} := \max\left(C_{Rd.c} \cdot k \cdot \left(100 \cdot \rho_l \cdot f_{ck}\right)^{\frac{1}{3}} \cdot \mathbf{MPa}^{\frac{2}{3}} + k_1 \cdot \sigma_{cp}, V_{min} + k_1 \cdot \sigma_{cp}\right) = 0.712\ \mathbf{MPa}$ 6.4.4 (6.47)

$V_{Rd.c} \geq V_{Ed} = 1$ Ikke behov for skjærarmering

SKJÆRARMERING, $V_{Rd.cs}$:

$$v := 0.6 \cdot \left(1 - \frac{f_{ck}}{250\ MPa}\right)$$ EN (6.6N)

$V_{Rd.max} := 0.4 \cdot v \cdot f_{cd} = 4.094\ MPa$ Maks skjærkraft

$$V_{Ed1} := \frac{\beta \cdot v_{Ed}}{u_0 \cdot d_v} = 0.929\ MPa$$

EN 6.4.5 (6.53)

$V_{Ed1} \le V_{Rd.max} = 1$

$$u_{out} := \frac{\beta \cdot v_{Ed}}{V_{Rd.c} \cdot d_v} = 977.92\ mm$$ Ytre kontrollperimeter EN 6.4.5 (6.54)

$$d_{out} := \frac{(u_{out} - b_x - b_y) \cdot 2}{\pi} = 304.254\ mm$$ Avstand fra søyleliv til uout.

$s_0 := 60\ mm$ $s_0 \ge 0.3 \cdot d_v = 1$ Avstand fra søyleliv til første bøyle EN 9.4.3 Fig 9.10a

$s_{r.max} := 0.75 \cdot d_v = 137.25\ mm$ Radiell avstand mellom skjærarm. utover EN 9.4.3 Fig 9.10a

$s_r := 130\ mm$

$$n_s := \frac{d_{out} - k \cdot d_v - s_0}{s_r} = -0.937$$ Antall bøyler i et snitt fra søyleliv og ut til kontrollsnitt det er behov for skjærarmering

$1.5 \cdot d_v = 274.5\ mm$ Tangentiell avstand innenfor kontrollsnittet EN 9.4.3 (1)

$2 \cdot d_v = 366\ mm$ Tangentiell avstand utenfor kontrollsnittet EN 9.4.3 (1)

$s_{t.max} := 1.5 \cdot d_v = 274.5\ mm$ Tangentiell avstand innenfor kontrollsnittet EN 6.4.5 Fig 6.22

$$n_t := \frac{u_1}{s_{t.max}} = 3.916$$

$n_t := 4$

$$s_t := \frac{u_1}{n_t} = 268.728\ mm$$ Tangentiell avstand innenfor kontrollsnittet

$$f_{ywd} := \frac{f_{yk}}{\gamma_s} = 434.783\ MPa$$

$$f_{ywd.ef} := min\left(250\ MPa + 0.25 \cdot d_v \cdot \frac{N}{mm^3}\right) = 295.75\ MPa$$ EN 6.4.5(6.52)

$$A_{sw} := \frac{\left(V_{Ed} - 0.75 \cdot V_{Rd.c}\right) \cdot s_r \cdot u_1}{1.5 \cdot f_{ywd.ef}} = 35.855\ mm^2$$

Areal av skjærarmering langs omkretsen av et snitt — EN 6.4.5

$$A_{sw.min} := \frac{0.08 \cdot \sqrt{f_{ck}} \cdot MPa^{\frac{1}{2}} \cdot \left(s_r \cdot s_t\right)}{1.5 \cdot f_{yk}} = 22.045\ mm^2$$

Min. arm av en armeringsstang — EN 9.4.3 (9.11)

$$\phi_v := \sqrt{\frac{A_{sw} \cdot 4}{n_t \cdot \pi}} = 3.378\ mm$$

Diameter behov rundt kontrollsnitt

$$\phi_v := 6\ mm$$

$$A_{sw} := n_t \cdot \frac{\pi \cdot \phi_v^{\,2}}{4} = 113.097\ mm^2$$

$$\rho_{sw} := \frac{\pi \cdot \phi_v^{\,2}}{4\ s_r \cdot s_t} = 0.00081$$

Armeringsforhold

$$V_{Rd.cs} := 0.75 \cdot V_{Rd.c} + 1.5 \cdot \frac{d}{s_r} \cdot A_{sw} \cdot f_{ywd.ef} \cdot \left(\frac{1}{u_1 \cdot d_v}\right) = 0.986\ MPa$$

EN 6.4.5(6.52)

$$k_{max} := 1.5$$

$$k_{max} \cdot V_{Rd.c} = 1.069\ MPa$$

$$V_{Rd.cs} \le k_{max} \cdot V_{Rd.c} = 1$$

EN 6.4.5(6.52)

$$V_{Rd.cs} \ge V_{Ed} = 1$$

Gjennomlokking - Innvendig søyle - prEN

Disclaimer: Beregningsmetodene som presenteres her er tiltenkt å bli lest i sammenheng med Eurokode 2 og det norske nasjonale tillegget. Det bemerkes her at den endelige versjonen av Eurokode 2 ikke var publisert ved utarbeidelsen av dette mathcadarket, og leseren bør bekrefte numeriske verdier gitt i denne metoden med den endelige versjonen av Eurokoden og det norske nasjonale tillegget.

KONSTANTE PARAMETERE:

$\alpha_{cc} := 0.85$	En koeffisient som tar hensyn til virkninger av langtidslast på trykkfastheten samt ugunstige virkninger som er en følge av måten lasten påføres.	NA.3.1.6
$\gamma_c := 1.5$	Materialkoeffisient for betong	Tabell NA 2.1N
$\gamma_v := 1.4$	Materialkoeffisient for skjær- og gjennomlokkingskapasitet uten skjærarmering. MERK: Ved dimensjonering i ulykkestilstand anvendes 1.15	Tabell 4.3(NDP)
$\gamma_s := 1.15$	Materialkoeffisient for stål	Tabell NA 2.1N

TVERRSNITT DEKKE:

$d := 230\ mm$	Tverrsnittykkelse	
$c_{min} := 25\ mm$	Minste overdekning	prEN 6.5.2.1
$\Delta c_{dev} := 10\ mm$	Største tillatte negative avvik	prEN 6.5.3
$c_{nom} := c_{min} + \Delta c_{dev} = 35\ mm$	Nominell overdekning	prEN 6.5.1(1)
$\phi_x := 12\ mm$	Stangdiameter i x-retning	
$\phi_y := 12\ mm$	Stangdiameter i y-retning	
$a_{s.x} := 200\ mm$	Senteravstand mellom slakkarmering i x-retning	
$a_{s.y} := 200\ mm$	Senteravstand mellom slakkarmering i y-retning	
$d_v := d - c_{nom} - \frac{\phi_x + \phi_y}{2} = 183\ mm$	Effektiv tverrsnittykkelse	prEN 8.4.2(1) (8.75)

GEOMETRI SØYLE:

$b_x := 250\ mm$	Bredde x-retning på søyle	
$b_y := 250\ mm$	Bredde y-retning på søyle	

KRITISK KONTROLLSNITT:

$b_{0.5} := 2 \cdot (b_x + b_y) + \pi \cdot d_v = 1574.911\ mm$	Omkrets av kritisk kontrollsnitt	prEN 8.4.2(2) Figur 8.18
$b_0 := 2 \cdot (b_x + b_y) = 1000\ mm$	Omkrets av redusert kritisk kontrollsnitt	CEN TC250 (C8.17) prEN 8.4.2(2) Figur 8.18

Gjennomlokking - Innvendig søyle - prEN

BETONG:

$\begin{bmatrix} f_{ck} \\ f_{cd} \end{bmatrix}$:= Fasthetsklasse: B35

$f_{ck} = 35$ MPa	Karakteristisk sylindertrykkfasthet	NS-EN 1992-1-1 Tabell 3.1
$f_{cd} = 19.833$ MPa	Dimensjonerende betongtrykkfasthet	NS-EN 1992-1-1 3.1.6

$D_{lower} := 16$ mm — Tilslag — NY EC2 8.2.1 (4)

$d_{dg} := \begin{cases} \text{if } f_{ck} \le 60\ MPa \\ \quad 16\ mm + D_{lower} \\ \text{else if } f_{ck} > 60\ MPa \\ \quad 16\ mm + D_{lower} \cdot \left(\frac{60}{f_{ck}}\right)^4 \cdot MPa^4 \end{cases} = 32\ mm$ — NY EC2 8.2.1 (4)

ARMERING:

$\begin{bmatrix} f_{yk} \\ f_{yd} \end{bmatrix}$:= Kamstål : B500NC

$f_{yk} = 500$ MPa	Karakteristisk strekkfasthet
$f_{yd} = 434.78$ MPa	Dimensjonerende strekkfasthet

LASTER:

$V_{Ed} := 643$ kN — Opptredende skjærkraft

DIMENSJONERENDE SKJÆRKRAFT, τ_{Ed}:

$\beta_e := 1.15$ — Beta-verdi for innvendig søyle — prEN 8.4.2 Tabell 8.3

$\tau_{Ed} := \beta_e \cdot \frac{V_{Ed}}{b_{0.5} \cdot d_v} = 2.566$ MPa — Dimensjonerende skjærkraft — prEN 8.4.2 (6)

SPENNKABLER, PT:

INFO:
Konsentrerte kabler: 5 stk. over midt støtte i y-retning, c/c 140mm.
Fordelte kabler: spenner i x-retning med c/c 500mm

$b_{s.x1} := 5000\ mm$	Lengde påvirket område av spennkabler i x-retning	
$b_{s.y1} := 7500\ mm$	Lengde påvirket område av spennkabler i y-retning	
$n_y := 5$	Antall konsentrerte kabler over spennet i y-retning	
$n_x := \frac{b_{s.y1}}{500\ mm} = 15$	Antall fordelte kabler over spennet i x-retning	
$e_{p.y} := 40\ mm$	Eksentrisitet på spennkabel over støtte i y-retning	NY EC2 8.4.3 (1)
$e_{p.x} := 55\ mm$	Eksentrisitet på spennkabel over støtte i x-retning	NY EC2 8.4.3 (1)
$P_{mt} := 178\ kN$	Oppspenningskraft med antatt tap	
$P_{mt.y} := P_{mt} \cdot n_y = 890\ kN$	Normalkraft i tverrsnittet i y-retning	
$P_{mt.x} := P_{mt} \cdot n_x = 2670\ kN$	Normalkraft i tverrsnittet i x-retning	
$\sigma_{d.y} := \frac{P_{mt.y}}{b_{s.x1} \cdot d} = 0.774\ MPa$	Spenning i tverrsnittet i y-retning	NY EC2 8.4.3 (1)
$\sigma_{d.x} := \frac{P_{mt.x}}{b_{s.y1} \cdot d} = 1.548\ MPa$	Spenning i tverrsnittet i x-retning	NY EC2 8.4.3 (1)

DIMENSJONERENDE SKJÆRKRAFT, τ_{Rdc}:

$$k_{pb1} := \left(3.6 \cdot \sqrt{1 - \frac{b_0}{b_{0.5}}}\right) = 2.175$$

Forbedringskoeffisient for skjærgradient for gjennomlokking — prEN 8.4.3 (1) (8.80)

$$1 \le k_{pb1} \le 2.5 = 1$$

$$\mu_p := 8$$

Koeffisient som hensyntar skjærkraft og bøyemoment i det kritiske kontrollsnittet — CEN TC250 (C8.4.19)

$$k_{N.y} := \sqrt{1 + 1.2 \cdot \frac{b_{0.5} \cdot |\sigma_{d.y}|}{\mu_p \cdot d_v \cdot \sqrt{f_{ck}} \cdot MPa^{\frac{1}{2}}} \cdot \left(1 + 6 \cdot \frac{e_{p.y}}{d}\right)} = 1.16$$

prEN 8.4.3 (4) (8.87)

$$k_{N.x} := \sqrt{1 + 1.2 \cdot \frac{b_{0.5} \cdot |\sigma_{d.x}|}{\mu_p \cdot d_v \cdot \sqrt{f_{ck}} \cdot MPa^{\frac{1}{2}}} \cdot \left(1 + 6 \cdot \frac{e_{p.x}}{d}\right)} = 1.35$$

prEN 8.4.3 (4) (8.87)

$$k_{pp.y} := k_{N.y} = 1.16$$

prEN 8.4.3 (4) (8.83)

$$k_{pp.x} := k_{N.x} = 1.35$$

prEN 8.4.3 (4) (8.83)

$$k_{pp} := \sqrt{k_{pp.y} \cdot k_{pp.x}} = 1.251$$

prEN 8.4.3 (4) (8.86)

$$k_{pb} := k_{pb1} \cdot k_{pp} = 2.722$$

$$k_{pb} := 2.5$$

Krav: $1 \le k_{pb} \le 2.5$ — prEN 8.4.3 (4) (8.80)

$$b_{s.x} := \left(3 \cdot d_v\right) \cdot 2 + b_x = 1348\ mm$$

$$b_{s.y} := \left(3 \cdot d_v\right) \cdot 2 + b_y = 1348\ mm$$

Slakkarmering med heft i x- og y-retning over bredden 3dv fra søyleliv — prEN 8.4.3 (4) (8.79)

$$A_{sl.x} := \pi \cdot \frac{\varnothing_x^{\,2}}{4} \cdot \frac{b_{s.x}}{a_{s.x}} = 762.276\ mm^2$$

Areal armering i x-retning

$$A_{sl.y} := \pi \cdot \frac{\varnothing_x^{\,2}}{4} \cdot \frac{b_{s.y}}{a_{s.y}} = 762.276\ mm^2$$

Areal armering i y-retning

$$\rho_{l.x} := \frac{A_{sl.x}}{b_{s.x} \cdot d_v} = 0.003$$

Armeringsforhold i x-retning — prEN 8.4.3 (4) (8.79)

$$\rho_{l.y} := \frac{A_{sl.y}}{b_{s.y} \cdot d_v} = 0.003$$

Armeringsforhold i y-retning — prEN 8.4.3 (4) (8.79)

$$\rho_l := \sqrt{\rho_{l.x} \cdot \rho_{l.y}} = 0.003$$

prEN 8.4.3 (4) (8.79)

$$\tau_{Rdc} := \min\left(\frac{0.6}{\gamma_v}\cdot k_{pb}\cdot\left(100\cdot\rho_l\cdot f_{ck}\cdot\frac{d_{dg}}{d_v}\right)^{\frac{1}{3}}\cdot MPa^{\frac{2}{3}}, \frac{0.6}{\gamma_v}\cdot\sqrt{f_{ck}}\cdot MPa^{\frac{1}{2}}\right) = 1.325\ MPa$$ prEN 8.4.2 (8.78)

FIBERBIDRAGET, $\tau_{Rd.cF}$:

$\eta_c := min\left(\frac{\tau_{Rdc}}{\tau_{Ed}}, 1\right) = 0.516$ Reduksjonskoeffisient for skjærkapasitet prEN L.8.4.3 (1)

$\eta_F := 1$ prEN L.8.4.3 (1)

$f_{Ftud1} := \frac{\tau_{Ed} - \eta_c\cdot\tau_{Rdc}}{\eta_F} = 1.881\ MPa$ Dimensjonerende reststrekkfasthet behov

Table L.2 – Residual strength classes for SFRC

Ductility classes	Characteristic residual flexural strength $f_{R,1k}$									Analytical formulae
	1,0	1,5	2,0	2,5	3,0	4,0	5,0	6,0	8,0	
a	0,5	0,8	1,0	1,3	1,5	2,0	2,5	3,0	4,0	$f_{R,3k} = 0,5f_{R,1k}$
b	0,7	1,1	1,4	1,8	2,1	2,8	3,5	4,2	5,6	$f_{R,3k} = 0,7f_{R,1k}$
c	0,9	1,4	1,8	2,3	2,7	3,6	4,5	5,4	7,2	$f_{R,3k} = 0,9f_{R,1k}$
d	1,1	1,7	2,2	2,8	3,3	4,4	5,5	6,6	8,8	$f_{R,3k} = 1,1f_{R,1k}$
e	1,3	2,0	2,6	3,3	3,9	5,2	6,5	7,8	10,4	$f_{R,3k} = 1,3f_{R,1k}$

NOTE 1: All strength classes apply unless a National Annex excludes specific classes.
NOTE 2: Intermediate classes can be used, if included in a National Annex.

Velger for videre beregning klasse D5. Må vurdere opp mot tester, dokumentasjoner og leverandør

$\gamma_{SF} := 1.5$ Materialfaktor fiber NB38 - 3.4.4

$\eta_F := 1$ Mangler forklaring?? for fiber prEN L.8.4.3 (1)

$k_0 := 1$ Kapasitetsfaktor prEN L.5.1.6.1 (4)

$F_{R.1k} := 5\ MPa$ Velger karakteristisk restbøyestrekkfasthet fiber, 0.5mm prEN L.5.1.2 (1)

$f_{R.3K} := 1.1\cdot F_{R.1k} = 5.5\ MPa$ Karakteristisk restbøyestrekkfasthet fiber, 2.5mm, duktilitetsklasse D. prEN L.5.1.2 (1)

$f_{Ftsd} := k_0\cdot 0.4\cdot\frac{F_{R.1k}}{\gamma_{SF}} = 1.333\ MPa$ Dimensjonerende reststrekkfasthet i bruksgrense prEN L.5.1.6.1 (2) (L.2)

$f_{Ftud} := k_0\cdot 0.37\cdot\frac{f_{R.3K}}{\gamma_{SF}} = 1.357\ MPa$ Dimensjonerende reststrekkfasthet i bruddgrense prEN L.5.1.6.1 (2) (L.3)

$\tau_{Rd.cF} := \eta_c\cdot\tau_{Rdc} + \eta_F\cdot f_{Ftud} = 2.041\ MPa$ prEN L.8.4.3 (L.23)

$\tau_{Rd.c.min} := \frac{11}{\gamma_v} \cdot \sqrt{\frac{f_{ck}}{f_{yd}} \cdot \frac{d_{dg}}{d_v}} \cdot MPa = 0.932\ MPa$ prEN 8.2.1 (4) (8.11)

$\tau_{Rd.cF} := \max\left(\eta_c \cdot \tau_{Rdc} + \eta_F \cdot f_{Ftud}, \eta_c \cdot \tau_{Rd.c.min} + f_{Ftud}\right) = 2.041\ MPa$ prEN L.8.4.3 (L.23)

$\tau_{Rd.cF} \geq \tau_{Ed} = 0$ Behov for skjærarmering!

SKJÆRARMERING, $\tau_{Rd.cs}$:

$\eta_c := \frac{\tau_{Rdc}}{\tau_{Ed}} = 0.516$ Reduksjonskoeffisient for skjærkapasitet prEN 8.4.4 (8.88)

$d_{v.out} := d_v - c_{nom} = 148\ mm$ Avstand mellom arm.lagene i OK og UK prEN 8.4.4 - Fig. 8.23

$b_{0.5.out} := b_{0.5} \cdot \left(\frac{1}{\eta_c}\right)^{\frac{3}{2}} \cdot \left(\frac{d_v}{d_{v.out}}\right)^{\frac{3}{2}} = 5834.836\ mm$ Ytre kontrollperimeter prEN 8.4.4 (8.94)

$d_{out} := \frac{b_{0.5.out} - 2 \cdot (b_x + b_y)}{2 \cdot \pi} = 769.488\ mm$ Avstand fra søyleliv til ytre kontrollsnitt

$s_0 := 60\ mm$ Krav: $0.3 \leq \frac{s_0}{d_v} \leq 0.5 = 1$ Avstand fra søyleliv til første bøyle prEN 12.5.1 Fig. 12.8a

$s_r := 0.67 \cdot d_v = 122.61\ mm$ prEN 8.4.4 (8.91)

$s_r := 120\ mm$ Avstand mellom bøyler utover

$n_s := \frac{d_{out} - 0.5 \cdot d_{v.out} - s_0}{s_r} = 5.296$ Antall bøyler i et snitt fra søyleliv og ut til kontrollsnitt det er behov for skjærarmering

$d_{sys} := 160\ mm$ Høyde på bøyle prEN 8.4.4 - Fig. 8.23

$\eta_{sys} := 1.15 \cdot \frac{d_{sys}}{d_v} + 0.63 \cdot \left(\frac{b_0}{d_v}\right)^{\frac{1}{4}} - 0.85 \cdot \frac{s_0}{d_{sys}} = 1.65$ prEN 8.4.4 (8.93)

$\tau_{Rd.max} := \eta_{sys} \cdot \tau_{Rdc} = 2.186\ MPa$ Maks skjærspenning prEN 8.4.4 (8.93)

$\tau_{Rd.max} \geq \tau_{Ed} = 0$

$\frac{\tau_{Ed}}{\tau_{Rd.max}} = 1.174$ Utnyttelse

$\eta_s := 0.8$ — prEN 8.4.4 (8.90)

$f_{ywd} := f_{yd} = 434.783\ MPa$

$\rho_w := \frac{\tau_{Ed}}{f_{ywd}} \cdot min\left(\frac{1-\eta_c^{\,2}}{\eta_s}, 1\right) = 0.00541$ — Armeringsforhold, behov — prEN 8.4.4 (8.91)

$\rho_w \cdot 100 = 0.541$

$1.5 \cdot d_v = 274.5\ mm$ — Tangentiell avstand innenfor 2dv

$3 \cdot d_v = 549\ mm$ — Tangentiell avstand utenfor 2dv

$s_{t.max} := 1.5 \cdot d_v = 0.275\ m$ — Maks tangentiell avstand — prEN 12.5.1 Fig. 12.8a

$b_{2dv} := 2 \cdot \left(b_x + b_y\right) + \pi \cdot 4 \cdot d_v = 3299.646\ mm$ — Omkrets kontrollsnitt 2dv

$n_t := \frac{b_{2dv}}{s_{t.max}} = 12.021$

$n_t := 12$

$s_t := \frac{b_{0.5}}{n_t} = 131.243\ mm$ — Tangentiell avstand ved kritisk kontrollsnitt 0.5dv

$d_{b.w} := \sqrt{s_r \cdot s_t \cdot \frac{4 \cdot \rho_w}{\pi}} = 10.415\ mm$ — Diameter bøyle — CEN TC250 Design ex.

$\phi_v := 10\ mm$

$A_{sw} := \frac{\pi \cdot \phi_v^{\,2}}{4} = 78.54\ mm^2$ — Arm. areal

$A_{sw.o} := A_{sw} \cdot n_t = 942.478\ mm^2$ — Arm. areal rundt et snitt

$\rho_{sw} := \frac{A_{sw}}{s_r \cdot s_t} = 0.00499$ — Armeringsforhold

$\eta_s := min\left(\sqrt{15 \cdot \frac{d_{dg}}{d_v}} \cdot \left(\frac{1}{\eta_c \cdot k_{pb}}\right)^{\frac{3}{2}} + \frac{d_v}{150 \cdot \phi_v}, 0.8\right) = 0.8$ — prEN 8.4.4 (8.90)

$\tau_{Rd.cs1} := \eta_c \cdot \tau_{Rdc} + \eta_s \cdot \rho_{sw} \cdot f_{ywd} + \eta_F \cdot f_{Ftud} = 3.776$ **MPa** prEN L.8.4.4 (8L.24)

$\tau_{Rd.csmin} := \rho_w \cdot f_{ywd} + \eta_F \cdot f_{Ftud} = 3.708$ **MPa** prEN L.8.4.4 (8L.24)

$\tau_{Rd.cs} := \max\left(\tau_{Rd.cs1}, \tau_{Rd.csmin}\right) = 3.776$ **MPa** prEN L.8.4.4 (8L.24)

$\tau_{Rd.cs} > \tau_{Ed} = 1$

Gjennomlokking - Rand søyle - prEN

Disclaimer: Beregningsmetodene som presenteres her er tiltenkt å bli lest i sammenheng med Eurokode 2 og det norske nasjonale tillegget. Det bemerkes her at den endelige versjonen av Eurokode 2 ikke var publisert ved utarbeidelsen av dette mathcadarket, og leseren bør bekrefte numeriske verdier gitt i denne metoden med den endelige versjonen av Eurokoden og det norske nasjonale tillegget.

KONSTANTE PARAMETERE:

$\alpha_{cc} := 0.85$	En koeffisient som tar hensyn til virkninger av langtidslast på trykkfastheten samt ugunstige virkninger som er en følge av måten lasten påføres.	NA.3.1.6
$\gamma_c := 1.5$	Materialkoeffisient for betong	Tabell NA 2.1N
$\gamma_v := 1.4$	Materialkoeffisient for skjær- og gjennomlokkingskapasitet uten skjærarmering. MERK: Ved dimensjonering i ulykkestilstand anvendes 1.15	Tabell 4.3(NDP)
$\gamma_s := 1.15$	Materialkoeffisient for stål	Tabell NA 2.1N

TVERRSNITT DEKKE:

$d := 230\ mm$	Tverrsnittykkelse	
$c_{min} := 25\ mm$	Minste overdekning	prEN 6.5.2.1
$\Delta c_{dev} := 10\ mm$	Største tillatte negative avvik	prEN 6.5.3
$c_{nom} := c_{min} + \Delta c_{dev} = 35\ mm$	Nominell overdekning	prEN 6.5.1(1)
$\varnothing_x := 12\ mm$	Stangdiameter i x-retning	
$\varnothing_y := 12\ mm$	Stangdiameter i y-retning	
$a_{s.x} := 200\ mm$	Senteravstand mellom slakkarmering i x-retning	
$a_{s.y} := 200\ mm$	Senteravstand mellom slakkarmering i y-retning	
$d_v := d - c_{nom} - \frac{\varnothing_x + \varnothing_y}{2} = 183\ mm$	Effektiv tverrsnittykkelse	prEN 8.4.2(1) (8.75)

GEOMETRI SØYLE:

$b_x := 250\ mm$	Bredde x-retning på søyle	
$b_y := 250\ mm$	Bredde y-retning på søyle	

KRITISK KONTROLLSNITT:

$b_{0.5} := 2\ b_x + b_y + \frac{\pi \cdot d_v}{2} = 1037.456\ mm$	Omkrets av kritisk kontrollsnitt	prEN 8.4.2(2) Figur 8.18
$b_0 := 2\ b_x + b_y = 750\ mm$	Omkrets av redusert kritisk kontrollsnitt	prEN 8.4.2(2) Figur 8.18

Gjennomlokking - Rand søyle - prEN

BETONG:

$\begin{bmatrix} f_{ck} \\ f_{cd} \end{bmatrix}$:= Fasthetsklasse: B35

$f_{ck} = 35$ MPa	Karakteristisk sylindertrykkfasthet	EN Tabell 3.1
$f_{cd} = 19.833$ MPa	Dimensjonerende betongtrykkfasthet	EN 3.1.6

$D_{lower} := 16$ mm — Tilslag — prEn 8.2.1 (4)

$d_{dg} := \begin{cases} \text{if } f_{ck} \le 60\ MPa \\ \quad 16\ mm + D_{lower} \\ \text{else if } f_{ck} > 60\ MPa \\ \quad 16\ mm + D_{lower} \cdot \left(\frac{60}{f_{ck}}\right)^4 \cdot MPa^4 \end{cases} = 32\ mm$ — prEN 8.2.1 (4)

ARMERING:

$\begin{bmatrix} f_{yk} \\ f_{yd} \end{bmatrix}$:= Kamstål : B500NC

$f_{yk} = 500$ MPa	Karakteristisk strekkfasthet
$f_{yd} = 434.78$ MPa	Dimensjonerende strekkfasthet

LASTER:

$V_{Ed} := 206$ kN — Opptredende skjærkraft

DIMENSJONERENDE SKJÆRKRAFT, τ_{Ed}:

$\beta_e := 1.4$ — Beta-verdi for innvendig søyle — prEN 8.4.2 Tabell 8.3

$\tau_{Ed} := \beta_e \cdot \frac{V_{Ed}}{b_{0.5} \cdot d_v} = 1.519$ MPa — Dimensjonerende skjærkraft — prEN 8.4.2 (6)

SPENNKABLER, PT:

INFO:
Konsentrerte kabler: 3 stk. over støtte på rand, c/c 140mm
Fordelte kabler: spenner i x-retning med c/c 500mm

$b_{s.x1} := 2500\ mm - 150\ mm = 2350\ mm$ Lengde påvirket område av spennkabler i x-retning

$b_{s.y1} := 7500\ mm$ Lengde påvirket område av spennkabler i y-retning

$n_y := 3$ Antall konsentrerte kabler over spennet i y-retning

$n_x := \frac{b_{s.y1}}{500\ mm} = 15$ Antall fordelte kabler over spennet i x-retning

$e_{p.y} := 40\ mm$ Eksentrisitet på spennkabel over støtte i y-retning NY EC2 8.4.3 (1)

$e_{p.x} := 0\ mm$ Eksentrisitet på spennkabel over støtte i x-retning NY EC2 8.4.3 (1)

$P_{mt} := 178\ kN$ Oppspenningskraft med antatt tap

$P_{mt.y} := P_{mt} \cdot n_y = 534\ kN$ Normalkraft i tverrsnittet i y-retning

$P_{mt.x} := P_{mt} \cdot n_x = 2670\ kN$ Normalkraft i tverrsnittet i x-retning

$\sigma_{d.y} := \frac{P_{mt.y}}{b_{s.x1} \cdot d} = 0.988\ MPa$ Spenning i tverrsnittet i y-retning NY EC2 8.4.3 (1)

$\sigma_{d.x} := \frac{P_{mt.x}}{b_{s.y1} \cdot d} = 1.548\ MPa$ Spenning i tverrsnittet i x-retning NY EC2 8.4.3 (1)

DIMENSJONERENDE SKJÆRKRAFT, τ_{Rdc}:

$$k_{pb1} := \left(3.6 \cdot \sqrt{1 - \frac{b_0}{b_{0.5}}}\right) = 1.895$$

Forbedringskoeffisient for skjærgradient for gjennomlokking — prEN 8.4.3 (1) (8.80)

$$1 \le k_{pb1} \le 2.5 = 1$$

$$\mu_p := 4$$

Koeffisient som hensyntar skjærkraft og bøyemoment i det kritiske kontrollsnittet — CEN TC250 (C8.4.19)

$$k_{N.y} := \sqrt{1 + 1.2 \cdot \frac{b_{0.5} \cdot |\sigma_{d.y}|}{\mu_p \cdot d_v \cdot \sqrt{f_{ck}} \cdot MPa^{\frac{1}{2}}} \cdot \left(1 + 6 \cdot \frac{e_{p.y}}{d}\right)} = 1.257$$

prEN 8.4.3 (4) (8.87)

$$k_{N.x} := \sqrt{1 + 1.2 \cdot \frac{b_{0.5} \cdot |\sigma_{d.x}|}{\mu_p \cdot d_v \cdot \sqrt{f_{ck}} \cdot MPa^{\frac{1}{2}}} \cdot \left(1 + 6 \cdot \frac{e_{p.x}}{d}\right)} = 1.202$$

prEN 8.4.3 (4) (8.87)

$$k_{pp.y} := k_{N.y} = 1.257$$

prEN 8.4.3 (4) (8.83)

$$k_{pp.x} := k_{N.x} = 1.202$$

prEN 8.4.3 (4) (8.83)

$$k_{pp} := \sqrt{k_{pp.y} \cdot k_{pp.x}} = 1.229$$

prEN 8.4.3 (4) (8.86)

$$k_{pb} := k_{pb1} \cdot k_{pp} = 2.329$$

Krav: $1 \le k_{pb} \le 2.5$ — prEN 8.4.3 (4) (8.80)

$$b_{s.x} := \left(3 \cdot d_v\right) + b_x = 799\ mm$$

Slakkarmering med heft i x- og y-retning over bredden 3dv fra søyleliv — prEN 8.4.3 (4) (8.79)

$$b_{s.y} := 3\ b_y = 750\ mm$$

$$A_{sl.x} := \pi \cdot \frac{\text{ø}_x^{\,2}}{4} \cdot \frac{b_{s.x}}{a_{s.x}} = 451.824\ mm^2$$

Areal armering i x-retning

$$A_{sl.y} := \pi \cdot \frac{\text{ø}_x^{\,2}}{4} \cdot \frac{b_{s.y}}{a_{s.y}} = 424.115\ mm^2$$

Areal armering i y-retning

$$\rho_{l.x} := \frac{A_{sl.x}}{b_{s.x} \cdot d_v} = 0.003$$

Armeringsforhold i x-retning — prEN 8.4.3 (4) (8.79)

$$\rho_{l.y} := \frac{A_{sl.y}}{b_{s.y} \cdot d_v} = 0.003$$

Armeringsforhold i y-retning — prEN 8.4.3 (4) (8.79)

$$\rho_l := \sqrt{\rho_{l.x} \cdot \rho_{l.y}} = 0.003$$

prEN 8.4.3 (4) (8.79)

$$\tau_{Rdc} := \min\left(\frac{0.6}{\gamma_v}\cdot k_{pb}\cdot\left(100\cdot\rho_l\cdot f_{ck}\cdot\frac{d_{dg}}{d_v}\right)^{\frac{1}{3}}\cdot MPa^{\frac{2}{3}}, \frac{0.6}{\gamma_v}\cdot\sqrt{f_{ck}}\cdot MPa^{\frac{1}{2}}\right) = 1.2346\ MPa$$ prEN 8.4.2 (8.78)

$\tau_{Rdc} \geq \tau_{Ed} = 0$

FIBERBIDRAGET, $\tau_{Rd.cF}$:

$\eta_c := min\left(\frac{\tau_{Rdc}}{\tau_{Ed}}, 1\right) = 0.813$ Reduksjonskoeffisient for skjærkapasitet prEN L.8.4.3 (1)

$\eta_F := 1$ prEN L.8.4.3 (1)

$f_{Ftud1} := \frac{\tau_{Ed} - \eta_c\cdot\tau_{Rdc}}{\eta_F} = 0.516\ MPa$ Dimensjonerende reststrekkfasthet behov

Table L.2 – Residual strength classes for SFRC

Ductility classes	Characteristic residual flexural strength $f_{R,1k}$									Analytical formulae
	1,0	1,5	2,0	2,5	3,0	4,0	5,0	6,0	8,0	
a	0,5	0,8	1,0	1,3	1,5	2,0	2,5	3,0	4,0	$f_{R,3k} = 0,5f_{R,1k}$
b	0,7	1,1	1,4	1,8	2,1	2,8	3,5	4,2	5,6	$f_{R,3k} = 0,7f_{R,1k}$
c	0,9	1,4	1,8	2,3	2,7	3,6	4,5	5,4	7,2	$f_{R,3k} = 0,9f_{R,1k}$
d	1,1	1,7	2,2	2,8	3,3	4,4	5,5	6,6	8,8	$f_{R,3k} = 1,1f_{R,1k}$
e	1,3	2,0	2,6	3,3	3,9	5,2	6,5	7,8	10,4	$f_{R,3k} = 1,3f_{R,1k}$

NOTE 1: All strength classes apply unless a National Annex excludes specific classes.
NOTE 2: Intermediate classes can be used, if included in a National Annex.

Velger for videre beregning klasse D5. Må vurdere opp mot tester, dokumentasjoner og leverandør

$\gamma_{SF} := 1.5$ Materialfaktor fiber NB38 - 3.4.4

$\eta_F := 1$ Mangler forklaring?? for fiber prEN L.8.4.3 (1)

$k_0 := 1$ Kapasitetsfaktor prEN L.5.1.6.1 (4)

$F_{R.1k} := 5\ MPa$ Velger karakteristisk restbøyestrekkfasthet fiber, 0.5mm prEN L.5.1.2 (1)

$f_{R.3K} := 1.1\cdot F_{R.1k} = 5.5\ MPa$ Karakteristisk restbøyestrekkfasthet fiber, 2.5mm, duktilitetsklasse D. prEN L.5.1.2 (1)

$f_{Ftsd} := k_0\cdot 0.4\cdot\frac{F_{R.1k}}{\gamma_{SF}} = 1.333\ MPa$ Dimensjonerende reststrekkfasthet i bruksgrense prEN L.5.1.6.1 (2) (L.2)

$f_{Ftud} := k_0\cdot 0.37\cdot\frac{f_{R.3K}}{\gamma_{SF}} = 1.357\ MPa$ Dimensjonerende reststrekkfasthet i bruddgrense prEN L.5.1.6.1 (2) (L.3)

$\tau_{Rd.cF} := \eta_c\cdot\tau_{Rdc} + \eta_F\cdot f_{Ftud} = 2.36\ MPa$ prEN L.8.4.3 (L.23)

$\tau_{Rd.c.min} := \frac{11}{\gamma_v}\cdot\sqrt{\frac{f_{ck}}{f_{yd}}\cdot\frac{d_{dg}}{d_v}}\cdot MPa = 0.932\ MPa$ prEN 8.2.1 (4) (8.11)

$\tau_{Rd.cF} := \max\left(\eta_c\cdot\tau_{Rdc} + \eta_F\cdot f_{Ftud}, \eta_c\cdot\tau_{Rd.c.min} + f_{Ftud}\right) = 2.36\ MPa$ prEN L.8.4.3 (L.23)

$\tau_{Rd.cF} \geq \tau_{Ed} = 1$ Ikke behov for skjærarmering! Se vekk ifra skjærarmering beregning på neste side

SKJÆRARMERING, $\tau_{Rd.cs}$:

$\eta_c := \frac{\tau_{Rdc}}{\tau_{Ed}} = 0.813$ — Reduksjonskoeffisient for skjærkapasitet — prEN 8.4.4 (8.88)

$d_{v.out} := d_v - c_{nom} = 148\ mm$ — Avstand mellom arm.lagene i OK og UK — prEN 8.4.4 - Fig. 8.23

$b_{0.5.out} := b_{0.5} \cdot \left(\frac{1}{\eta_c}\right)^{\frac{3}{2}} \cdot \left(\frac{d_v}{d_{v.out}}\right)^{\frac{3}{2}} = 1946.809\ mm$ — Ytre kontrollperimeter — prEN 8.4.4 (8.94)

$d_{out} := \frac{\left(b_{0.5.out} - 2\ b_x - b_y\right)}{\pi} = 380.956\ mm$ — Avstand fra søyleliv til ytre kontrollsnitt

$s_0 := 60\ mm$ Krav: $0.3 \le \frac{s_0}{d_v} \le 0.5 = 1$ — Avstand fra søyleliv til første bøyle — prEN 12.5.1 Fig. 12.8a

$s_r := 0.67 \cdot d_v = 122.61\ mm$ — prEN 8.4.4 (8.91)

$s_r := 120\ mm$ — Avstand mellom bøyler utover

$n_s := \frac{d_{out} - 0.5 \cdot d_{v.out} - s_0}{s_r} = 2.058$ — Antall bøyler i et snitt fra søyleliv og ut til kontrollsnitt det er behov for skjærarmering

$d_{sys} := 160\ mm = 160\ mm$ — Høyde på bøyle — prEN 8.4.4 - Fig. 8.23

$\eta_{sys} := 1.15 \cdot \frac{d_{sys}}{d_v} + 0.63 \cdot \left(\frac{b_0}{d_v}\right)^{\frac{1}{4}} - 0.85 \cdot \frac{s_0}{d_{sys}} = 1.583$ — prEN 8.4.4 (8.93)

$\tau_{Rd.max} := \eta_{sys} \cdot \tau_{Rdc} = 1.954\ MPa$ — Maks skjærspenning — prEN 8.4.4 (8.93)

$\tau_{Rd.max} \ge \tau_{Ed} = 1$

$\frac{\tau_{Ed}}{\tau_{Rd.max}} = 0.777$

$\eta_s := 0.8$ — prEN 8.4.4 (8.90)

$f_{ywd} := f_{yd} = 434.783\ MPa$

$\rho_w := \frac{\tau_{Ed}}{f_{ywd}} \cdot min\left(\frac{1 - \eta_c^{\ 2}}{\eta_s}, 1\right) = 0.00148$ — Armeringsforhold, behov — prEN 8.4.4 (8.91)

$\rho_w \cdot 100 = 0.148$

$1.5 \cdot d_v = 274.5\ mm$ Tangentiell avstand innenfor kontrollsnitt 2dv

$3 \cdot d_v = 549\ mm$ Tangentiell avstand utenfor kontrollsnitt 2dv

$s_{t.max} := 1.5 \cdot d_v = 0.275\ m$ Maks avstand mellom rader innenfor kontrollsnittet 2dv — prEN 12.5.1 Fig. 12.8a

$b_{2dv} := 2 \cdot b_x + b_y + \frac{\pi \cdot 4 \cdot d_v}{2} = 1899.823\ mm$ Omkrets kontrollsnitt 2dv

$n_t := \frac{b_{2dv}}{s_{t.max}} = 6.921$

$n_t := 7$

$s_t := \frac{b_{0.5}}{n_t} = 148.208\ mm$ Tangentiell avstand ved kritisk kontrollsnitt 0.5dv

$d_{b.w} := \sqrt{s_r \cdot s_t \cdot \frac{4 \cdot \rho_w}{\pi}} = 5.794\ mm$ Diameter bøyle — CEN TC250 Design ex.

$\varnothing_v := 8\ mm$

$A_{sw} := \frac{\pi \cdot \varnothing_v^{\,2}}{4} = 50.265\ mm^2$ Arm. areal

$A_{sw.o} := A_{sw} \cdot 8 = 402.124\ mm^2$ Arm. areal rundt et snitt

$\rho_{sw} := \frac{A_{sw}}{s_r \cdot s_t} = 0.00283$ Armeringsforhold

$\eta_s := min\left(\sqrt{15 \cdot \frac{d_{dg}}{d_v}} \cdot \left(\frac{1}{\eta_c \cdot k_{pb}}\right)^{\frac{3}{2}} + \frac{d_v}{150 \cdot \varnothing_v}, 0.8\right) = 0.774$ — prEN 8.4.4 (8.90)

$\tau_{Rd.cs1} := \eta_c \cdot \tau_{Rdc} + \eta_s \cdot \rho_{sw} \cdot f_{ywd} + \eta_F \cdot f_{Ftud} = 3.311\ \mathbf{MPa}$

$\tau_{Rd.csmin} := \rho_w \cdot f_{ywd} + \eta_F \cdot f_{Ftud} = 2.001\ \mathbf{MPa}$ — prEN L.8.4.4 (8L.24)

$\tau_{Rd.cs} := \max\left(\tau_{Rd.cs1}, \tau_{Rd.csmin}\right) = 3.311\ \mathbf{MPa}$ — prEN L.8.4.4 (8L.24)

$\tau_{Rd.cs} > \tau_{Ed} = 1$

Gjennomlokking - Hjørne søyle - prEN

Disclaimer: Beregningsmetodene som presenteres her er tiltenkt å bli lest i sammenheng med Eurokode 2 og det norske nasjonale tillegget. Det bemerkes her at den endelige versjonen av Eurokode 2 ikke var publisert ved utarbeidelsen av dette mathcadarket, og leseren bør bekrefte numeriske verdier gitt i denne metoden med den endelige versjonen av Eurokoden og det norske nasjonale tillegget.

KONSTANTE PARAMETERE:

$\alpha_{cc} := 0.85$	En koeffisient som tar hensyn til virkninger av langtidslast på trykkfastheten samt ugunstige virkninger som er en følge av måten lasten påføres.	NA.3.1.6
$\gamma_c := 1.5$	Materialkoeffisient for betong	Tabell NA 2.1N
$\gamma_v := 1.4$	Materialkoeffisient for skjær- og gjennomlokkingskapasitet uten skjærarmering. MERK: Ved dimensjonering i ulykkestilstand anvendes 1.15	Tabell 4.3(NDP)
$\gamma_s := 1.15$	Materialkoeffisient for stål	Tabell NA 2.1N

TVERRSNITT DEKKE:

$d := 230\ mm$	Tverrsnittykkelse	
$c_{min} := 25\ mm$	Minste overdekning	prEN 6.5.2.1
$\Delta c_{dev} := 10\ mm$	Største tillatte negative avvik	prEN 6.5.3
$c_{nom} := c_{min} + \Delta c_{dev} = 35\ mm$	Nominell overdekning	prEN 6.5.1(1)
$\varnothing_x := 12\ mm$	Stangdiameter i x-retning	
$\varnothing_y := 12\ mm$	Stangdiameter i y-retning	
$a_{s.x} := 200\ mm$	Senteravstand mellom slakkarmering i x-retning	
$a_{s.y} := 200\ mm$	Senteravstand mellom slakkarmering i y-retning	
$d_v := d - c_{nom} - \frac{\varnothing_x + \varnothing_y}{2} = 183\ mm$	Effektiv tverrsnittykkelse	prEN 8.4.2(1) (8.75)

GEOMETRI SØYLE:

$b_x := 250\ mm$	Bredde x-retning på søyle
$b_y := 250\ mm$	Bredde y-retning på søyle

KRITISK KONTROLLSNITT:

$b_{0.5} := b_x + b_y + \frac{\pi \cdot d_v}{4} = 643.728\ mm$	Omkrets av kritisk kontrollsnitt	prEN 8.4.2(2) Figur 8.18
$b_0 := b_x + b_y = 500\ mm$	Omkrets av redusert kritisk kontrollsnitt	prEN 8.4.2(2) Figur 8.18

Gjennomlokking - Hjørne søyle - prEN

BETONG: f_{ck}

$\begin{bmatrix} \\ f_{cd} \end{bmatrix}$:= Fasthetsklasse: B35

$f_{ck} = 35$ MPa	Karakteristisk sylindertrykkfasthet	NS-EN 1992-1-1 Tabell 3.1
$f_{cd} = 19.833$ MPa	Dimensjonerende betongtrykkfasthet	NS-EN 1992-1-1 3.1.6

$D_{lower} := 16$ mm — Tilslag — NY EC2 8.2.1 (4)

$d_{dg} := \begin{cases} \text{if } f_{ck} \le 60\ MPa \\ \quad 16\ mm + D_{lower} \\ \text{else if } f_{ck} > 60\ MPa \\ \quad 16\ mm + D_{lower} \cdot \left(\frac{60}{f_{ck}}\right)^4 \cdot MPa^4 \end{cases} = 32\ mm$ — NY EC2 8.2.1 (4)

ARMERING:

$\begin{bmatrix} f_{yk} \\ f_{yd} \end{bmatrix}$:= Kamstål : B500NC

$f_{yk} = 500$ MPa	Karakteristisk strekkfasthet
$f_{yd} = 434.78$ MPa	Dimensjonerende strekkfasthet

LASTER:

$V_{Ed} := 85$ kN — Opptredende skjærkraft

DIMENSJONERENDE SKJÆRKRAFT, τ_{Ed}:

$\beta_e := 1.5$ — Beta-verdi for innvendig søyle — prEN 8.4.2 Tabell 8.3

$\tau_{Ed} := \beta_e \cdot \frac{V_{Ed}}{b_{0.5} \cdot d_v} = 1.082$ MPa — Dimensjonerende skjærkraft — prEN 8.4.2 (6)

SPENNKABLER, PT:

INFO:
Konsentrerte kabler: 3 stk. over midt støtte i y-retning, c/c 140mm.
Fordelte kabler: spenner i x-retning med c/c 500mm

$b_{s.x1} := 2500\ mm - 150\ mm = 2350\ mm$ Lengde påvirket område av spennkabler i x-retning

$b_{s.y1} := 4000\ mm - 150\ mm = 3850\ mm$ Lengde påvirket område av spennkabler i y-retning

$n_y := 3$ Antall konsentrerte kabler over spennet i y-retning

$n_x := \frac{b_{s.y1}}{500\ mm} = 7.7$ Antall fordelte kabler over spennet i x-retning

$e_{p.y} := 0\ mm$ Eksentrisitet på spennkabel over støtte i y-retning NY EC2 8.4.3 (1)

$e_{p.x} := 0\ mm$ Eksentrisitet på spennkabel over støtte i x-retning NY EC2 8.4.3 (1)

$P_{mt} := 178\ kN$ Oppspenningskraft med antatt tap

$P_{mt.y} := P_{mt} \cdot n_y = 534\ kN$ Normalkraft i tverrsnittet i y-retning

$P_{mt.x} := P_{mt} \cdot n_x = 1370.6\ kN$ Normalkraft i tverrsnittet i x-retning

$\sigma_{d.y} := \frac{P_{mt.y}}{b_{s.x1} \cdot d} = 0.988\ MPa$ Spenning i tverrsnittet i y-retning NY EC2 8.4.3 (1)

$\sigma_{d.x} := \frac{P_{mt.x}}{b_{s.y1} \cdot d} = 1.548\ MPa$ Spenning i tverrsnittet i x-retning NY EC2 8.4.3 (1)

DIMENSJONERENDE SKJÆRKRAFT, τ_{Rdc}:

$$k_{pb1} := \left(3.6 \cdot \sqrt{1 - \frac{b_0}{b_{0.5}}}\right) = 1.701$$

Forbedringskoeffisient for skjærgradient for gjennomlokking — prEN 8.4.3 (1) (8.80)

$$1 \le k_{pb1} \le 2.5 = 1$$

$$\mu_p := 2$$

Koeffisient som hensyntar skjærkraft og bøyemoment i det kritiske kontrollsnittet — CEN TC250 (C8.4.19)

$$k_{N.y} := \sqrt{1 + 1.2 \cdot \frac{b_{0.5} \cdot |\sigma_{d.y}|}{\mu_p \cdot d_v \cdot \sqrt{f_{ck}} \cdot MPa^{\frac{1}{2}}} \cdot \left(1 + 6 \cdot \frac{e_{p.y}}{d}\right)} = 1.163$$

prEN 8.4.3 (4) (8.87)

$$k_{N.x} := \sqrt{1 + 1.2 \cdot \frac{b_{0.5} \cdot |\sigma_{d.x}|}{\mu_p \cdot d_v \cdot \sqrt{f_{ck}} \cdot MPa^{\frac{1}{2}}} \cdot \left(1 + 6 \cdot \frac{e_{p.x}}{d}\right)} = 1.246$$

prEN 8.4.3 (4) (8.87)

$$k_{pp.y} := k_{N.y} = 1.163$$

prEN 8.4.3 (4) (8.83)

$$k_{pp.x} := k_{N.x} = 1.246$$

prEN 8.4.3 (4) (8.83)

$$k_{pp} := \sqrt{k_{pp.y} \cdot k_{pp.x}} = 1.204$$

prEN 8.4.3 (4) (8.86)

$$k_{pb} := k_{pb1} \cdot k_{pp} = 2.048$$

Krav: $1 \le k_{pb} \le 2.5$ — prEN 8.4.3 (4) (8.80)

$$b_{s.x} := 2 \cdot b_x = 500\ mm$$

Slakkarmering med heft i x- og y-retning over bredden 3dv fra søyleliv — prEN 8.4.3 (4) (8.79)

$$b_{s.y} := 2 \cdot b_y = 500\ mm$$

$$A_{sl.x} := \pi \cdot \frac{\text{ø}_x^{\,2}}{4} \cdot \frac{b_{s.x}}{a_{s.x}} = 282.743\ mm^2$$

Areal armering i x-retning

$$A_{sl.y} := \pi \cdot \frac{\text{ø}_x^{\,2}}{4} \cdot \frac{b_{s.y}}{a_{s.y}} = 282.743\ mm^2$$

Areal armering i y-retning

$$\rho_{l.x} := \frac{A_{sl.x}}{b_{s.x} \cdot d_v} = 0.003$$

Armeringsforhold i x-retning — prEN 8.4.3 (4) (8.79)

$$\rho_{l.y} := \frac{A_{sl.y}}{b_{s.y} \cdot d_v} = 0.003$$

Armeringsforhold i y-retning — prEN 8.4.3 (4) (8.79)

$$\rho_l := \sqrt{\rho_{l.x} \cdot \rho_{l.y}} = 0.003$$

prEN 8.4.3 (4) (8.79)

$$\tau_{Rdc} := \min\left(\frac{0.6}{\gamma_v}\cdot k_{pb}\cdot\left(100\cdot\rho_l\cdot f_{ck}\cdot\frac{d_{dg}}{d_v}\right)^{\frac{1}{3}}\cdot MPa^{\frac{2}{3}}, \frac{0.6}{\gamma_v}\cdot\sqrt{f_{ck}}\cdot MPa^{\frac{1}{2}}\right) = 1.0852\ MPa$$ NY EC2 8.4.2 (8.78)

$\tau_{Rdc} \geq \tau_{Ed} = 1$ Ikke behov for mer skjærarmering eller fiberbidrag

FIBERBIDRAGET, $\tau_{Rd.cF}$:

$\eta_c := min\left(\frac{\tau_{Rdc}}{\tau_{Ed}}, 1\right) = 1$ Reduksjonskoeffisient for skjærkapasitet prEN L.8.4.3 (1)

$\eta_F := 1$ prEN L.8.4.3 (1)

$f_{Ftud1} := \frac{\tau_{Ed} - \eta_c\cdot\tau_{Rdc}}{\eta_F} = -0.003\ MPa$ Dimensjonerende reststrekkfasthet behov

Table L.2 – Residual strength classes for SFRC

Ductility classes	Characteristic residual flexural strength $f_{R,1k}$									Analytical formulae
	1,0	1,5	2,0	2,5	3,0	4,0	5,0	6,0	8,0	
a	0,5	0,8	1,0	1,3	1,5	2,0	2,5	3,0	4,0	$f_{R,3k} = 0,5f_{R,1k}$
b	0,7	1,1	1,4	1,8	2,1	2,8	3,5	4,2	5,6	$f_{R,3k} = 0,7f_{R,1k}$
c	0,9	1,4	1,8	2,3	2,7	3,6	4,5	5,4	7,2	$f_{R,3k} = 0,9f_{R,1k}$
d	1,1	1,7	2,2	2,8	3,3	4,4	5,5	6,6	8,8	$f_{R,3k} = 1,1f_{R,1k}$
e	1,3	2,0	2,6	3,3	3,9	5,2	6,5	7,8	10,4	$f_{R,3k} = 1,3f_{R,1k}$

NOTE 1: All strength classes apply unless a National Annex excludes specific classes.
NOTE 2: Intermediate classes can be used, if included in a National Annex.

Velger for videre beregning klasse D5. Må vurdere opp mot tester, dokumentasjoner og leverandør

$\gamma_{SF} := 1.5$ Materialfaktor fiber NB38 - 3.4.4

$\eta_F := 1$ Mangler forklaring?? for fiber prEN L.8.4.3 (1)

$k_0 := 1$ Kapasitetsfaktor prEN L.5.1.6.1 (4)

$F_{R.1k} := 5\ MPa$ Velger karakteristisk restbøyestrekkfasthet fiber, 0.5mm prEN L.5.1.2 (1)

$f_{R.3K} := 1.1\cdot F_{R.1k} = 5.5\ MPa$ Karakteristisk restbøyestrekkfasthet fiber, 2.5mm, duktilitetsklasse D. prEN L.5.1.2 (1)

$f_{Ftsd} := k_0\cdot 0.4\cdot\frac{F_{R.1k}}{\gamma_{SF}} = 1.333\ MPa$ Dimensjonerende reststrekkfasthet i bruksgrense prEN L.5.1.6.1 (2) (L.2)

$f_{Ftud} := k_0\cdot 0.37\cdot\frac{f_{R.3K}}{\gamma_{SF}} = 1.357\ MPa$ Dimensjonerende reststrekkfasthet i bruddgrense prEN L.5.1.6.1 (2) (L.3)

$\tau_{Rd.cF} := \eta_c \cdot \tau_{Rdc} + \eta_F \cdot f_{Ftud} = 2.442\ MPa$ prEN L.8.4.3 (L.23)

$\tau_{Rd.c.min} := \frac{11}{\gamma_v} \cdot \sqrt{\frac{f_{ck}}{f_{yd}} \cdot \frac{d_{dg}}{d_v}} \cdot MPa = 0.932\ MPa$ prEN 8.2.1 (4) (8.11)

$\tau_{Rd.cF} := \max\left(\eta_c \cdot \tau_{Rdc} + \eta_F \cdot f_{Ftud}, \eta_c \cdot \tau_{Rd.c.min} + f_{Ftud}\right) = 2.442\ MPa$ prEN L.8.4.3 (L.23)

$\tau_{Rd.cF} \geq \tau_{Ed} = 1$

Ikke behov for skjærarmering! Se vekk ifra skjærarmering beregning på neste side

SKJÆRARMERING, $\tau_{Rd.cs}$:

$\eta_c := \frac{\tau_{Rdc}}{\tau_{Ed}} = 1.003$ Reduksjonskoeffisient for skjærkapasitet prEN 8.4.4 (8.88)

$d_{v.out} := d_v - c_{nom} = 148\ mm$ Avstand mellom arm.lagene i OK og UK prEN 8.4.4 - Fig. 8.23

$b_{0.5.out} := b_{0.5} \cdot \left(\frac{1}{\eta_c}\right)^{\frac{3}{2}} \cdot \left(\frac{d_v}{d_{v.out}}\right)^{\frac{3}{2}} = 881.573\ mm$ Ytre kontrollperimeter prEN 8.4.4 (8.94)

$d_{out} := \frac{\left(b_{0.5.out} - b_x - b_y\right) \cdot 4}{2\ \pi} = 242.917\ mm$ Avstand fra søyleliv til ytre kontrollsnitt

$s_0 := 60\ mm$ Krav: $0.3 \leq \frac{s_0}{d_v} \leq 0.5 = 1$ Avstand fra søyleliv til første bøyle prEN 12.5.1 Fig. 12.8a

$s_r := 0.67 \cdot d_v = 122.61\ mm$ prEN 8.4.4 (8.91)

$s_r := 120\ mm$ Avstand mellom bøyler utover

$n_s := \frac{d_{out} - 0.5 \cdot d_{v.out} - s_0}{s_r} = 0.908$ Antall bøyler i et snitt fra søyleliv og ut til kontrollsnitt det er behov for skjærarmering

$d_{sys} := 160\ mm = 160\ mm$ Høyde på bøyle prEN 8.4.4 - Fig. 8.23

$\eta_{sys} := 1.15 \cdot \frac{d_{sys}}{d_v} + 0.63 \cdot \left(\frac{b_0}{d_v}\right)^{\frac{1}{4}} - 0.85 \cdot \frac{s_0}{d_{sys}} = 1.497$ prEN 8.4.4 (8.93)

$\tau_{Rd.max} := \eta_{sys} \cdot \tau_{Rdc} = 1.624\ MPa$ Maks skjærspenning prEN 8.4.4 (8.93)

$\tau_{Rd.max} \geq \tau_{Ed} = 1$

$\frac{\tau_{Ed}}{\tau_{Rd.max}} = 0.666$

$\eta_s := 0.8$ prEN 8.4.4 (8.90)

$f_{ywd} := f_{yd} = 434.783\ MPa$

$\rho_w := \frac{\tau_{Ed}}{f_{ywd}} \cdot min\left(\frac{1-\eta_c^{\,2}}{\eta_s}, 1\right) = -0.00002$ Armeringsforhold, behov prEN 8.4.4 (8.91)

$\rho_w \cdot 100 = -0.002$

$1.5 \cdot d_v = 274.5\ mm$ Tangentiell avstand innenfor kontrollsnitt 2dv

$3 \cdot d_v = 549\ mm$ Tangentiell avstand utenfor kontrollsnitt 2dv

$s_{t.max} := 1.5 \cdot d_v = 0.275\ m$ Maks avstand mellom rader innenfor kontrollsnittet 2dv prEN 12.5.1 Fig. 12.8a

$b_{2dv} := b_x + b_y + \frac{\pi \cdot 4\ d_v}{4} = 1074.911\ mm$ Omkrets kontrollsnitt 2dv

$n_t := \frac{b_{2dv}}{s_{t.max}} = 3.916$

$n_t := 4$

$s_t := \frac{b_{0.5}}{n_t} = 160.932\ mm$ Tangentiell avstand ved kritisk kontrollsnitt 0.5dv

$d_{b.w} := \sqrt{s_r \cdot s_t \cdot \frac{4 \cdot \rho_w}{\pi}} = 0.638i\ mm$ Diameter bøyle CEN TC250 Design ex.

$\varnothing_v := 6\ mm$

$A_{sw} := \frac{\pi \cdot \varnothing_v^{\,2}}{4} = 28.274\ mm^2$ Arm. areal

$A_{sw.o} := A_{sw} \cdot 8 = 226.195\ mm^2$ Arm. areal rundt et snitt

$\rho_{sw} := \frac{A_{sw}}{s_r \cdot s_t} = 0.00146$ Armeringsforhold

$\eta_s := min\left(\sqrt{15 \cdot \frac{d_{dg}}{d_v}} \cdot \left(\frac{1}{\eta_c \cdot k_{pb}}\right)^{\frac{3}{2}} + \frac{d_v}{150 \cdot \varnothing_v}, 0.8\right) = 0.754$ prEN 8.4.4 (8.90)

$\tau_{Rd.cs1} := \eta_c \cdot \tau_{Rdc} + \eta_s \cdot \rho_{sw} \cdot f_{ywd} + \eta_F \cdot f_{Ftud} = 2.925\ \mathbf{MPa}$

$\tau_{Rd.csmin} := \rho_w \cdot f_{ywd} + \eta_F \cdot f_{Ftud} = 1.349\ \mathbf{MPa}$ prEN L.8.4.4 (8L.24)

$\tau_{Rd.cs} := \max\left(\tau_{Rd.cs1}, \tau_{Rd.csmin}\right) = 2.925\ \mathbf{MPa}$ prEN L.8.4.4 (8L.24)

$\tau_{Rd.cs} > \tau_{Ed} = 1$

FEM-DESIGN REPORT

LOADS:

Dead load (kN/m^2)	1
Live load (kN/m^2)	2
Jacking stress (MPa)	1487

FEM-design calculates self-weight of flat-slab automatic

LOAD COMBINATIONS:

No.	Name	Type	Factor	Load cases
1	LC1ULS	Ultimate	1.350	Egenlast (+Struc. dead load)
			1.050	Nyttelast
2	LC2ULS	Ultimate	1.200	Egenlast (+Struc. dead load)
			1.500	Nyttelast
3	LC1SqLS	Quasi-permanent	1.000	Egenlast (+Struc. dead load)
			0.300	Nyttelast
4	LC1ScLS	Characteristic	1.000	Egenlast (+Struc. dead load)
			1.000	Nyttelast
5	LC3ULS	Ultimate	1.350	Egenlast (+Struc. dead load)
			1.000	PTC T8 (Post tensioning)
			1.050	Nyttelast
6	LC4ULS	Ultimate	1.200	Egenlast (+Struc. dead load)
			1.000	PTC T8 (Post tensioning)
			1.500	Nyttelast
7	LC2SqLS	Quasi-permanent	1.000	Egenlast (+Struc. dead load)
			1.000	PTC T8 (Post tensioning)
			0.300	Nyttelast
8	LC2ScLS	Characteristic	1.000	Egenlast (+Struc. dead load)
			1.000	PTC T8 (Post tensioning)
			1.000	Nyttelast
9	LC5ULS	Ultimate	1.350	Egenlast (+Struc. dead load)
			1.000	PTC T0 (Post tensioning)
			1.050	Nyttelast
10	LC6ULS	Ultimate	1.200	Egenlast (+Struc. dead load)
			1.000	PTC T0 (Post tensioning)
			1.500	Nyttelast
11	LC3SqLS	Quasi-permanent	1.000	Egenlast (+Struc. dead load)
			1.000	PTC T0 (Post tensioning)
			0.300	Nyttelast
12	LC3ScLS	Characteristic	1.000	Egenlast (+Struc. dead load)
			1.000	PTC T0 (Post tensioning)
			1.000	Nyttelast

FINITE ELEMENT:

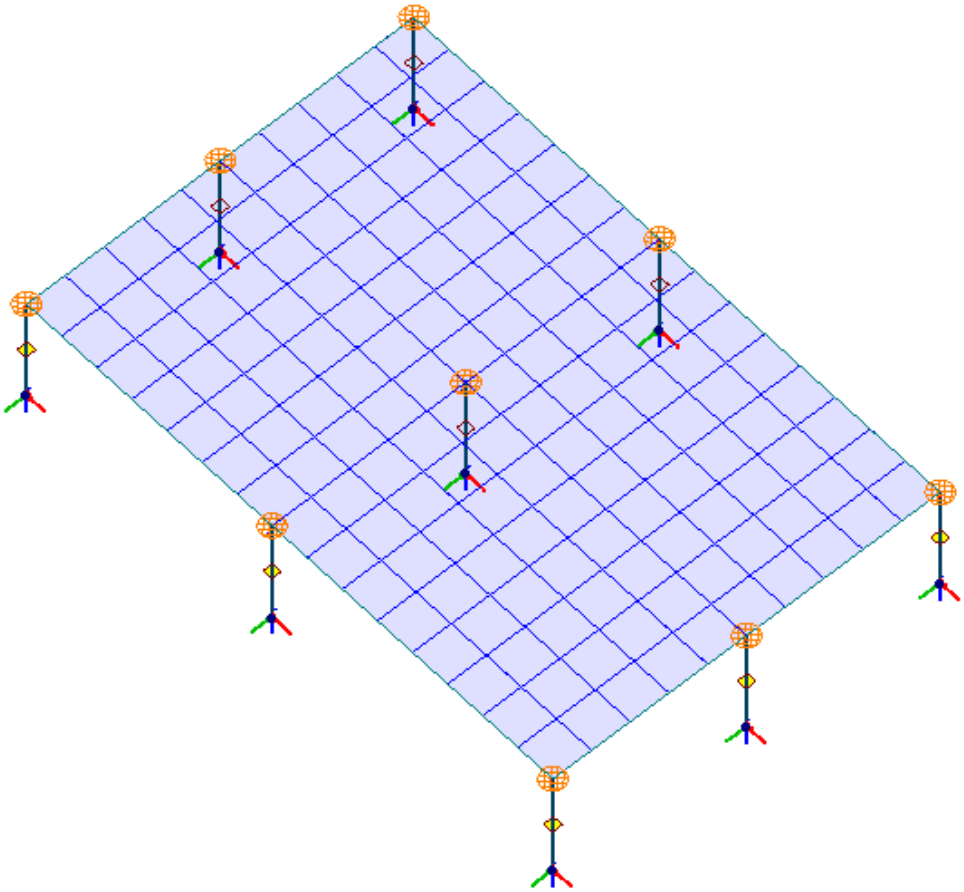

DEFLECTION:

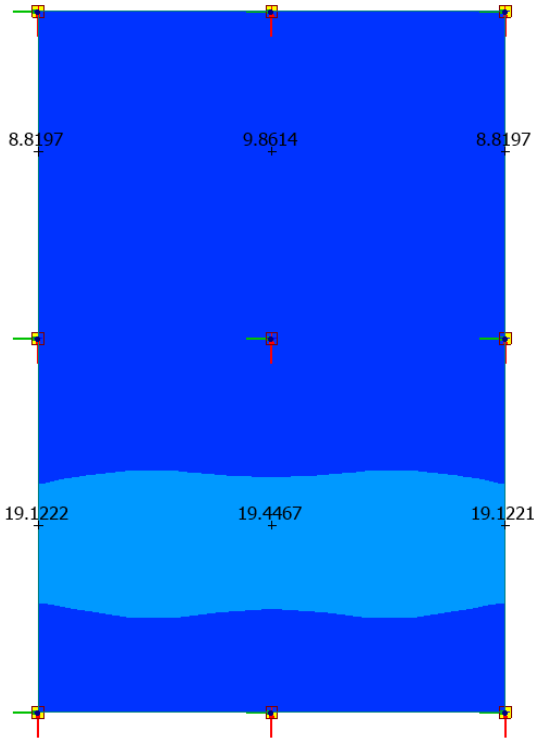

Without post-tensioned tendons

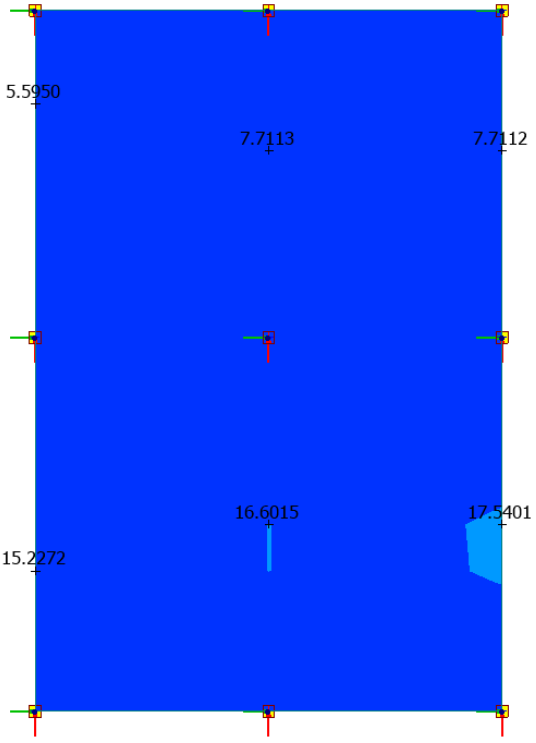

With post-tensioned tendons

REACTIONS:

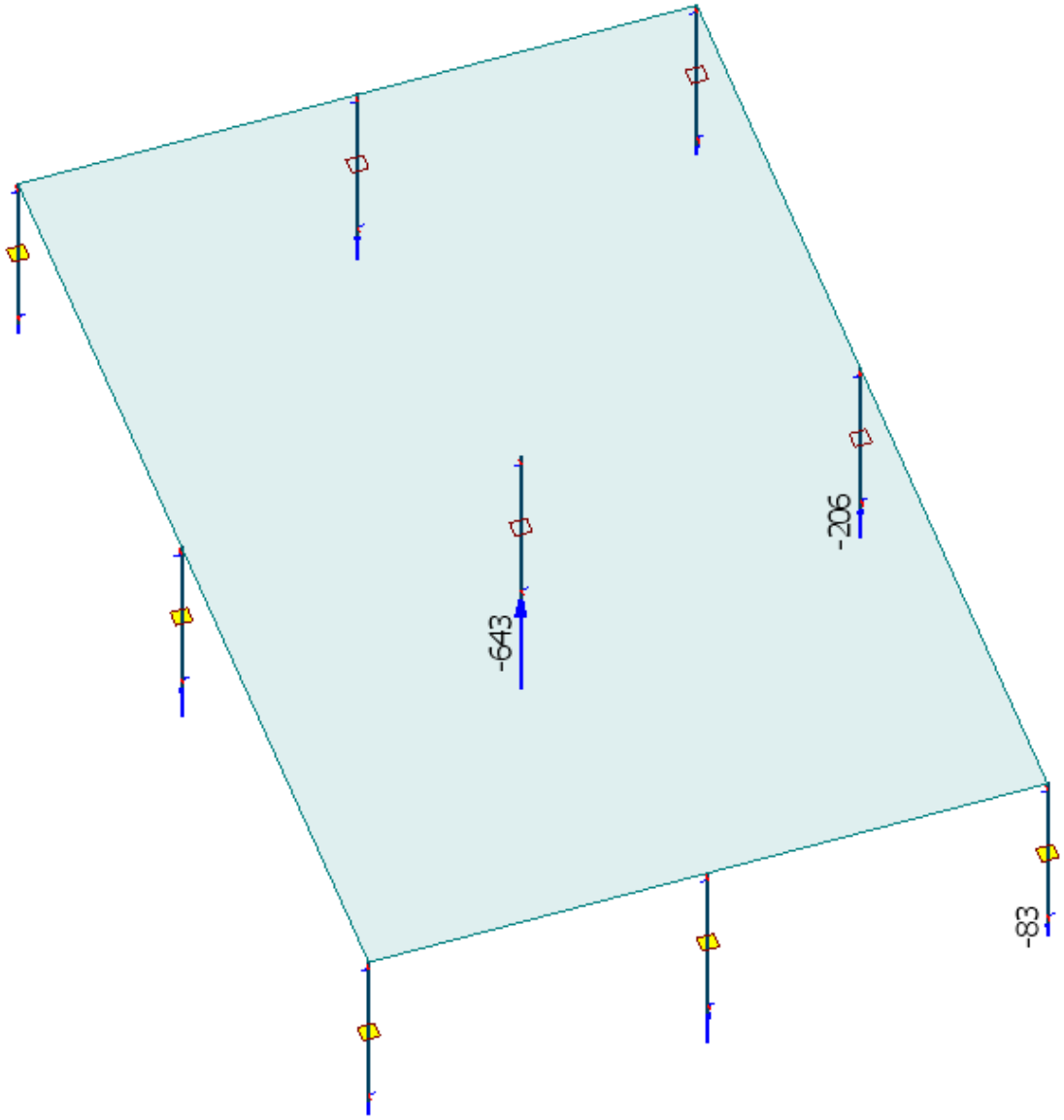

DETAILED RESULTS:

Result of internal column with load combination without post-tensioned tendons:

PU.(C.4).1
Load combination: 'LC2ULS'

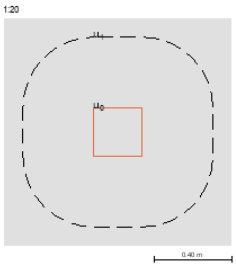

C35/45
t = 230.00 mm
f_{cd} = 19.83 N/mm²
f_{ck} = 35.00 N/mm²
k_{max} = 1.50

Summary

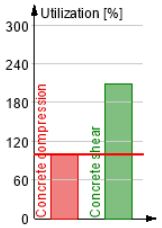

Concrete compression resistance - Part 1.1: 6.4.3

$$v_{Ed} = \frac{\beta \cdot V_{Ed,0}}{u_0 \cdot d} = \frac{1.15 \cdot 638939.40}{1000 \cdot 183} = 4.02 \text{ N/mm}^2 \quad (6.38)$$

$v_{Rd,max} = 4.09$ N/mm² is calculated according to National Annex.

$v_{Ed} = 4.02 \text{ N/mm}^2 \le v_{Rd,max} = 4.09 \text{ N/mm}^2$ (6.53) - OK

Shear reinforcement resistance - Part 1.1: 6.4.3

$$v_{Ed} = \frac{\beta \cdot V_{Ed}}{u_1 \cdot d} \quad (6.38)$$

$$v_{Rd,sw} = 1.5 \frac{d}{s_r} \cdot A_{sw} \, f_{ywd,ef} \, \frac{1}{u_1 \, d} \sin(\alpha)$$

$$v_{Rd,cs} = \min(0.75 \, v_{Rd,c} + v_{Rd,sw}, \, k_{max} \, v_{Rd,c})$$

Concrete shear resistance - Part 1.1: 6.4.3

$$v_{Ed} = \frac{\beta \cdot V_{Ed}}{u_{Out} \cdot d} = \frac{1.15 \cdot 638939.40}{3296 \cdot 183} = 1.22 \text{ N/mm}^2 \quad (6.38)$$

$$v_{Rd,c} = \max\left(C_{Rd,c} \cdot k \, (100 \cdot \rho_l \cdot f_{ck})^{1/3}, \, v_{min}\right) + k_1 \cdot \sigma_{cp} =$$

$$= \max\left(0.12 \cdot 2.00 \, (100 \cdot 0.0031 \cdot 35.00)^{1/3}, \, 0.59\right) + 0.10 \cdot 0.00 = 0.59 \text{ N/mm}^2 \quad (6.47)$$

$v_{Ed} = 1.22 \text{ N/mm}^2 > v_{Rd,c} = 0.59 \text{ N/mm}^2$ - Not OK
Shear reinforcement should be extended!

Result of internal column with load combination with post-tensioned tendons:

PU.(C.4).1
Load combination: 'LC4ULS'

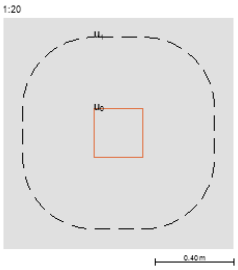

C35/45
t = 230.00 mm
f_{cd} = 19.83 N/mm²
f_{ck} = 35.00 N/mm²
k_{max} = 1.50

Summary

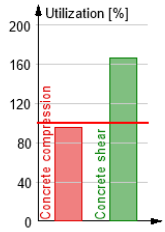

Concrete compression resistance - Part 1.1: 6.4.3

$$v_{Ed} = \frac{\beta \cdot V_{Ed,0}}{u_0 \cdot d} = \frac{1.15 \cdot 621665.14}{1000 \cdot 183} = 3.91 \text{ N/mm}^2 \quad (6.38)$$

$v_{Rd,max} = 4.09$ N/mm² is calculated according to National Annex.

$v_{Ed} = 3.91 \text{ N/mm}^2 \le v_{Rd,max} = 4.09 \text{ N/mm}^2$ (6.53) - OK

Shear reinforcement resistance - Part 1.1: 6.4.3

$$v_{Ed} = \frac{\beta \cdot V_{Ed}}{u_1 \cdot d} \quad (6.38)$$

$$v_{Rd,sw} = 1.5 \frac{d}{s_r} \cdot A_{sw} \, f_{ywd,ef} \, \frac{1}{u_1 \, d} \sin(\alpha)$$

$$v_{Rd,cs} = \min(0.75 \, v_{Rd,c} + v_{Rd,sw}, \, k_{max} \, v_{Rd,c})$$

Concrete shear resistance - Part 1.1: 6.4.3

$$v_{Ed} = \frac{\beta \cdot V_{Ed}}{u_{Out} \cdot d} = \frac{1.15 \cdot 621665.14}{3296 \cdot 183} = 1.19 \text{ N/mm}^2 \quad (6.38)$$

$$v_{Rd,c} = \max\left(C_{Rd,c} \cdot k \, (100 \cdot \rho_l \cdot f_{ck})^{1/3}, \, v_{min}\right) + k_1 \cdot \sigma_{cp} =$$

$$= \max\left(0.12 \cdot 2.00 \, (100 \cdot 0.0031 \cdot 35.00)^{1/3}, \, 0.59\right) + 0.10 \cdot 1.24 = 0.71 \text{ N/mm}^2 \quad (6.47)$$

$v_{Ed} = 1.19 \text{ N/mm}^2 > v_{Rd,c} = 0.71 \text{ N/mm}^2$ - Not OK
Shear reinforcement should be extended!

Result of edge column with load combination without post-tensioned tendons:

PU.(C.45).1
Load combination: 'LC2ULS'

1:20

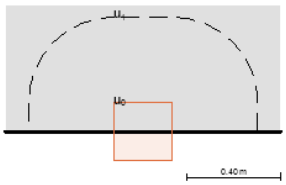

C35/45
$t = 230.00$ mm
$f_{cd} = 19.83$ N/mm^2
$f_{ck} = 35.00$ N/mm^2
$k_{max} = 1.50$

Summary

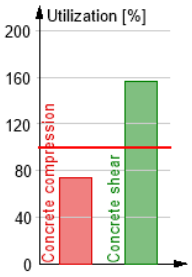

Concrete compression resistance - Part 1.1: 6.4.3

$$v_{Ed} = \frac{\beta \cdot V_{Ed,0}}{u_0 \cdot d} = \frac{1.40 \cdot 196924.55}{500 \cdot 183} = 3.01 \text{ N/mm}^2 \quad (6.38)$$

$v_{Rd,max} = 4.09$ N/mm^2 is calculated according to National Annex.

$v_{Ed} = 3.01$ N/mm$^2 \le v_{Rd,max} = 4.09$ N/mm^2 (6.53) - OK

Concrete shear resistance - Part 1.1: 6.4.3

$$v_{Ed} = \frac{\beta \cdot V_{Ed}}{u_1 \cdot d} = \frac{1.40 \cdot 196924.55}{1648 \cdot 183} = 0.91 \text{ N/mm}^2 \quad (6.38)$$

$$v_{Rd,c} = \max\left(C_{Rd,c} \cdot k \, (100 \cdot \rho_l \cdot f_{ck})^{1/3}, v_{min} \right) + k_1 \cdot \sigma_{cp} =$$
$$= \max\left(0.12 \cdot 2.00 \, (100 \cdot 0.0031 \cdot 35.00)^{1/3}, 0.59 \right) + 0.10 \cdot 0.00 = 0.59 \text{ N/mm}^2 \quad (6.47)$$

$v_{Ed} = 0.91$ N/mm$^2 > v_{Rd,c} = 0.59$ N/mm^2 - Not OK

Shear reinforcement is needed!

Result of edge column with load combination with post-tensioned tendons:

PU.(C.45).1
Load combination: 'LC4ULS'

1:20

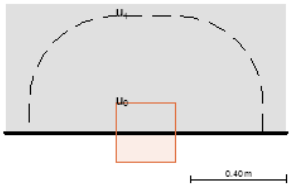

C35/45
$t = 230.00$ mm
$f_{cd} = 19.83$ N/mm^2
$f_{ck} = 35.00$ N/mm^2
$k_{max} = 1.50$

Summary

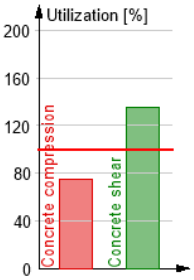

Concrete compression resistance - Part 1.1: 6.4.3

$$v_{Ed} = \frac{\beta \cdot V_{Ed,0}}{u_0 \cdot d} = \frac{1.40 \cdot 199280.39}{500 \cdot 183} = 3.05 \text{ N/mm}^2 \quad (6.38)$$

$v_{Rd,max} = 4.09$ N/mm^2 is calculated according to National Annex.

$v_{Ed} = 3.05$ N/mm$^2 \le v_{Rd,max} = 4.09$ N/mm^2 (6.53) - OK

Concrete shear resistance - Part 1.1: 6.4.3

$$v_{Ed} = \frac{\beta \cdot V_{Ed}}{u_1 \cdot d} = \frac{1.40 \cdot 199280.39}{1648 \cdot 183} = 0.93 \text{ N/mm}^2 \quad (6.38)$$

$$v_{Rd,c} = \max\left(C_{Rd,c} \cdot k \, (100 \cdot \rho_l \cdot f_{ck})^{1/3}, v_{min} \right) + k_1 \cdot \sigma_{cp} =$$
$$= \max\left(0.12 \cdot 2.00 \, (100 \cdot 0.0031 \cdot 35.00)^{1/3}, 0.59 \right) + 0.10 \cdot 0.98 = 0.68 \text{ N/mm}^2 \quad (6.47)$$

$v_{Ed} = 0.93$ N/mm$^2 > v_{Rd,c} = 0.68$ N/mm^2 - Not OK

Shear reinforcement is needed!

Result of corner column with load combination without post-tensioned tendons:

PU.(C.7).1
Load combination: 'LC2ULS'

1:20

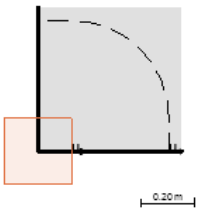

C35/45
t = 230.00 mm
f_{cd} = 19.83 N/mm²
f_{ck} = 35.00 N/mm²
k_{max} = 1.50

Summary

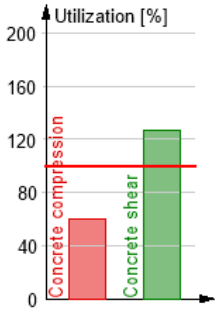

Concrete compression resistance - Part 1.1: 6.4.3

$$v_{Ed} = \frac{\beta \cdot V_{Ed,0}}{u_0 \cdot d} = \frac{1.50 \cdot 74458.89}{250 \cdot 183} = 2.44 \text{ N/mm}^2 \quad (6.38)$$

$v_{Rd,max}$ = 4.09 N/mm² is calculated according to National Annex.

v_{Ed} = 2.44 N/mm² ≤ $v_{Rd,max}$ = 4.09 N/mm² (6.53) - OK

Concrete shear resistance - Part 1.1: 6.4.3

$$v_{Ed} = \frac{\beta \cdot V_{Ed}}{u_1 \cdot d} = \frac{1.50 \cdot 74458.89}{824 \cdot 183} = 0.74 \text{ N/mm}^2 \quad (6.38)$$

$$v_{Rd,c} = \max\left(C_{Rd,c} \cdot k \left(100 \cdot \rho_l \cdot f_{ck} \right)^{1/3}, v_{min} \right) + k_1 \cdot \sigma_{cp} =$$

$$= \max\left(0.12 \cdot 2.00 \left(100 \cdot 0.0031 \cdot 35.00 \right)^{1/3}, 0.59 \right) + 0.10 \cdot 0.00 = 0.59 \text{ N/mm}^2 \quad (6.47)$$

v_{Ed} = 0.74 N/mm² > $v_{Rd,c}$ = 0.59 N/mm² - Not OK

Shear reinforcement is needed!

Result of corner column with load combination with post-tensioned tendons:

PU.(C.7).1
Load combination: 'LC4ULS'

1:20

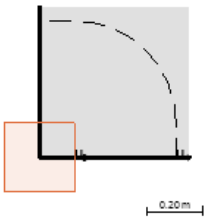

C35/45
t = 230.00 mm
f_{cd} = 19.83 N/mm²
f_{ck} = 35.00 N/mm²
k_{max} = 1.50

Summary

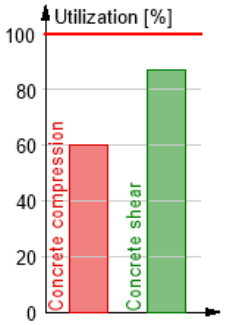

Concrete compression resistance - Part 1.1: 6.4.3

$$v_{Ed} = \frac{\beta \cdot V_{Ed,0}}{u_0 \cdot d} = \frac{1.50 \cdot 75199.88}{250 \cdot 183} = 2.47 \text{ N/mm}^2 \quad (6.38)$$

$v_{Rd,max}$ = 4.09 N/mm² is calculated according to National Annex.

v_{Ed} = 2.47 N/mm² ≤ $v_{Rd,max}$ = 4.09 N/mm² (6.53) - OK

Concrete shear resistance - Part 1.1: 6.4.3

$$v_{Ed} = \frac{\beta \cdot V_{Ed}}{u_1 \cdot d} = \frac{1.50 \cdot 75199.88}{824 \cdot 183} = 0.75 \text{ N/mm}^2 \quad (6.38)$$

$$v_{Rd,c} = \max\left(C_{Rd,c} \cdot k \left(100 \cdot \rho_l \cdot f_{ck} \right)^{1/3}, v_{min} \right) + k_1 \cdot \sigma_{cp} =$$

$$= \max\left(0.12 \cdot 2.00 \left(100 \cdot 0.0031 \cdot 35.00 \right)^{1/3}, 0.59 \right) + 0.10 \cdot 2.75 = 0.86 \text{ N/mm}^2 \quad (6.47)$$

v_{Ed} = 0.75 N/mm² ≤ $v_{Rd,c}$ = 0.86 N/mm² - OK

ADAPT REPORT

LOADS:

Dead load (kN/m^2)	1
Live load (kN/m^2)	2
Jacking stress (MPa)	1478

Self-weight of the structure is automatic added and calculated

LOAD COMBINATIONS:

146.40 LOAD COMBINATIONS

Name: Service (quasi-perm)
Evaluation: Service Quasi-Permanent
Combination detail: 1.00 x Selfweight + 1.00 x Dead load + 0.30 x Live load + 1.00 x Prestressing

Name: ULS_135G_1P
Evaluation: STRENGTH
Combination detail: 1.35 x Selfweight + 1.35 x Dead load + 1.05 x Live load + 1.00 x Prestressing

Name: ULS_12G_1P
Evaluation: STRENGTH
Combination detail: 1.20 x Selfweight + 1.20 x Dead load + 1.50 x Live load + 1.00 x Prestressing

Name: Serv1
Evaluation: Service Frequent
Combination detail: 1.00 x Selfweight + 1.00 x Dead load + 1.00 x Live load + 1.00 x Prestressing

Name: ULs_135_ UPT
Evaluation: STRENGTH
Combination detail: 1.35 x Selfweight + 1.35 x Dead load + 1.05 x Live load

Name: ULS_120_UPT
Evaluation: Service Frequent
Combination detail: 1.20 x Selfweight + 1.20 x Dead load + 1.50 x Live load

Name: SQ_UPT
Evaluation: Service Quasi-Permanent
Combination detail: 1.00 x Selfweight + 1.00 x Dead load + 0.30 x Live load

FINITE ELEMENT:

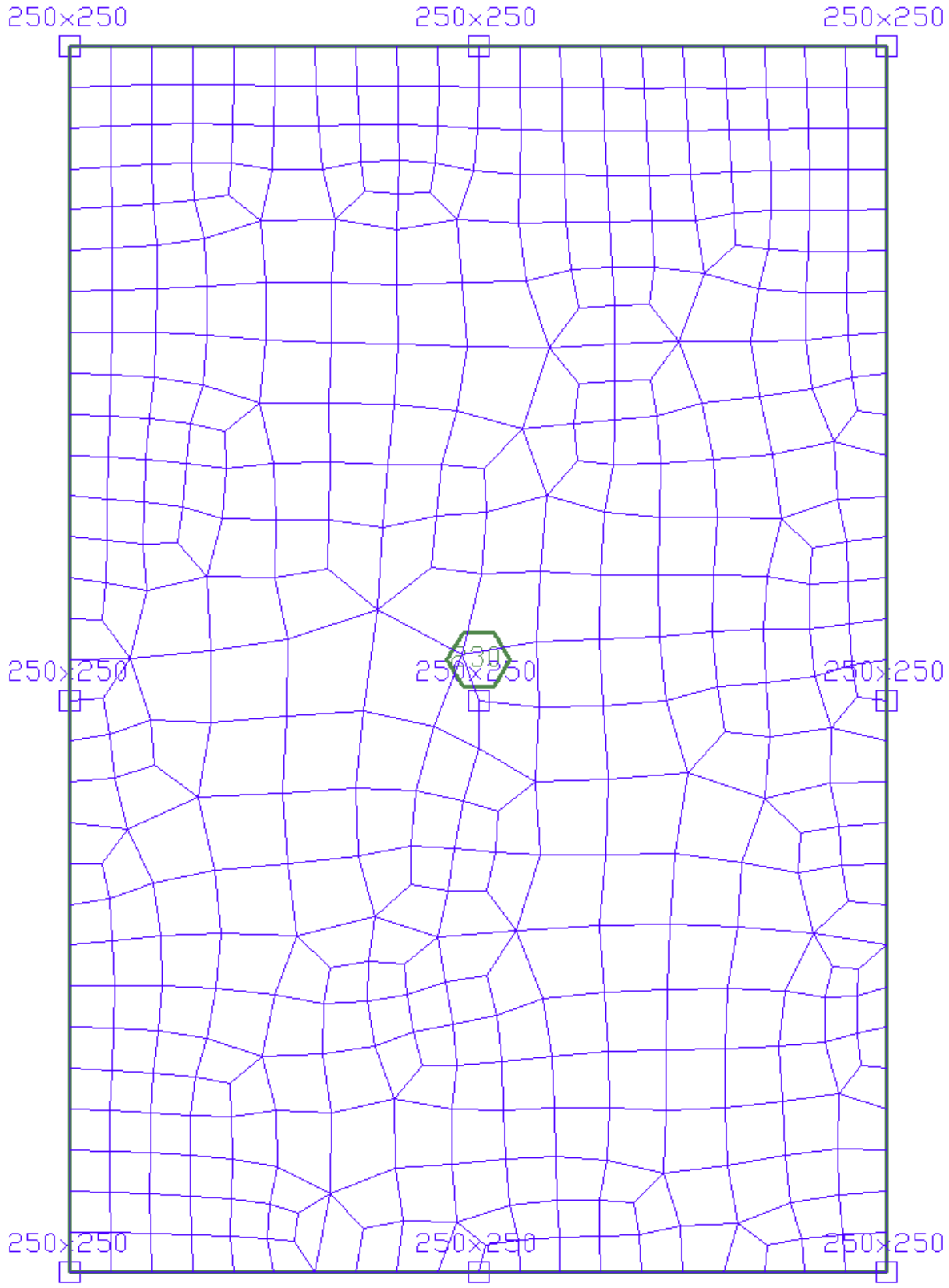

PUNCHING SHEAR

Label	ID	Stress Check	Load Combination	Factored shear (kN	Mrr (kN-m)	Mss (kN-m)	Critical sectior	Shear stress (MPa)	Allowable stress (MPa)
Column 2	2	OK	ULS_135G_1P	-191.57	10.88	0.06	1	0.412	0.672
			ULS_12G_1P	-190.35	10.80	0.05	1	0.409	0.672
			ULs_135_ UPT	-194.71	13.36	0.20	1	0.418	0.672
Column 4	4	OK	ULS_135G_1P	-80.19	8.85	-3.27	1	0.172	0.672
			ULS_12G_1P	-79.65	8.79	-3.24	1	0.171	0.672
			ULs_135_ UPT	-77.07	10.54	-6.14	1	0.166	0.672
Column 5	5	OK	ULS_135G_1P	-79.39	8.64	3.08	1	0.171	0.672
			ULS_12G_1P	-78.87	8.59	3.05	1	0.169	0.672
			ULs_135_ UPT	-76.24	10.31	6.42	1	0.164	0.672
Column 6	6	OK	ULS_135G_1P	-212.55	-11.68	13.07	1	0.428	0.672
			ULS_12G_1P	-211.27	-11.61	12.93	1	0.426	0.672
			ULs_135_ UPT	-200.83	-11.90	23.18	1	0.405	0.672
Column 7	7	Reinforce	ULS_135G_1P	-560.56	-7.44	0.14	1	1.205	0.672
							2	0.944	0.672
							3	0.776	0.672
							4	0.659	0.672
			ULS_12G_1P	-556.93	-7.39	0.14	1	1.197	0.672
							2	0.938	0.672
							3	0.771	0.672
							4	0.655	0.672
			ULs_135_ UPT	-591.43	-8.85	0.30	1	1.271	0.672
							2	0.996	0.672
							3	0.819	0.672
							4	0.696	0.672
							5	0.604	0.672
Column 8	8	OK	ULS_135G_1P	-209.78	-5.65	-6.17	1	0.451	0.672
			ULS_12G_1P	-208.57	-5.61	-6.11	1	0.448	0.672
			ULs_135_ UPT	-196.76	-5.78	-10.30	1	0.423	0.672
Column 9	9	OK	ULS_135G_1P	-63.82	-6.94	2.44	1	0.137	0.672
			ULS_12G_1P	-63.37	-6.89	2.41	1	0.136	0.672
			ULs_135_ UPT	-61.05	-8.83	5.36	1	0.131	0.672
Column 10	10	OK	ULS_135G_1P	-161.28	-12.85	0.12	1	0.347	0.672
			ULS_12G_1P	-160.23	-12.75	0.12	1	0.344	0.672
			ULs_135_ UPT	-164.03	-17.10	0.26	1	0.353	0.672
Column 11	11	OK	ULS_135G_1P	-63.85	-7.05	-2.67	1	0.137	0.672
			ULS_12G_1P	-63.41	-7.00	-2.64	1	0.136	0.672
			ULs_135_ UPT	-60.87	-9.06	-5.11	1	0.131	0.672

SKJÆRKAPASITET I BETONG

		Rev. EC2		NS-EN 1992											
BETONGKLASSER	Fck	INNVENDIG SØYLE	Internal column prEN	Cir. column prEN	Internal column EN	Cir. column NS-EN	RANDSØYLE	Edge column prEN	Sirk. Søyle prEN	Edge column EN	Sirk. Søyle NS-EN	HJØRNESØYLE	Corner column prEN	Sirk. Søyle prEN	Corner column EN	Sirk. Søyle NS-EN
	0	0	0	0	0		0	0	0	0		0	0	0	0
	5	0.6026	0.689	0.2775	0.2775		0.525	0.597	0.277	0.277		0.471	0.534	0.277	0.277
	12	0.8068	0.9231	0.3715	0.3715		0.703	0.8	0.371	0.371		0.631	0.715	0.371	0.371
	16	0.888	1.016	0.40886	0.40886		0.774	0.88	0.409	0.409		0.695	0.787	0.409	0.409
	20	0.9566	1.0944	0.44272	0.44272		0.833	0.948	0.443	0.443		0.748	0.848	0.443	0.443
	25	1.0305	1.1789	0.49497	0.49497		0.898	1.021	0.4949	0.495		0.806	0.914	0.495	0.495
	30	1.095	1.2528	0.5422	0.5422		0.954	1.085	0.542	0.542		0.856	0.971	0.542	0.542
	35	1.1528	1.3189	0.5856	0.5856		1.004	1.143	0.586	0.586		0.902	1.022	0.586	0.586
	45	1.2535	1.4341	0.6641	0.6641		1.092	1.242	0.664	0.664		0.98	1.111	0.664	0.664
	55	1.3402	1.5333	0.7342	0.7342		1.168	1.328	0.734	0.734		1.048	1.188	0.734	0.734
	65	1.3491	1.5434	0.79812	0.79812		1.175	1.337	0.798	0.798		1.055	1.196	0.798	0.798
	75	1.3226	1.513	0.85732	0.85732		1.152	1.311	0.857	0.857		1.034	1.173	0.857	0.857
	85	1.3242	1.515	0.91269	0.91269		1.154	1.312	0.913	0.913		1.036	1.174	0.913	0.913
	95	1.3407	1.5338	0.96488	0.96488		1.168	1.329	0.96488	0.96488		1.049	1.189	0.96488	0.96488

DEKKETYKKELSE	Dekketykkelse	INNVENDIG SØYLE	Internal column prEN	Cir. column prEN	Internal column EN	Cir. column NS-EN	RAND SØYLE	Edge column prEN	Cir. column prEN	Edge column EN	Cir. column NS-EN	HJØRNESØYLE	Corner column prEN	Sirk. Søyle prEN	Corner column EN	Sirk. Søyle NS-EN
	100		1.6467	1.995	0.8022	0.8022		1.378	1.627	0.8022	0.8022	under kpb	1.211	1.408	0.8022	0.8022
	150		1.3839	1.6318	0.6428	0.6428		1.179	1.369	0.6428	0.6428		1.044	1.203	0.6428	0.6428
	175		1.2967	1.5126	0.5979	0.5979		1.113	1.284	0.5979	0.5979		0.991	1.135	0.5979	0.5979
	200		1.2249	1.4154	0.5856	0.5856		1.059	1.213	0.5856	0.5856		0.946	1.079	0.5856	0.5856
	230		1.1528	1.3189	0.5856	0.5856		1.004	1.143	0.5856	0.5856		0.902	1.022	0.5856	0.5856
	250		1.1111	1.2365	0.5824	0.5824		0.972	1.102	0.5824	0.582		0.875	0.989	0.5824	0.582
	275		1.0645	1.1443	0.558	0.558		0.937	1.056	0.558	0.558		0.846	0.952	0.558	0.558
	300		1.0231	1.0677	0.5376	0.5376		0.905	1.015	0.5376	0.53763		0.82	0.919	0.5376	0.53763
	325		0.9858	1.003	0.5203	0.5203		0.876	0.978	0.5203	0.5202		0.796	0.889	0.5203	0.5202
Overskrede kpb	350		0.9467	0.9467	0.5053	0.5053		0.849	0.945	0.5053	0.4921		0.774	0.862	0.5053	0.4921
	375		0.898	0.898	0.4921	0.4921		0.825	0.898	0.4921	0.4921		0.754	0.837	0.4921	0.4921
	400		0.8551	0.8551	0.4805	0.4805		0.803	0.855	0.4805	0.48047		0.735	0.814	0.4805	0.48047
	425		0.8169	0.8169	0.4701	0.4701		0.782	0.817	0.4701	0.4701		0.718	0.793	0.4701	0.4701
	450		0.7828	0.7828	0.461	0.461		0.763	0.783	0.461	0.4607		0.702	0.773	0.461	0.4607
	475		0.752	0.752	0.4523	0.4523		0.744	0.752	0.4523	0.4523		0.687	0.752	0.4523	0.4523
	500		0.7241	0.7241	0.4446	0.445	kpb overskrede	0.724	0.724	0.4446	0.445		0.672	0.724	0.4446	0.445

SØYLEBREDDE	Bredde søyle	INNVENDIG SØYLE	Internal column prEN	Cir. column prEN	Internal column EN	Cir. column NS-EN	RAND SØYLE	Edge column prEN	Cir. column prEN	Edge column EN	Cir. column NS-EN	HJØRNESØYLE	Corner column prEN	Sirk. Søyle prEN	Corner column EN	Sirk. Søyle NS-EN
	50		1.325	1.325	0.5856	0.5856		1.325	1.325	0.5856	0.5856		1.325	1.325	0.5856	0.5856
	100		1.325	1.325	0.5856	0.5856		1.325	1.325	0.5856	0.5856		1.234	1.274	0.5856	0.5856
	150		1.325	1.325	0.5856	0.5856		1.191	1.247	0.5856	0.5856		1.086	1.128	0.5856	0.5856
	200		1.2338	1.3189	0.5856	0.5856		1.086	1.143	0.5856	0.5856		0.981	1.022	0.5856	0.5856
	250		1.1528	1.2404	0.5856	0.5856		1.004	1.061	0.5856	0.5856		0.902	0.942	0.5856	0.5856
	300		1.0859	1.1744	0.5856	0.5856		0.939	0.994	0.5856	0.5856		0.839	0.878	0.5856	0.5856
	350		1.0294	1.118	0.5856	0.5856		0.885	0.939	0.5856	0.5856		0.787	0.825	0.5856	0.5856
	400		0.981	1.069	0.5856	0.5856		0.839	0.892	0.5856	0.5856		0.745	0.781	0.5856	0.5856
	450		0.9387	1.0259	0.5856	0.5856		0.799	0.851	0.5856	0.5856		0.708	0.743	0.5856	0.5856
	500		0.9016	0.9876	0.5856	0.5856		0.765	0.816	0.5856	0.5856		0.676	0.711	0.5856	0.5856
	550		0.8685	0.9533	0.5856	0.5856		0.735	0.784	0.5856	0.5856		0.649	0.682	0.5856	0.5856
	600		0.8388	0.9224	0.5856	0.5856		0.708	0.756	0.5856	0.5856		0.624	0.656	0.5856	0.5856

TILSLAG:	Tilslag	INNVENDIG SØYLE	Internal column prEN	Cir. column prEN	Internal column EN	Cir. column NS-EN	RAND SØYLE	Edge column prEN	Cir. column prEN	Edge column EN	Cir. column NS-EN	HJØRNESØYLE	Corner column prEN	Sirk. Søyle prEN	Corner column EN	Sirk. Søyle NS-EN
	10		1.0757	1.2307	0.4423	0.4423		0.937	1.066	0.4423	0.4423		0.841	0.954	0.4423	0.4423
	11		1.0893	1.2462	0.4423	0.4423		0.949	1.08	0.4423	0.4423		0.852	0.966	0.4423	0.4423
	12		1.1026	1.2614	0.4423	0.4423		0.961	1.093	0.4423	0.4423		0.862	0.978	0.4423	0.4423
	14		1.1282	1.2908	0.4423	0.4423		0.983	1.118	0.4423	0.4423		0.882	1	0.4423	0.4423
	15		1.1406	1.305	0.4423	0.4423		0.994	1.131	0.4423	0.4423		0.892	1.011	0.4423	0.4423
	16		1.1528	1.3189	0.5308	0.5308		1.004	1.143	0.5308	0.5308		0.902	1.022	0.5308	0.5308
	18		1.1763	1.3458	0.5308	0.5308		1.025	1.166	0.5308	0.5308		0.92	1.043	0.5308	0.5308
	20		1.1989	1.3717	0.5308	0.5308		1.045	1.188	0.5308	0.5308		0.938	1.063	0.5308	0.5308
	22		1.2207	1.3966	0.5308	0.5308		1.064	1.21	0.5308	0.5308		0.955	1.082	0.5308	0.5308
	24		1.2418	1.4207	0.5308	0.5308		1.082	1.231	0.5308	0.5308		0.971	1.101	0.5308	0.5308

ARMERINGSRATIO	Arm.ratio	INNVENDIG SØYLE	Internal column prEN	Cir. column prEN	Internal column EN	Cir. column NS-EN	RAND SØYLE	Edge column prEN	Cir. column prEN	Edge column EN	Cir. column NS-EN	HJØRNESØYLE	Corner column prEN	Sirk. Søyle prEN	Corner column EN	Sirk. Søyle NS-EN
	0		0	0	0	0		0	0	0	0		0	0	0	0
c/c 400	0.0015		0.915	1.046	0.5856	0.5856		0.797	0.907	0.5856	0.5856		0.716	0.811	0.5856	0.5856
c/c 350	0.0017		0.9566	1.094	0.5856	0.5856		0.833	0.948	0.5856	0.5856		0.748	0.848	0.5856	0.5856
c/c 300	0.002		1.007	1.15	0.5856	0.5856		0.877	0.998	0.5856	0.5856		0.788	0.893	0.5856	0.5856
c/c 250	0.0025		1.0701	1.2243	0.5856	0.5856		0.932	1.061	0.5856	0.5856		0.837	0.949	0.5856	0.5856
c/c 200	0.0031		1.1528	1.31	0.5856	0.5856		1.004	1.143	0.5856	0.5856		0.902	1.022	0.5856	0.5856
c/c 175	0.0035		1.2052	1.37	0.5856	0.5856		1.05	1.195	0.5856	0.5856		0.943	1.069	0.5856	0.5856
c/c 150	0.004		1.2688	1.45	0.5856	0.5856		1.105	1.258	0.5856	0.5856		0.992	1.125	0.5856	0.5856
c/c 125	0.005		1.3483	1.54	0.6207	0.6207		1.175	1.336	0.6207	0.6207		1.054	1.195	0.6207	0.6207
c/c 100	0.006		1.4524	1.6617	0.6687	0.6687		1.265	1.44	0.6687	0.6687		1.136	1.288	0.6687	0.6687
c/c 75	0.008		1.5986	1.82	0.736	0.736		1.393	1.584	0.736	0.736		1.25	1.417	0.736	0.736
c/c 50	0.01		1.8299	2.09	0.8425	0.8425		1.594	1.814	0.8425	0.8425		1.431	1.623	0.8425	0.8425
c/c 40	0.015		1.9712	2.2552	0.90757	0.90757		1.717	1.954	0.90757	0.90757		1.542	1.748	0.90757	0.90757
c/c 30	0.02		2.1696	2.48	0.9891	0.9891		1.89	2.15	0.9891	0.9891		1.697	1.924	0.9891	0.9891
c/c 25	0.025		2.3055	2.5355	0.9891	0.9891		2.009	2.285	0.9891	0.9891		1.803	2.044	0.9891	0.9891
c/c 20	0.03		2.4836	2.5355	0.9891	0.9891		2.164	2.462	0.9891	0.9891		1.942	2.202	0.9891	0.9891
c/c 17.5	0.035		2.5355	2.5355	0.9891	0.9891		2.262	2.535	0.9891	0.9891		2.031	2.302	0.9891	0.9891
c/c 15	0.04		2.5355	2.5355	0.9891	0.9891		2.382	2.535	0.9891	0.9891		2.138	2.424	0.9891	0.9891
	0.045		2.5355	2.5355	0.9891	0.9891		2.437	2.535	0.9891	0.9891		2.188	2.535	0.9891	0.9891
	0.05		2.5355	2.5355	0.9891	0.9891		2.535	2.535	0.9891	0.9891		2.272	2.535	0.9891	0.9891

SKJÆRKAPASITET I BETONG MED PT-KABLER

BETONGKLASSER	Fck	INNVENDIG SØYLE	with PT prEN	without PT prEN	with PT EN	without PT EN	RANDSØYLE	with PT prEN	without PT prEN	with PT EN	without PT EN	HJØRNESØYLE	with PT prEN	without PT prEN	with PT EN	without PT EN	
	0		0	0	0	0		0	0	0	0		0	0	0	0	Overskrider kpb for innvendig søyle prEN
Overskrider kpb	5		0.6926	0.6026	0.423	0.2775		0.6926	0.525	0.421	0.277		0.6489	0.471	0.396	0.277	Overskrider kpb for rand søyle prEN at B5,
	12		0.9274	0.8068	0.517	0.3715		0.9274	0.703	0.515	0.371		0.7929	0.631	0.49	0.371	
	16		1.0207	0.888	0.555	0.40886		1.0179	0.774	0.553	0.409		0.851	0.695	0.527	0.409	
	20		1.0995	0.9566	0.589	0.44272		1.0718	0.833	0.586	0.443		0.9004	0.748	0.561	0.443	
	25		1.1844	1.0305	0.641	0.49497		1.1302	0.898	0.639	0.4949		0.954	0.806	0.614	0.495	
	30		1.2586	1.095	0.688	0.5422		1.1816	0.954	0.686	0.542		1.0011	0.856	0.661	0.542	
maks kpb	35		1.325	1.1528	0.732	0.5856		1.2277	1.004	0.729	0.586		1.0434	0.902	0.704	0.586	
	45		1.4408	1.2535	0.81	0.6641		1.3087	1.092	0.808	0.664		1.1175	0.98	0.783	0.664	
	55		1.5404	1.3402	0.88	0.7342		1.3788	1.168	0.878	0.734		1.1816	1.048	0.853	0.734	
	65		1.5506	1.3491	0.944	0.79812		1.3721	1.175	0.942	0.798		1.1792	1.055	0.917	0.798	
	75		1.5202	1.3226	1.003	0.85732		1.3328	1.152	1.001	0.857		1.1481	1.034	0.976	0.857	
	85		1.522	1.3242	1.059	0.91269		1.3242	1.154	1.056	0.913		1.1429	1.036	1.031	0.913	
	95		1.541	1.3407	1.111	0.96488		1.3319	1.168	1.109	0.96488		1.1515	1.049	1.083	0.96488	

Spennkraft på 178 kN per kabel, 5 kons for innv. 3 kons.kabler i rand. Kabler og fordelte med cc500

			Rev. EC2	NS-EN 1992		Rev. EC2	NS-EN 1992		Rev. EC2	NS-EN 1992
TENSIONING FORCE	Pmt	INNVENDIG SØYLE	Internal prEN	Internal EN	RANDSØYLE	Edge prEN	Edge EN	HJØRNESØYLE	Corner prEN	Corner EN
	0		1.1528	0.586		1.004	0.586		0.9016	0.586
	50		1.2644	0.627		1.0741	0.626		0.9436	0.619
	100		1.325	0.668		1.1396	0.666		0.9838	0.652
	150		1.325	0.709		1.2014	0.707		1.0224	0.686
	200		1.325	0.75		1.2601	0.747		1.0595	0.719
	250		1.325	0.791		1.3162	0.787		1.0954	0.752
	300		1.325	0.832		1.325	0.828		1.1301	0.785
	350		1.325	0.873		1.325	0.868		1.1638	0.819
	400		1.325	0.914		1.325	0.909		1.1965	0.852
	450		1.325	0.955		1.325	0.949		1.2283	0.885
	500		1.325	0.995		1.325	0.989		1.2593	0.919

Samme antall kabler, kun endret på jacking force for å se på endringene. B35, og alt annet forblir det samme

Overhøyde kabel	ep	INNVENDIG/RAND/HJØRNE SØYLE	Internal column prEN	Edge column prEN	Internal column EN
	0		1.5438	1.3042	0.845
	10		1.6055	1.332	0.845
	20		1.6648	1.3581	0.845
	30		1.7219	1.3827	0.845
	40		1.777	1.4062	0.845
	50		1.8304	1.4285	0.845
	60		1.8821	1.4498	0.845

UTEN begrensning av kpb

BETONGKAP + FRC

BETONGKLASSER	Fck	INNVENDIG SØYLE	Int. colum w/ FRC	Int. colum w/o FRC	RAND SØYLE	Edge colum w/ FRC	Edge colum w/o FRC	HJØRNE SØYLE	Corner colum w/ FRC	Corner colum w/o FRC
	0		0	0		0	0		0	0
	5		1.498	0.6026		1.5381	0.525		1.5747	0.471
	12		1.61	0.8068		1.6819	0.703		1.7475	0.631
	16		1.664	0.888		1.7507	0.774		1.8302	0.695
	20		1.713	0.9566		1.8139	0.833		1.906	0.748
	25		1.771	1.0305		1.8872	0.898		1.9942	0.806
	30		1.824	1.095		1.9558	0.954		2.076	0.856
	35		1.875	1.1528		2.0207	1.004		2.15	0.902
	45		1.969	1.2535		2.1418	1.092		2.3	0.98
	55		2.057	1.3402		2.2549	1.168		2.4	1.048
dlower	65		2.066	1.3491		2.266	1.175		2.41	1.055
	75		2.038	1.3226		2.2307	1.152		2.39	1.034
	85		2.04	1.3242		2.2328	1.154		2.39	1.036
	95		2.057	1.3407		2.2548	1.168		2.4	1.049

Benyttet duktilitetsklasse D og Frk 5 for å ikke bruke for høy fiberkapasitet.

			Rev. EC2			Rev. EC2			Rev. EC2	
COLUMN SIZE	B	INNVENDIG SØYLE	Int. colum w/ FRC	Int. colum w/o FRC	RAND SØYLE	Edge colum w/ FRC	Edge colum w/o FRC	HJØRNE SØYLE	Corner colum w/ FRC	Corner colum w/o FRC
	50		1.693	1.325		1.844	1.325		2	1.325
	100		1.78	1.325		2.011	1.325		2.154	1.234
	150		1.867	1.325		2.0207	1.191		2.154	1.086
	200		1.875	1.2338		2.0207	1.086		2.154	0.981
	250		1.875	1.1528		2.0207	1.004		2.154	0.902
	300		1.875	1.0859		2.0207	0.939		2.154	0.839
	350		1.875	1.0294		2.0207	0.885		2.144	0.787
nc stoppe å øke på hjørnesøyle, og vi f	400		1.875	0.981		2.0207	0.839		2.1012	0.745
	450		1.875	0.9387		2.0207	0.799		2.064	0.708
	500		1.875	0.9016		2.0207	0.765		2.03	0.676
	550		1.875	0.8685		2.0207	0.735		2.005	0.649
	600		1.875	0.8388		2.0207	0.708		1.98067	0.624

			Rev. EC2			Rev. EC2			Rev. EC2	
DEKKETYKKELSE	Dekketykkelse		Int. colum w/ FRC	Int. colum w/o FRC	RAND SØYLE	Edge colum w/ FRC	Edge colum w/o FRC	HJØRNE SØYLE	Corner colum w/ FRC	Corner colum w/o FRC
	100	under min. FRC max, øke	1.583	1.6467	under min. FRC max, øke f	1.6473	1.378	Under kpb, og krav	1.70734	1.211
	150		1.71	1.3839	under min. FRC max, øke f	1.8093	1.179	Under min. FRC ma	1.9006	1.044
	175		1.765	1.2967	under min. FRC max, øke f	1.8799	1.113	Under min. FRC ma	1.98539	0.991
	200		1.816	1.2249		1.946	1.059	Under min. FRC ma	2.06	0.946
	230		1.875	1.1528		2.0207	1.004		2.15	0.902
	250		1.912	1.1111		2.0682	0.972		2.21	0.875
	275		1.956	1.0645		2.1255	0.937	nc makset	2.202	0.846
	300		1.999	1.0231		2.1807	0.905		2.1765	0.82
kpn overskredet	350		2.074	0.9467	nc makset	2.2061	0.849		2.13	0.774
	400		2.113	0.8551		2.1594	0.803		2.09	0.735
	450		2.113	0.7828		2.1193	0.763		2.0585	0.702
nc makset	500		2.081	0.7241	kpb makset	2.08	0.724		2.028	0.672

DUKTILITETSKLASSE	FR.1k	INNVENDIG SØYLE	A	B	C	D	E
	1		0.641	0.691	0.74	0.789	0.839
	1.5		0.703	0.777	0.851	0.925	0.999
	2		0.765	0.863	0.962	1.061	1.159
	3		0.888	1.036	1.184	1.332	1.48
	4		1.011	1.209	1.406	1.603	1.801
	5		1.135	1.381	1.628	1.875	2.121
	6		1.258	1.554	1.85	2.146	2.442
	8		1.505	1.899	2.294	2.689	3.083

Betongkvalitet B35, arm ratio 0.0031 (cc200)

FR.1k	RAND SØYLE	A	B	C	D	E
1			0.787	0.837	0.886	0.935	0.985
1.5			0.849	0.923	0.997	1.071	1.145
2			0.911	1.009	1.108	1.207	1.305
3			1.034	1.182	1.33	1.478	1.626
4			1.157	1.355	1.552	1.749	1.947
5			1.281	1.527	1.774	2.021	2.267
6			1.404	1.7	1.996	2.292	2.588
8			1.651	2.045	2.44	2.835	3.229

FR.1k	HJØRNE SØYLE	A	B	C	D	E
1			0.921	0.971	1.02	1.069	1.119
1.5			0.983	1.057	1.131	1.205	1.279
2			1.045	1.143	1.242	1.341	1.439
3			1.168	1.316	1.464	1.612	1.76
4			1.291	1.489	1.686	1.883	2.081
5			1.415	1.661	1.908	2.155	2.401
6			1.538	1.834	2.13	2.426	2.722
8			1.785	2.179	2.574	2.969	3.363

BETONG + SKJÆRARMERING

Forhold mellom opptredn fck	VRd.c INTERNAL SØYLE Int. column prEN	Int. column EN		VRd.c prEN Edge column prEN	NS-EN Edge column EN		VRd.c prEN Corner column prEN	NS-EN Corner column EN	
5	2.192	6.063	EDGE SØYLE			INTERNAL SØYLE			
12	1.6372	2.601		1.555	3.1532		1.295	2.091	
16	1.4875	1.984		1.162	1.3525		0.967	0.8969	
20	1.3809	1.615		1.055	1.0317		0.879	0.6842	
25	1.2819	1.32		0.98	0.837		0.816	0.5568	
35	1.459	0.987		0.91	0.6867		0.757	0.4554	
45	1.0538	0.805		0.813	0.5133		0.677	0.3404	
55	0.9856	0.693		0.748	0.4187		0.622	0.2777	
65	0.9791	0.618		0.699	0.3602		0.582	0.2388	
75	0.9987	0.566		0.695	0.3212		0.578	0.213	
85	0.9975	0.53		0.709	0.2943		0.59	0.1952	
95	0.9853	0.504		0.708	0.2754		0.589	0.1826	
				0.699	0.2623		0.582	0.174	

SKJÆRARMERING

Int. column prEN	Int. column EN	Edge column prEN	Edge column EN	Corner column prEN	Corner column EN		
0	0.699	0.439	0.664	0.439	0.751	0.439	
50	1.805	0.504	1.61	0.552	1.614	0.639	
75	2.358	0.537	2.083	0.609	2.045	0.738	
100	2.911	0.569	2.557	0.665	2.477	0.838	
113	3.199	0.568	2.803	0.649	2.701	0.878	
150	4.017	0.634	3.503	0.778	3.34	0.878	
200	5.123	0.699	4.4449	0.878	4.202	0.878	min 22mm2 = 0.49;Pa randEn
300	7.336	0.829	6.342	0.878	5.92	0.878	

BETONG+PT+FRC +SKJÆR

Kap bidrag

	Fck	Pmt	Armering
Inner column	1.325	2.041	1.735
Edge column	1.234	2.36	0
Corner column	1.04	2.363	0

12 rader rundt med ø10, avstand utover er 120mm(krav),
5 bøyler utover, krav om 1.5dv (274mm) radene innen 2dv kontrollsnitt, og 3dv (549mm) utenfor 2dv kontrollsnitt

Total Kap med alle bidrag

	Int. prEN	Int. EN	Edge prEN	Edge EN	Corner prEN	Corner EN
Only concrete	2.253	1.664	1.647	1.234	1.26	0.891
PT	2.419	1.751	1.955	1.329	1.568	0.986
FRC	3.934		3.311		2.925	

Skjærarm. Behov etter alle bidrag

	Int. prEN	Int. EN	Edge prEN	Edge EN	Corner prEN	Corner EN
Only concrete	1112.62	759.4	306.04	217.279	148.15	65.808
PT	1022.26	675.185	185.6	164.4	0	0
FRC	511.929		0		0	

Opptredne skjærkraft (Mpa)

OPPTREDNE SKJÆRKRAFT

KVADRATISKE SØYLER

Rev. EC2 — NS-EN 1992

fck		Fck	prEN b0 Int. column prEN	b0.5 Int. column prEN	b0 Edge column prEN	b0.5 Edge column prEN	b0 Corner column prEN	b0.5 Corner column prEN	NS-EN b0 Int. column EN	b0.5 Int. column EN	b0 Edge column EN	b0.5 Edge column EN	b0 Corner column EN	b0.5 Corner column EN
	B5	5	4.041	2.566	2.101	1.519	1.393	1.082	4.041	1.225	2.101	0.83	1.393	0.648
	B12	12	4.041	2.566	2.101	1.519	1.393	1.082	4.041	1.225	2.101	0.83	1.393	0.648
	B16	16	4.041	2.566	2.101	1.519	1.393	1.082	4.041	1.225	2.101	0.83	1.393	0.648
	B20	20	4.041	2.566	2.101	1.519	1.393	1.082	4.041	1.225	2.101	0.83	1.393	0.648
	B25	25	4.041	2.566	2.101	1.519	1.393	1.082	4.041	1.225	2.101	0.83	1.393	0.648
	B30	30	4.041	2.566	2.101	1.519	1.393	1.082	4.041	1.225	2.101	0.83	1.393	0.648
	B35	35	4.041	2.566	2.101	1.519	1.393	1.082	4.041	1.225	2.101	0.83	1.393	0.648
	B45	45	4.041	2.566	2.101	1.519	1.393	1.082	4.041	1.225	2.101	0.83	1.393	0.648
	B55	55	4.041	2.566	2.101	1.519	1.393	1.082	4.041	1.225	2.101	0.83	1.393	0.648
	B65	65	4.041	2.566	2.101	1.519	1.393	1.082	4.041	1.225	2.101	0.83	1.393	0.648
	B75	75	4.041	2.566	2.101	1.519	1.393	1.082	4.041	1.225	2.101	0.83	1.393	0.648
	B85	85	4.041	2.566	2.101	1.519	1.393	1.082	4.041	1.225	2.101	0.83	1.393	0.648
	B95	95	4.041	2.566	2.101	1.519	1.393	1.082	4.041	1.225	2.101	0.83	1.393	0.648

	Bredde søyle	prEN b0 Int. column prEN	b0.5 Int. column prEN	b0 Edge column prEN	b0.5 Edge column prEN	b0 Corner column prEN	b0.5 Corner column prEN	NS-EN b0 Int. column EN	b0.5 Int. column EN	b0 Edge column EN	b0.5 Edge column EN	b0 Corner column EN	b0.5 Corner column EN
bredde søyler	50	20.204	5.214	10.506	3.603	6.967	2.859	20.204	1.617	10.506	1.212	6.967	1.032
	100	10.102	4.145	5.253	2.683	3.484	2.027	10.102	1.497	5.253	1.087	3.484	0.899
	150	6.735	3.439	3.502	2.137	2.322	1.57	6.735	1.394	3.502	0.985	2.322	0.796
	200	5.051	2.939	2.627	1.776	1.742	1.281	5.051	1.304	2.627	0.901	1.742	0.715
	250	4.041	2.566	2.101	1.519	1.393	1.082	4.041	1.225	2.101	0.83	1.393	0.648
	300	3.367	2.277	1.751	1.327	1.161	0.937	3.367	1.155	1.751	0.769	1.161	0.593
	350	2.886	2.046	1.501	1.178	0.995	0.826	2.886	1.092	1.501	0.716	0.995	0.546
	400	2.525	1.858	1.313	1.059	0.871	0.738	2.525	1.036	1.313	0.671	0.871	0.507
	450	2.245	1.701	1.167	0.962	0.774	0.668	2.245	0.986	1.167	0.63	0.774	0.472
	500	2.02	1.569	1.051	0.882	0.697	0.609	2.02	0.94	1.051	0.595	0.697	0.442
	550	1.837	1.456	0.955	0.813	0.633	0.56	1.837	0.898	0.955	0.563	0.633	0.416
	600	1.684	1.358	0.876	0.755	0.581	0.518	1.684	0.86	0.876	0.534	0.581	0.393

	Dekketykkelse	prEN b0 Int. column prEN	b0.5 Int. column prEN	b0 Edge column prEN	b0.5 Edge column prEN	b0 Corner column prEN	b0.5 Corner column prEN	NS-EN b0 Int. column EN	b0.5 Int. column EN	b0 Edge column EN	b0.5 Edge column EN	b0 Corner column EN	b0.5 Corner column EN
dekketykkelse	100	13.952	11.96	7.255	6.53	4.811	4.442	13.952	8.374	7.255	5.024	4.811	3.609
	150	7.179	5.424	3.733	3.071	2.476	2.131	7.179	3.129	3.733	2.004	2.476	1.503
	200	4.833	3.264	2.513	1.903	1.667	1.344	4.833	1.654	2.513	1.101	1.667	0.85
	230	4.041	2.566	2.101	1.519	1.393	1.082	4.041	1.225	2.101	0.83	1.393	0.648
	250	3.643	2.224	1.894	1.329	1.256	0.952	3.643	1.026	1.894	0.701	1.256	0.552
	300	2.923	1.628	1.52	0.993	1.008	0.721	2.923	0.699	1.520	0.487	1.008	0.389
	350	2.44	1.250	1.269	0.776	0.842	0.570	2.440	0.508	1.269	0.359	0.842	0.29
	400	2.095	0.993	1.089	0.626	0.722	0.465	2.095	0.385	1.089	0.275	0.722	0.224
	450	1.835	0.810	0.954	0.517	0.633	0.387	1.835	0.303	0.954	0.218	0.633	0.179
	500	1.632	0.674	0.849	0.436	0.563	0.329	1.632	0.244	0.849	0.177	0.563	0.146

APPENDIX B

BETA-VERDIER ETTER prEN 1992-1-1

$d := 230\ mm$	Tverrsnittykkelse	
$c_{min} := 25\ mm$	Minste overdekning	
$\Delta c_{dev} := 10\ mm$	Største tillatte negative avvik	
$c_{nom} := c_{min} + \Delta c_{dev} = 35\ mm$	Nominell overdekning	
$\varnothing_x := 12\ mm$	Stangdiameter i x-retning	
$\varnothing_y := 12\ mm$	Stangdiameter i y-retning	
$a_{sx} := 200\ mm$	Senteravstand slakkarmering i x-retning	
$a_{sy} := 200\ mm$	Senteravstand slakkarmering i y-retning	
$d_v := d - c_{nom} - \frac{\varnothing_x + \varnothing_y}{2} = 183\ mm$	Effektiv tverrsnittykkelse	6.4.2 (6.32)

GEOMETRI SØYLE:

$b_x := 250\ mm$	Bredde x-retning på søyle	
$b_y := 250\ mm$	Bredde y-retning på søyle	

INNVENDIG SØYLE:

$V_{Ed} := 801\ kN$

$M_{Ed.x} := 138.1\ kN \cdot m$

$M_{Ed.y} := 173.37\ kN \cdot m$

$b_{b.min} := b_x + d_v = 433\ mm$

$b_{b.max} := b_y + d_v = 433\ mm$ Kvadratisk tverrsnitt

$b_b := \sqrt{b_{b.min} \cdot b_{b.max}} = 433\ mm$ prEN 8.4.2(2) Tabell 8.3

$e_{b.x} := \frac{M_{Ed.x}}{V_{Ed}} = 0.172\ m$

$e_{b.y} := \frac{M_{Ed.y}}{V_{Ed}} = 0.216\ m$ prEN 8.4.2(2) Figur 8.21

$e_b := \sqrt{e_{b.x}^2 + e_{b.y}^2} = 276.717\ mm$ Eksentrisitet prEN 8.4.2(2) Figur 8.21

$\beta_e := 1 + 1.1 \cdot \frac{e_b}{b_b} = 1.703$ prEN 8.4.2(2) Figur 8.21

BETA-VERDIER ETTER prEN 1992-1-1

RANDSØYLE:

$V_{Ed.r} := 329\ \mathbf{kN}$

$M_{Ed.x.r} := 29.9\ \mathbf{kN \cdot m}$

$M_{Ed.y.r} := 136.7\ \mathbf{kN \cdot m}$

$b_{br.min} := b_x + 0.5 \cdot d_v = 341.5\ \mathbf{mm}$

$b_{br.max} := b_x + d_v = 433\ \mathbf{mm}$

$b_{b.r} := \sqrt{b_{br.min} \cdot b_{br.max}} = 384.538\ \mathbf{mm}$ prEN 8.4.2(2) Figur 8.21

$e_{bx.r} := \frac{M_{Ed.x.r}}{V_{Ed.r}} = 90.881\ \mathbf{mm}$

$e_{by.r} := \frac{M_{Ed.y.r}}{V_{Ed.r}} = 415.502\ \mathbf{mm}$

$e_{bk} := 0.5 \cdot \left(e_{bx.r} + e_{by.r}\right) = 253.191\ \mathbf{mm}$ prEN 8.4.2(2) Figur 8.21

$\beta_e := 1 + 1.1 \cdot \frac{e_{bk}}{b_{b.r}} = 1.724$ prEN 8.4.2(2) Figur 8.21

HJØRNESØYLE:

$V_{Ed.h} := 146\ \mathbf{kN}$

$M_{Ed.x.h} := 25.14\ \mathbf{kN \cdot m}$

$M_{Ed.y.h} := 26.82\ \mathbf{kN \cdot m}$

$b_{bh.min} := b_x + 0.5 \cdot d_v = 341.5\ \mathbf{mm}$

$b_{bh.max} := b_x + 0.5 \cdot d_v = 341.5\ \mathbf{mm}$

$b_{bh} := \sqrt{b_{bh.min} \cdot b_{bh.max}} = 341.5\ \mathbf{mm}$ prEN 8.4.2(2) Figur 8.21

$e_{b.xh} := \frac{M_{Ed.x.h}}{V_{Ed.h}} = 172.192\ \mathbf{mm}$

$e_{b.yh} := \frac{M_{Ed.y.h}}{V_{Ed.h}} = 183.699\ \mathbf{mm}$

$e_{bh} := \min\left(0.27 \cdot \left(e_{b.xh} + e_{b.yh}\right), 0.45\ b_{bh}\right) = 96.09\ \mathbf{mm}$ prEN 8.4.2(2) Figur 8.21

$\beta_e := 1 + 1.1 \cdot \frac{e_{bk}}{b_{bh}} = 1.816$ prEN 8.4.2(2) Figur 8.21

BETA-VERDIER ETTER prEN 1992-1-1

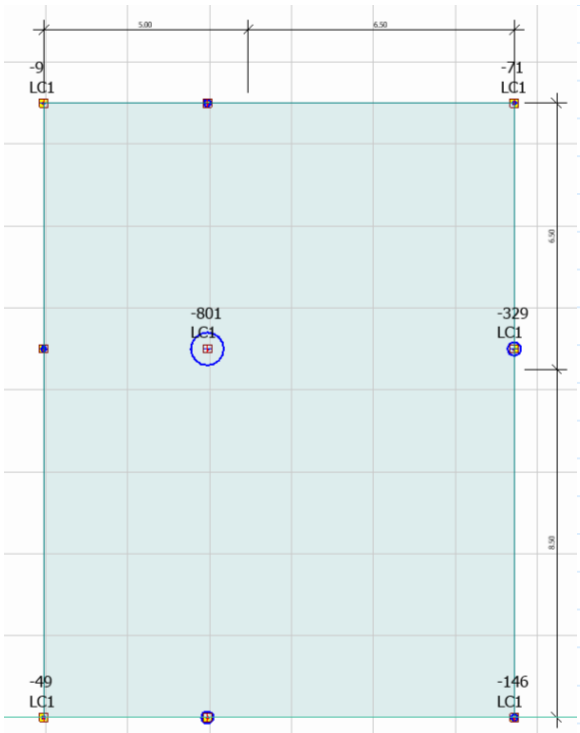

Opptredende skjærkraft (kN)

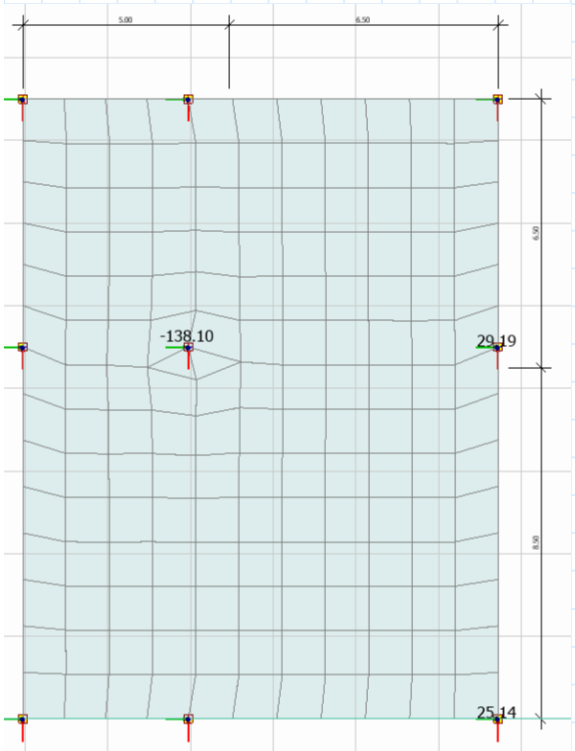

Opptredne moment om x-akse (kNm)

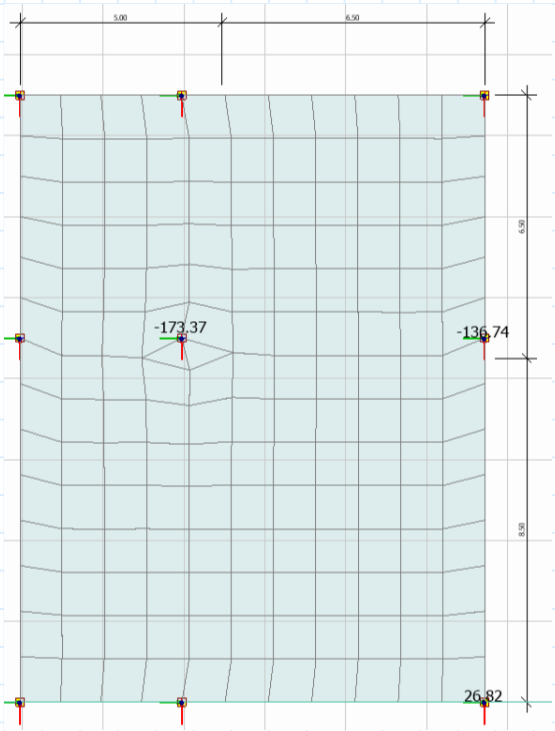

Opptredne moment om y-akse (kNm)

BETA-VERDIER ns-en 1992 og preEN

TVERRSNITT DEKKE:

$d := 230\ mm$	Tverrsnittykkelse	
$c_{min} := 25\ mm$	Minste overdekning	
$\Delta c_{dev} := 10\ mm$	Største tillatte negative avvik	
$c_{nom} := c_{min} + \Delta c_{dev} = 35\ mm$	Nominell overdekning	
$\phi_x := 12\ mm$	Stangdiameter i x-retning	
$\phi_y := 12\ mm$	Stangdiameter i y-retning	
$a_s := 200\ mm$	Senteravstand mellom slakkarmering	
$d_v := d - c_{nom} - \frac{\phi_x + \phi_y}{2} = 183\ mm$	Effektiv tverrsnittykkelse	6.4.2 (6.32)

GEOMETRI SØYLE:

$b_x := 250\ mm$	Bredde x-retning på søyle	
$b_y := 250\ mm$	Bredde y-retning på søyle	

KRITISK KONTROLLSNITT:

$u_1 := 2 \cdot (b_x + b_y) + \pi \cdot 4\ d_v = 3299.646\ mm$	Omkrets av kritisk kontrollsnitt	6.4.3 Figur 6.20 (6.32)
$k := 0.6$		

INNVENDIG SØYLE:

LASTER:

$V_{Ed} := 801\ kN$

$M_{Ed.x} := 138.1\ kN \cdot m$

$M_{Ed.y} := 173.37\ kN \cdot m$

$e_y := \frac{M_{Ed.y}}{V_{Ed}} = 0.216\ m$

$e_x := \frac{M_{Ed.x}}{V_{Ed}} = 0.172\ m$

$M_{Ed} := \sqrt{M_{Ed.x}^2 + M_{Ed.y}^2} = 221.65\ kN \cdot m$

BETA-VERDIER ns-en 1992 og preEN

$W_1 := \frac{b_x^2}{2} + b_x \cdot b_y + 4 \cdot b_y \cdot d_v + 16\, d_v^2 + 2 \cdot \pi \cdot d_v \cdot b_x = 1100029.728\ \mathbf{mm}^2$ 6.4.3 (6.41)

$\beta := 1 + k \cdot \frac{M_{Ed}}{V_{Ed}} \cdot \frac{u_1}{W_1} = 1.498$ Eksentrisk ift kontrolltverrsnittet 6.4.3 (6.39)

$\beta := 1 + 1.8 \cdot \sqrt{\left(\frac{e_y}{b_x + 4 \cdot d_v}\right)^2 + \left(\frac{e_x}{b_y + 4 \cdot d_v}\right)^2} = 1.507$ Innvendig rekt. søyle - eksentrisk belastet. 6.4.3 (6.43)

RANDSØYLE:

$V_{Ed.k} := 329\ \mathbf{kN}$

$M_{Ed.y.k} := 136.7\ \mathbf{kN \cdot m}$

$e_{par} := \frac{M_{Ed.y.k}}{V_{Ed.k}} = 0.416\ \mathbf{m}$

$W_{1.k} := \frac{b_y^2}{4} + b_x \cdot b_y + 4 \cdot b_x \cdot d_v + 8 \cdot d_v^2 + \pi \cdot d_v \cdot b_y = 672764.864\ \mathbf{mm}^2$ 6.4.3 (6.45)

$u_{1.k} := 2 \cdot b_x + b_y + \frac{\pi \cdot 4 \cdot d_v}{2} = 1899.823\ \mathbf{mm}$ Kritisk kontrollsnitt

$u_{.1k} := b_y + 2 \cdot \frac{b_x}{2} + \frac{\pi \cdot 4 \cdot d_v}{2} = 1649.823\ \mathbf{mm}$ Redusert kritisk kontrollsnitt

$\beta := \frac{u_{1.k}}{u_{.1k}} + k \cdot \frac{u_{1.k}}{W_{1.k}} \cdot e_{par} = 1.856$ For eksentrisk belastet kant rekt. søyle 6.4.3 (6.44)

HJØRNESØYLE:

$u_{1.h} := b_x + b_y + \frac{\pi \cdot 4 \cdot d_v}{4} = 1074.911\ \mathbf{mm}$ Kritisk kontrollsnitt

$u_{.1h} := \frac{b_x}{2} + \frac{b_y}{2} + \frac{\pi \cdot 4 \cdot d_v}{4} = 824.911\ \mathbf{mm}$ Redusert kritisk kontrollsnitt

$\beta := \frac{u_{1.h}}{u_{.1h}} = 1.303$ For søyler i hjørner 6.4.3 (6.46)

APPENDIX C

EN 1992-1-1

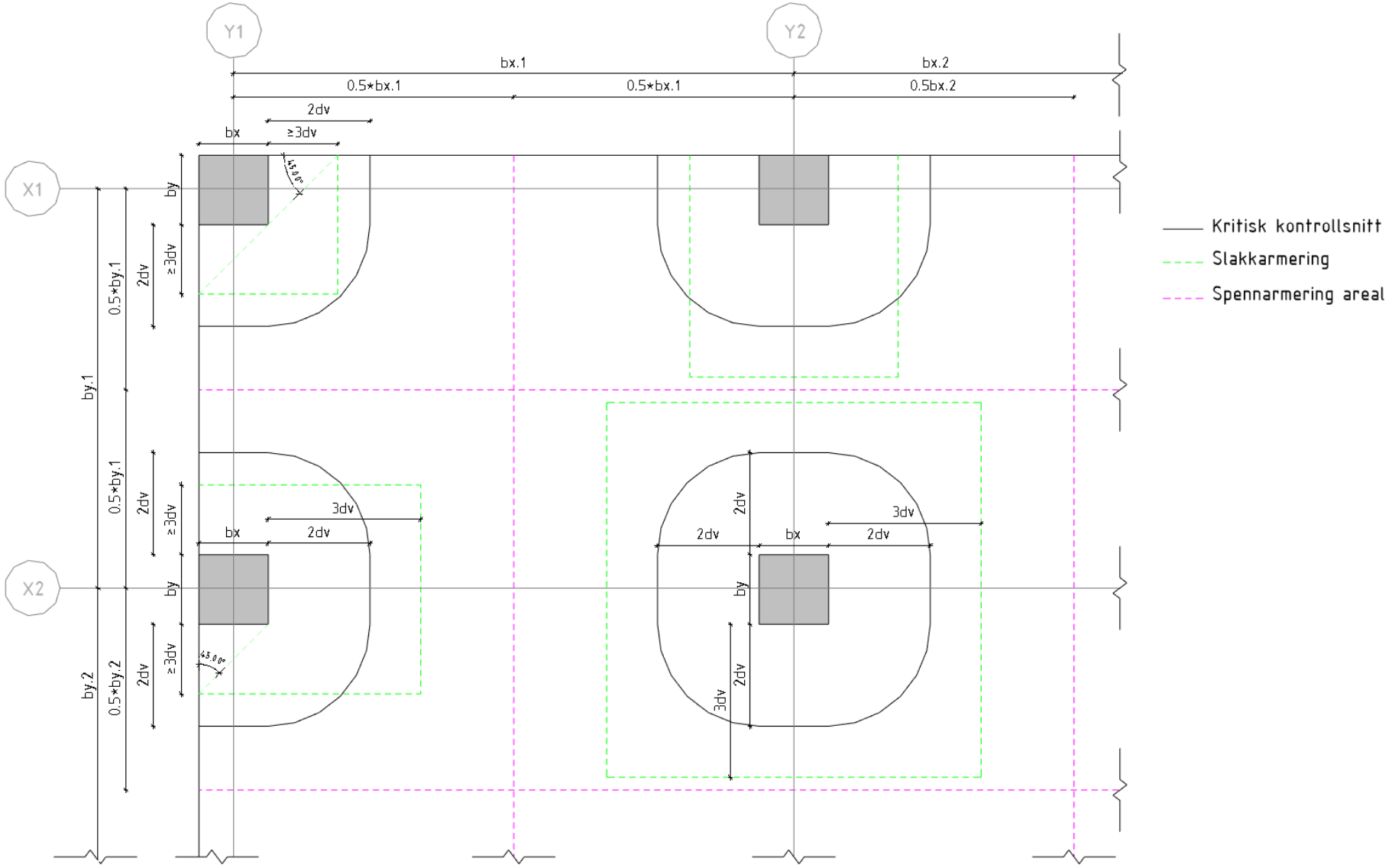

prEN 1992-1-1

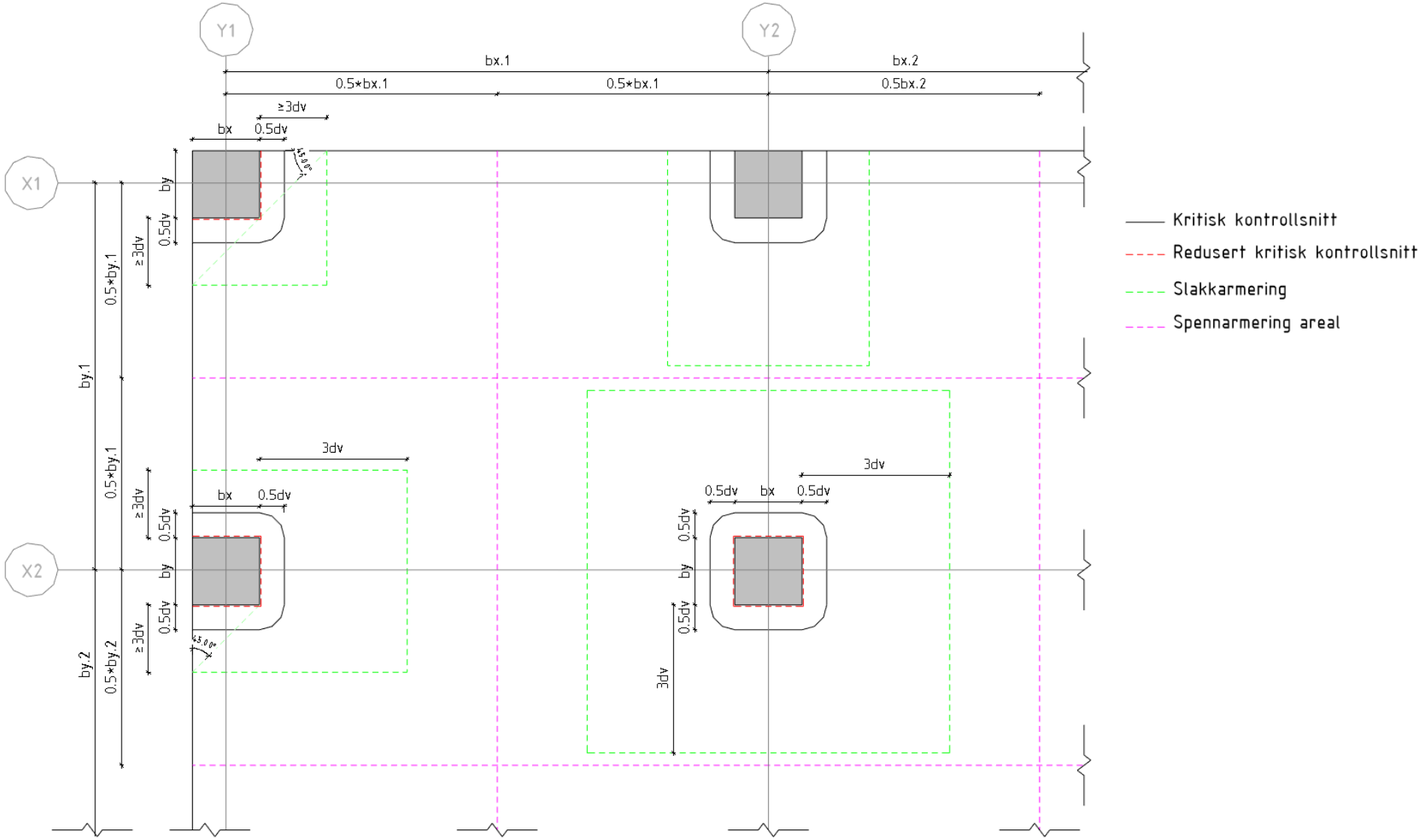
Y1
Y2
X1
X2
bx.1
0.5*bx.1
0.5*bx.1
bx.2
0.5bx.2
≥3dv
bx
0.5dv
by
0.5dv
≥3dv
0.5*by.1
by.1
45.0°
3dv
bx
0.5dv
0.5dv
bx
0.5dv
3dv
0.5dv
by
0.5dv
3dv
by.2
0.5*by.2
Kritisk kontrollsnitt
Redusert kritisk kontrollsnitt
Slakkarmering
Spennarmering areal

APPENDIX D

1st draft of the paper

Parametric study of punching shear resistance in fiber-reinforced PT slabs

T.Gjerdset, I.Nordvik, S. Samarakoon

Department of Mechanical and Structural Engineering and Material Science, University of Stavanger, Stavanger, Norway

Abstract

Post-tensioned flat slabs with fiber-reinforced concrete can reduce cracking and deflections, provide longer spans, thinner slabs and provide a reduction in the weight of the structure due to reduced floor dead load. The solution also provides benefits such as reduced storey height, a large reduction in conventional reinforcement, as well as an overall more flexible design [1]. However, the local shear per unit of length around columns in flat slabs can become very high, and this can result in local punching shear failure [2]. This paper investigates the punching shear resistance in post-tensioned flat slabs with fiber-reinforcement in accordance with proposed provisions in prEN 1992-1-1.

In this study, the punching shear resistance around different critical control sections in a flat slab was controlled, and then compared with results from ADAPT and FEM-design. Furthermore, the effect from different parameters in preEN 1992-1-1 and EN 1992-1-1 were compared.

The study showed that the fiber-reinforcement had the greatest contribution on the punching shear resistance according to the proposed provisions of Eurocode 2. The shear reinforcement had the second greatest contribution, although this contribution will vary. The purpose of the shear reinforcement is to account for the residual shear capacity and depending on the contribution from the fiber-reinforcement, post-tensioning and shear force, this value will therefore be different depending on the given case. If the contribution is e.g. sufficiently high from the fiber, the required amount of shear reinforcement will be lower/not required, because there will be a higher capacity in the slab to withstand the shear force.

Introduction

Reinforced concrete is the world's most widely used structural material, and it has maintained this position since the end of the nineteenth century.

Because reinforced concrete's tensile strength is limited, and the compressive strength is excessive, flexural cracks develop at early stages of loading. To prevent or reduce such cracks from developing, an eccentric or concentric force is imposed. The force is imposed in the longitudinal direction of the structural element, and it prevents the cracks from developing by eliminating or reducing the tensile stresses at critical midspan and support sections at service load. This will increase the shear, bending and torsional capacities of the sections, and the sections are then able to behave elastically. Such an imposed longitudinal force is called a prestressing force. Prestressing can either be done before or after the concrete is cast. If the prestressing is done after the concrete is cast, it is called post-tensioning [3].

Fiber-reinforced concrete is not a new concept, but there has been a lack of design guidelines, and today EN 1992-1-1 does not include guidelines for fiber reinforced concrete, although the work with a new revision is under preparation. However, the Norwegian Concrete Society issued NB38 in 2019 which united the industry in the development of guildlines regarding fiber-reinforced concrete.

For the design of reinforced slabs, there are numerous structural solutions, depending on the loading, geometry, economical factors and maybe also the preference of the designer and the customer. A common way to design slabs is by using a slab that is directly supported by columns without beams. This solution is called flat slabs and can provide a flexible and good structural design with many advantages.

The critical failure mode for flat slabs is punching shear. This is a phenomenon in slabs that is caused by concentrated support reactions inducing a cone shaped perforation starting from the top surface of the slab. The design approach with respect to punching shear is in various codes based on empirical results and observations from reinforced concrete slabs supported on concrete columns [4].

The combination of fiber and post-tensioning in flat slabs can offer numerous advantages, and the following sections presents the structural behavior, the critical areas in the slab that tends to exceed the punching shear limits, and different parameters that govern the punching shear resistance.

Methodology

A qualitative research method is chosen to understand and analyze the parametric study. The following methods were used:

- Literature study
  Empirical data was gathered to understand the case and to develop an understanding of how the punching shear resistance behavior of the flat slab

- Document study of building codes
  In order to increase knowledge and understanding about the current and the proposed provisions in Eurocode 2 regarding punching shear, a review of the current and proposed version, including a comparison of them, was performed

- Parametric study
  A parametric study was performed in order to investigate and analyze the effect on punching shear resistance in a flat slab with post-tensioning and fiber reinforcement. The study was performed on a fictive slab that included different cases of the critical control sections

- Digital tools and software
  The calculations were done using Mathcad, and thereafter these calculations were compared with results from analyses done in ADAPT and FEM-design

Geometry and Material Properties

A rectangular flat slab spanning 15m x 10m directly supported on columns was analyzed. This is shown in Figure 1. The structural loads considered besides the self-weight of the slab, and the loads due to pre-stressing, was a distributed live load of 2kN/m^2 and an additional dead load of 1 kN/m^2.
The study was performed with square columns, including interior, edge, and corner columns for the following cases: Without shear reinforcement, with post-tensioning, with fiber-reinforcement, with shear reinforcement and with PT (unbonded system), fiber, and shear reinforcement.

Figure 1 Geometry of the slab

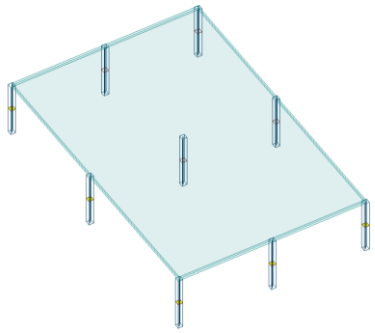

In every case, a set of parameters were varied (one at a time, while others stayed constant). The values of these parameters are presented in Table 1. The basis for these values were design shear- and moment values that were implemented from a FEM Design analysis, performed on the prerequisites presented initially in this chapter.

Table 1 Parameters varied

	Inner column	Edge column	Corner column
B [mm]	250	250	250
f_{ck} [Mpa]	35	35	35
η_c	0,42	0,61	0,901
ρ	0.0031	0.0031	0.0031
d_{dg} [mm]	32	32	32
e_x [mm]	40	40	40
e_y [mm]	55	55	55

Table 2 Values from FEM Design

	Inner column	Edge column	Corner column
V_{Ed} (kN)	643	206	85
$M_{Ed,x}$ (kNm)	103	16	15
$M_{Ed,y}$ (kNm)	126	96	17

Without Shear Reinforcement

Figure 2 Punching shear resistance without shear reinforcement for different characteristic compressive strengths

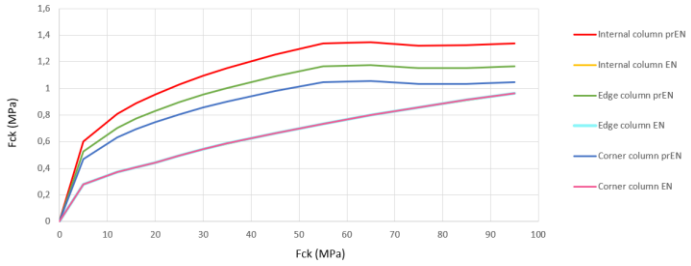

The change in compressive strength resulted in an increased shear resistance with increased compressive strength. It is however important to note that the all the values from the result cannot be considered realistic due the practical aspects. For a normal flat slab, the concrete quality will usually be between B30 and B45, both due to costs and structural behavior.

Figure 3 Punching shear resistance with different slab thickness

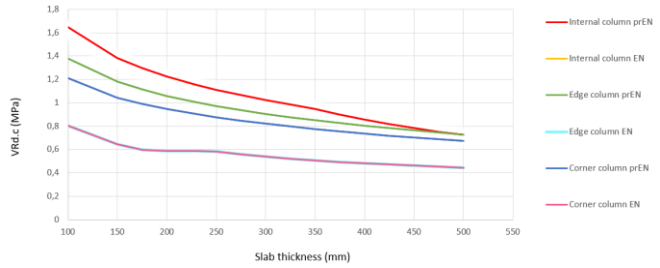

According to the formulas in EN 1992-1-1 the column placement did not affect the punching shear resistance, while prEN-1992-1-1 gave a different punching shear resistance depending on where the column was located. The results also showed that the punching shear resistance decreased with a thicker slab. It could be expected that a thicker member would have a higher punching shear resistance, but due to the nature of the formula, the resistance will in fact decrease when the value for d_v increases.

Formula 1 Punching shear resistance according to prEN 1992-1-1

$$\tau_{Rd.c} = \frac{0.6}{\gamma_v} \cdot k_{pb}(100 \cdot \rho_l \cdot f_{ck} \cdot \frac{d_{dg}}{d_v})^{\frac{1}{3}} \leq \frac{0.6}{\gamma_v} \cdot \sqrt{f_{ck}} \qquad [5]$$

Figure 4 varied parameters D_{lower} and k (aggregate)

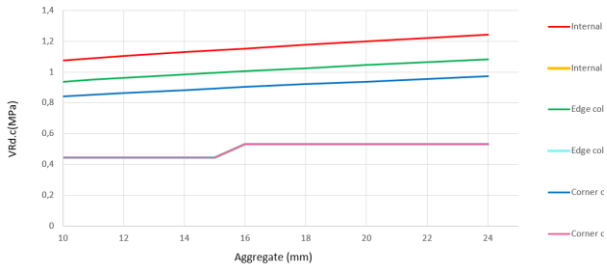

The parameters D_{lower} and k was also studied. D_{lower} is a parameter from prEN 1992-1-1 included in the formula for d_{dg}, and k is a factor from EN 1992-1-1. The results shows that the aggregate affects the punching shear resistance in prEN 1992-1-1, but in EN 1992-1-1 there are only two options for aggregate size, and therefore only two values are possible.

Prestressing

Figure 5 Punching shear resistance with post-tensioned mono strands for different characteristic compressive strengths (internal column)

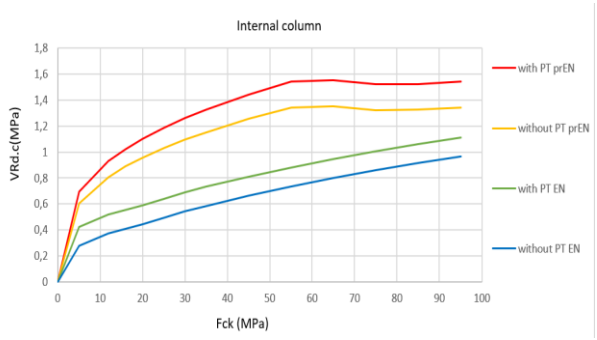

The results showed that there was an increased resistance with increased compressive strength. The results also showed that the resistance increased when the jacking force was increased, but according to prEN 1992-1-1 there is a limit due to factor k_{pb}.

The parameter that affected the punching shear resistance the least, was changing the eccentricity of cables in the section.

Figure 6 Punching shear resistance with post-tensioned mono strands for different characteristic compressive strengths (edge column)

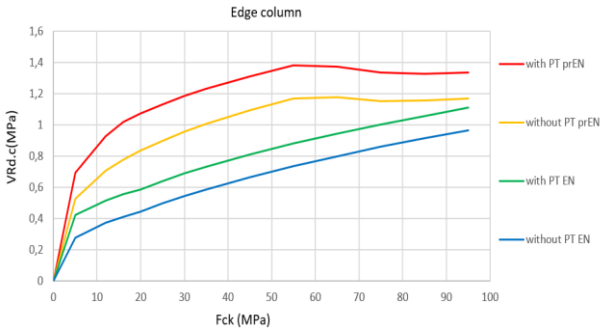

Figure 7 Punching shear resistance with post-tensioned mono strands for different characteristic compressive strengths (corner column)

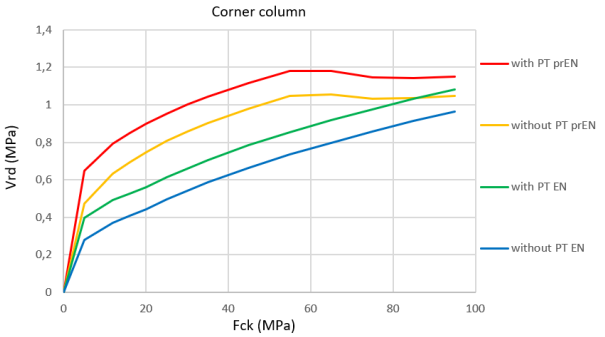

Fiber Reinforcement

Figure 8 Punching shear resistance with and without FRC for different characteristic compressive strengths

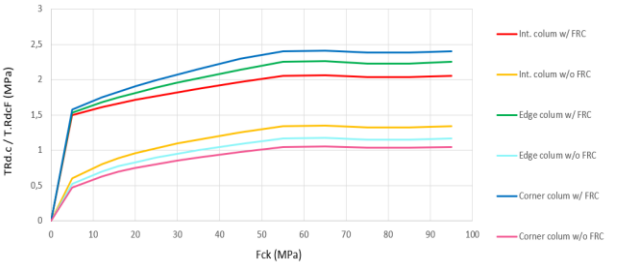

The results showed that there was an increased resistance with increased compressive strength. Also, the study showed that if the amount of fiber reinforcement was increased (kg/m^3), the residual tensile strength also increased. However, limitations regarding the amount of fiber that is possible needs to be taken into account. If the amount of fiber per cubic meter of concrete is too high, it will be difficult to cast the concrete. In addition to this, limitations regarding fiber is also governed by what the concrete producer can deliver in terms of fiber quality.

Figure 9 Residual tensile strength for internal column

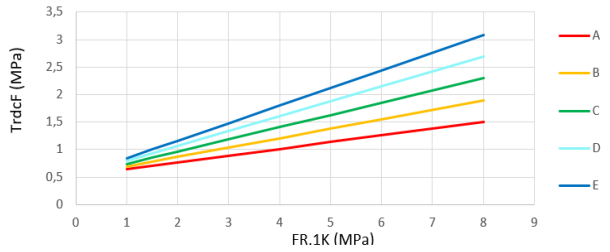

Figure 10 Residual tensile strength for edge column

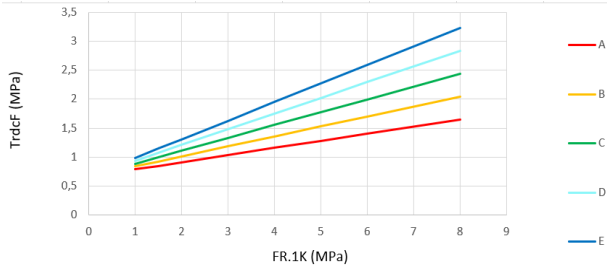

Figure 11 Residual tensile strength for corner

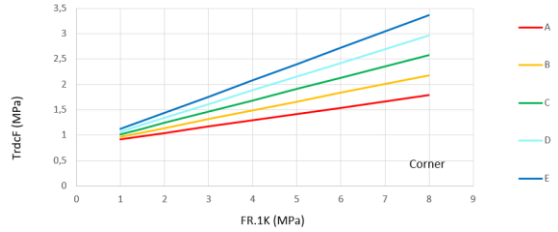

Summary of the results

In the light of the previous presented results from the parametric study, the main observations are summarized and presented in Table 3.

Table 3 Summary of results

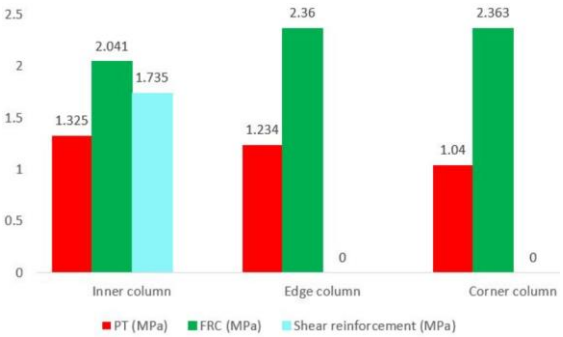

Conclusions and recommendations

Based on the calculations performed in Mathcad and analysis, the following conclusions have been drawn:

- The study showed that the fiber-reinforcement had the greatest contribution to the punching shear resistance according to the proposed provisions in Eurocode 2.
- The shear reinforcement had the second greatest contribution, although this contribution will vary. The purpose of the shear reinforcement is to account for the residual shear capacity and depending on the contribution from the fiber reinforcement, post-tensioning and shear force, this value will therefore be different depending on the given case.
- The prestressing affected the punching shear resistance in a relatively small manner.
- The punching shear resistance was lower for EN-1992-1-1 compared to prEN 1992-1-1. However, the proposed version will give a lower capacity because the design shear force is increased due to the decreased critical control section.

The punching shear resistance in post-tensioned flat slabs with fiber-reinforcement is a complex due to several reasons. The first being that the interaction between the different contributions are somehow intricate, and each contribution is governed by many parameters and factors.

When investigating the punching shear resistance in post-tensioned flat slabs with fiber reinforcement, more case studies are suggested with the advantage of the relation to reality. The interaction between the different contributions to the punching shear resistance is complex theoretically, and more studies should be conducted to confirm the theoretical trends and observations. Especially for the contribution from the fiber reinforcement, beam tests should be done in order to get exact input values.

References

[1] The concrete society . (2005). *Post-tensioned concrete floors: Design handbook Technical report No. 43.* Surrey: The concrete society

[2] Sørensen, S. I. (2013). *BETONGKONSTRUKSJONER Beregning og dimensjonering etter Eurokode 2.* Trondheim: Fagbokforlaget

[3] G.Nawy, E. (2003). *PRESTRESSED CONCRETE A fundamental Approach*. New Jersey: Pearson

[4] Ericsson, F. (2010). *Punching Shear in Reinforced Concrete – Slabs Supported on Edge Steel Columns.* Gøteborg: Chalmers University

[5] Norsk Standard. (2008). Prosjektering av betongkonstruksjoner. Oslo: Standard Norge